Climate4you update August 2018

Contents:

August 2018 global surface air temperature overview

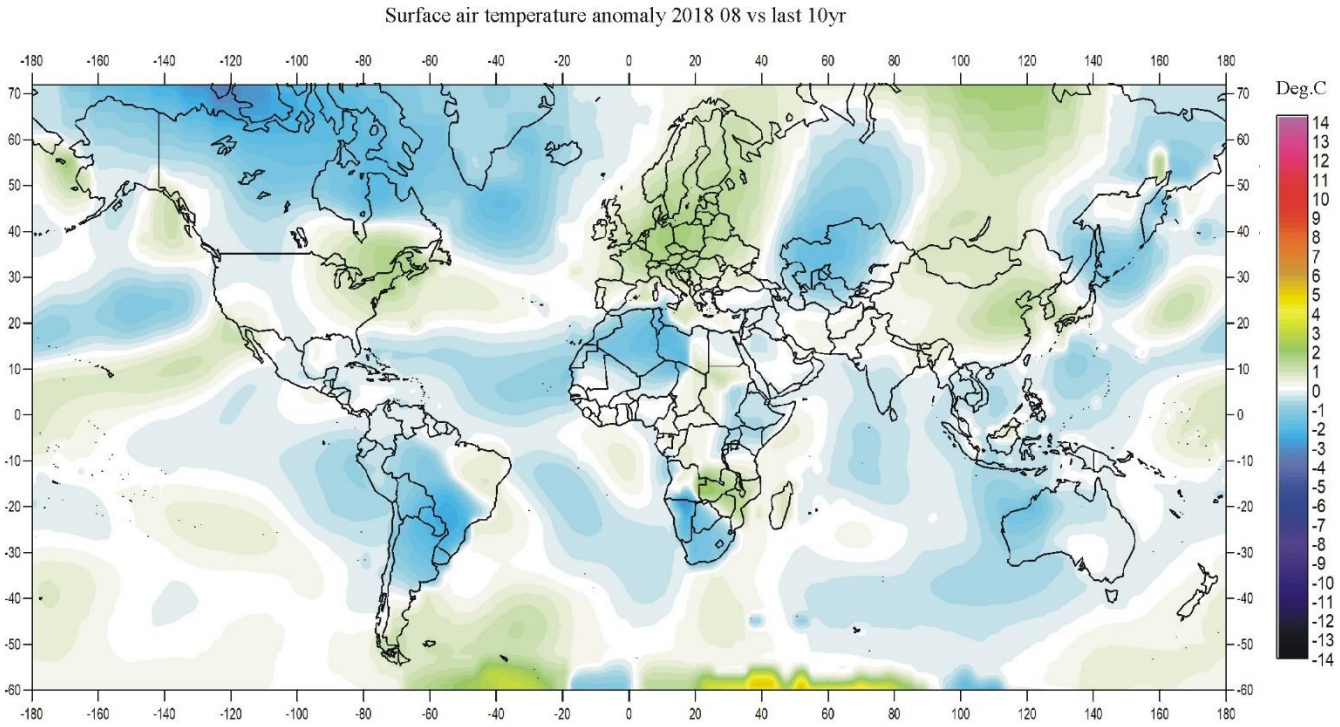

2

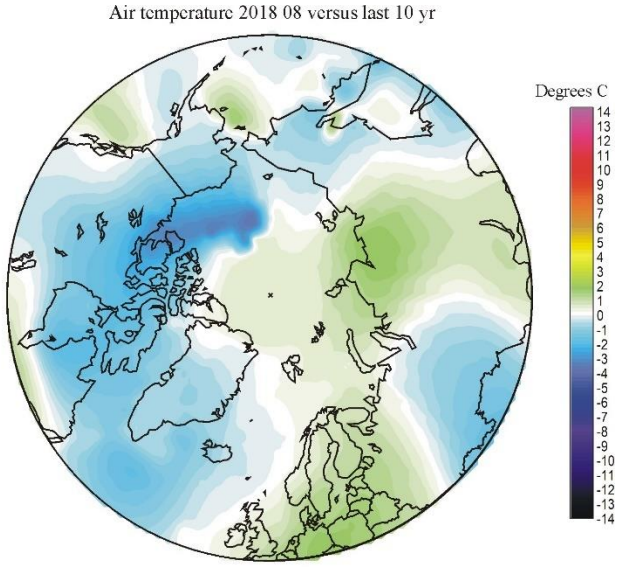

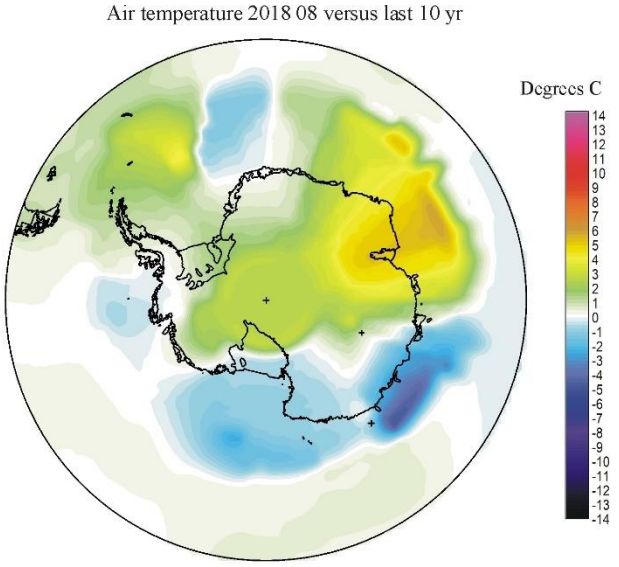

August 2018 surface air temperature compared to the average of the last 10 years. Green-yellow-red colours indicate areas with higher temperature than the 10-year average, while blue colours indicate lower than average temperatures. Data source: Goddard Institute for Space Studies (GISS) using ERSST_v4 ocean surface temperatures.

Comments to the August 2018 global surface air temperature overview

General: This newsletter contains graphs showing a selection of key meteorological variables for the past month. *All temperatures are given in degrees Celsius*.

In the above maps showing the geographical pattern of surface air temperatures, *the last previous 10 years are used as reference period*.

The rationale for comparing with this recent period instead of the official WMO 'normal' period 1961-1990, is that the latter period is affected by the cold period 1945-1980. Most comparisons with this time period will automatically appear as warm, and it will be difficult to decide if modern surface air temperatures are increasing or decreasing. Comparing instead with the last previous 10 years overcomes this problem and displays the modern dynamics of ongoing change. This decadal approach also corresponds well to the typical memory horizon for many people.

In addition, the GISS temperature data used for preparing the above diagrams display distinct temporal instability for data before the turn of the century (see p. 7). Any comparison with the WMO 'normal' period 1961-1990 is therefore influenced by ongoing monthly mainly administrative changes. An unstable value is clearly not suited as reference value. Simply comparing with the last previous 10 years makes more sense and is more useful.

The different air temperature records have been divided into three quality classes, QC1, QC2 and QC3, respectively, as described on page 7.

In many diagrams shown in this newsletter the thin line represents the monthly global average value, and the thick line indicate a simple running average, in most cases a simple moving 37-month average, nearly corresponding to a three-year average. The 37-month average is calculated from values covering a range from 18 months before to 18 months after, with equal weight given to all individual months.

The year 1979 has been chosen as starting point in many diagrams, as this roughly corresponds to both the beginning of satellite observations and the onset of the late 20th century warming period. However, several of the data series have a much longer record length, which may be inspected in greater detail on www.climate4you.com.

August 2018 global surface air temperatures

General: For August 2018 GISS supplied 15932 interpolated surface air data points; all published values are used to produce the diagrams shown on page 2. According to the GISS data, the average global August temperature anomaly was a little lower than in the previous month. Thus, the overall decrease of global surface air temperatures since the 2016-17 El Niño global temperature peak persists.

The Northern Hemisphere was characterised by rather small regional contrasts, and relative cooling dominate (see p. 2). Northern America, Greenland and eastern Siberia were cold compared to the previous 10 years, while Europe and western Siberia were relatively warm. The American-Greenland sector of the Arctic was cold, while the Europe-Siberia sector was warm. However, the GISS surface air temperatures north of 80° N still appears to have an issue with interpolation in this region. The Arctic sea ice still appears to be displaying an overall thickness increase, compared to the situation one year ago (see diagram on p.32).

Near the Equator temperatures were near or below the 10-year average.

The Southern Hemisphere temperatures were near or below the average for the previous 10 years. Especially the land areas represented by South America, South Africa and Australia was relatively cold. In contrast, large parts of the Antarctic were warmer than the average. As it still is winter in the Antarctica, this anomaly presumably is the result of advection of relatively warm air masses into the continent from lower latitudes. South of 80°S there the GISS anomaly pattern still is influenced by an interpolation artefact.

Temperature quality class 1: Lower troposphere temperature from satellites, updated to August 2018

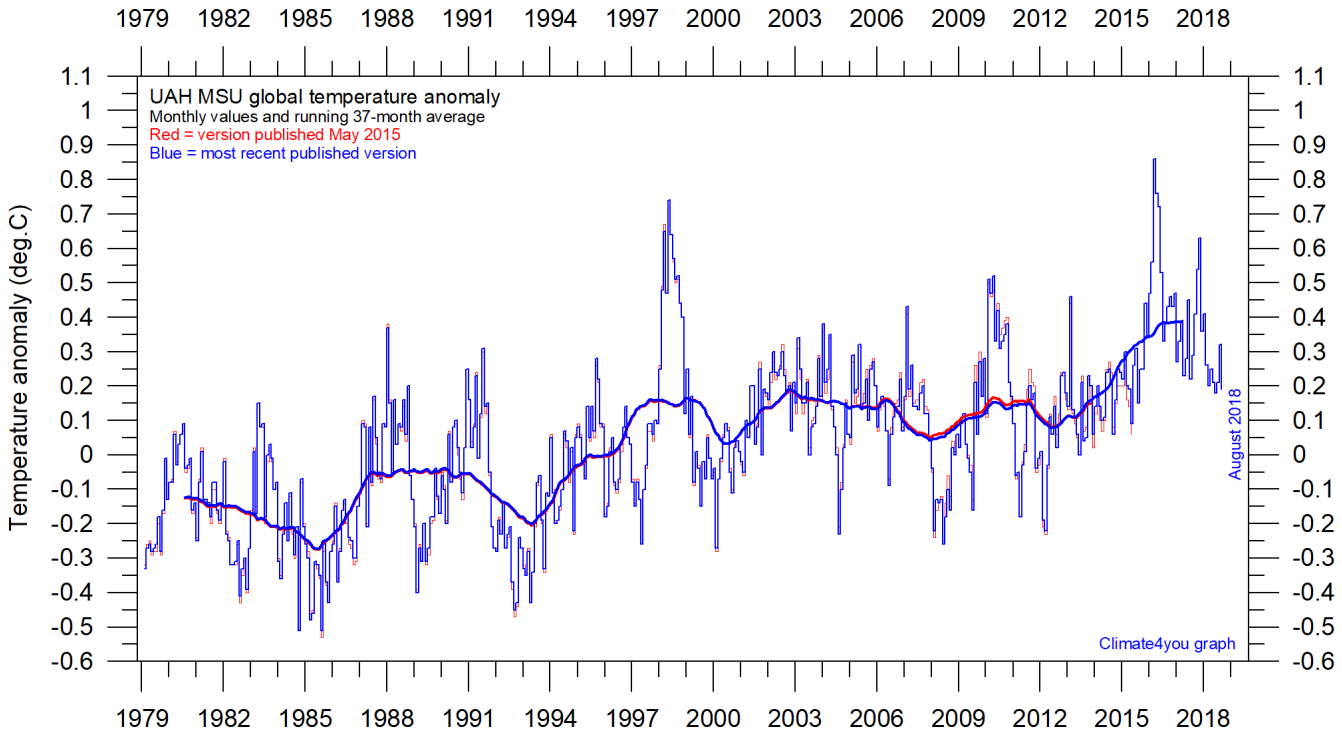

Global monthly average lower troposphere temperature (thin line) since 1979 according to University of Alabama at Huntsville, USA. The thick line is the simple running 37-month average.

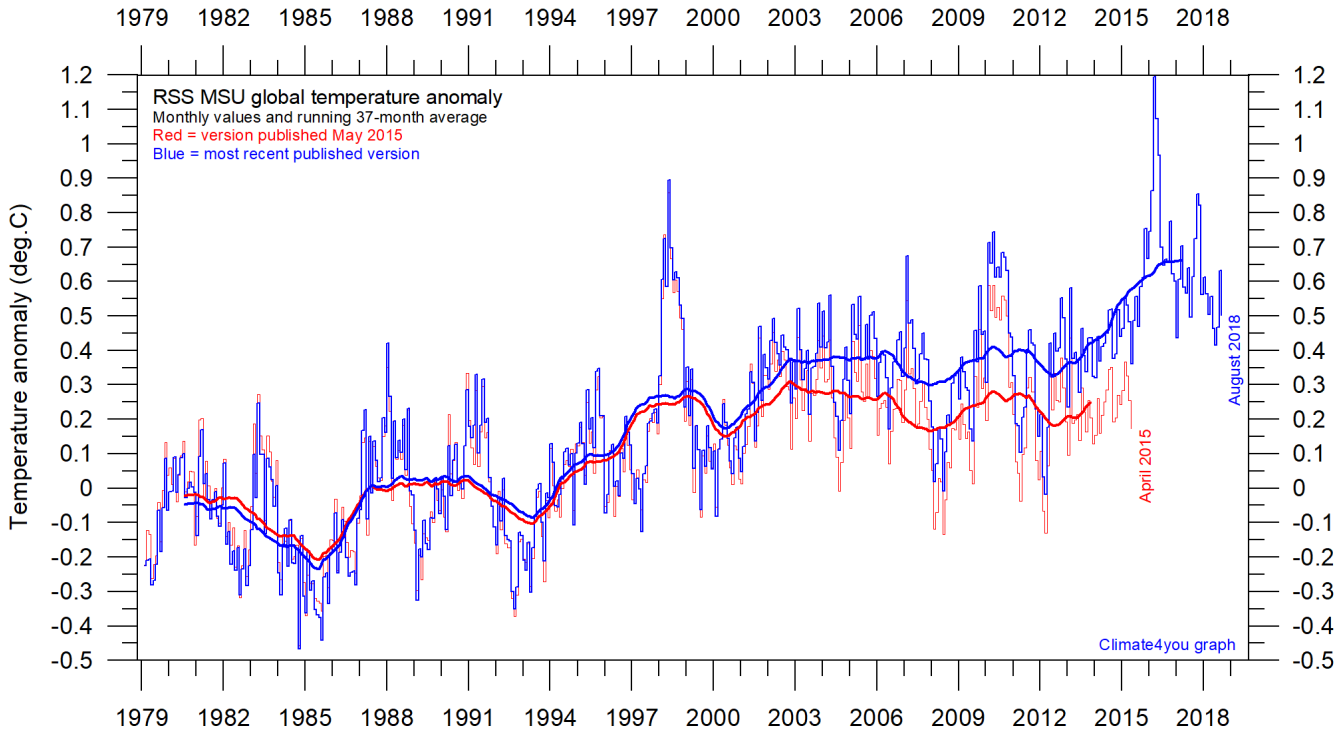

Global monthly average lower troposphere temperature (thin line) since 1979 according to according to Remote Sensing Systems (RSS), USA. The thick line is the simple running 37-month average.

Temperature quality class 2: HadCRUT global surface air temperature, updated to July 2018

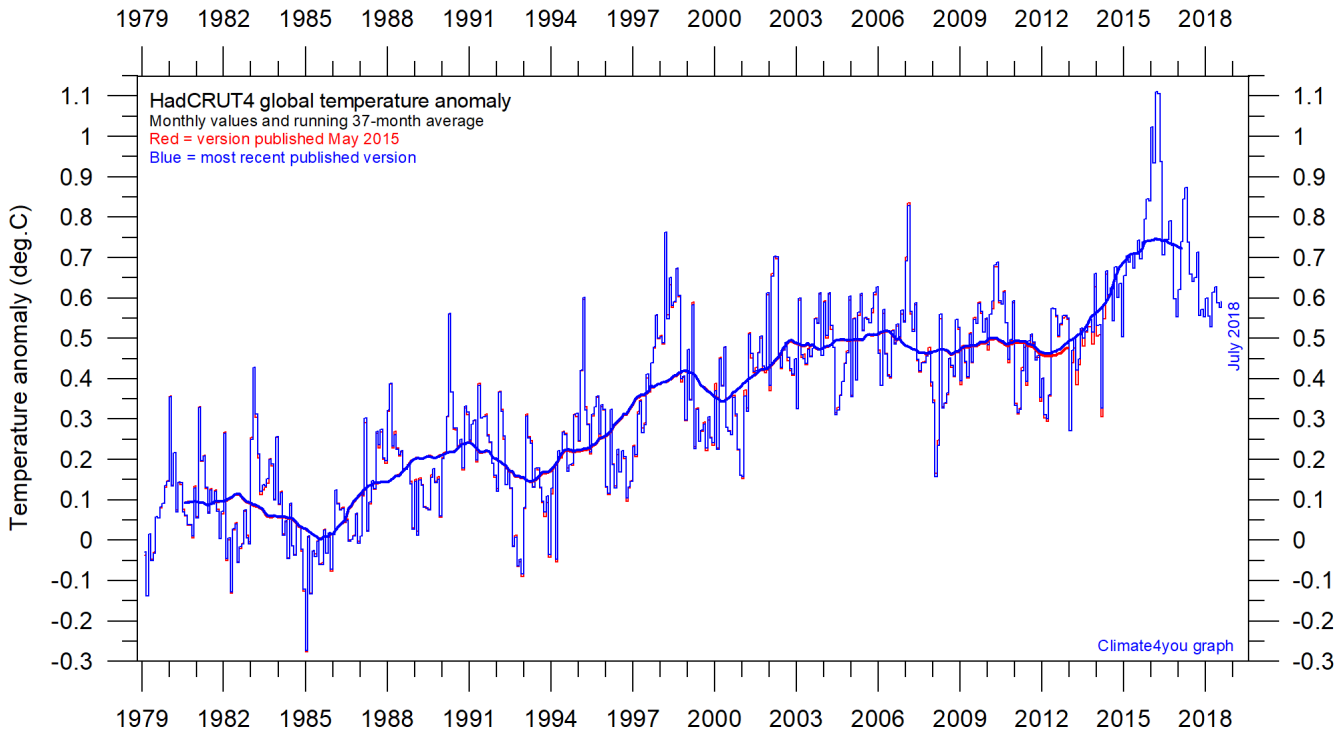

Global monthly average surface air temperature (thin line) since 1979 according to according to the Hadley Centre for Climate Prediction and Research and the University of East Anglia's Climatic Research Unit (CRU), UK. The thick line is the simple running 37-month average.

Temperature quality class 3: GISS and NCDC global surface air temperature, updated to August 2018

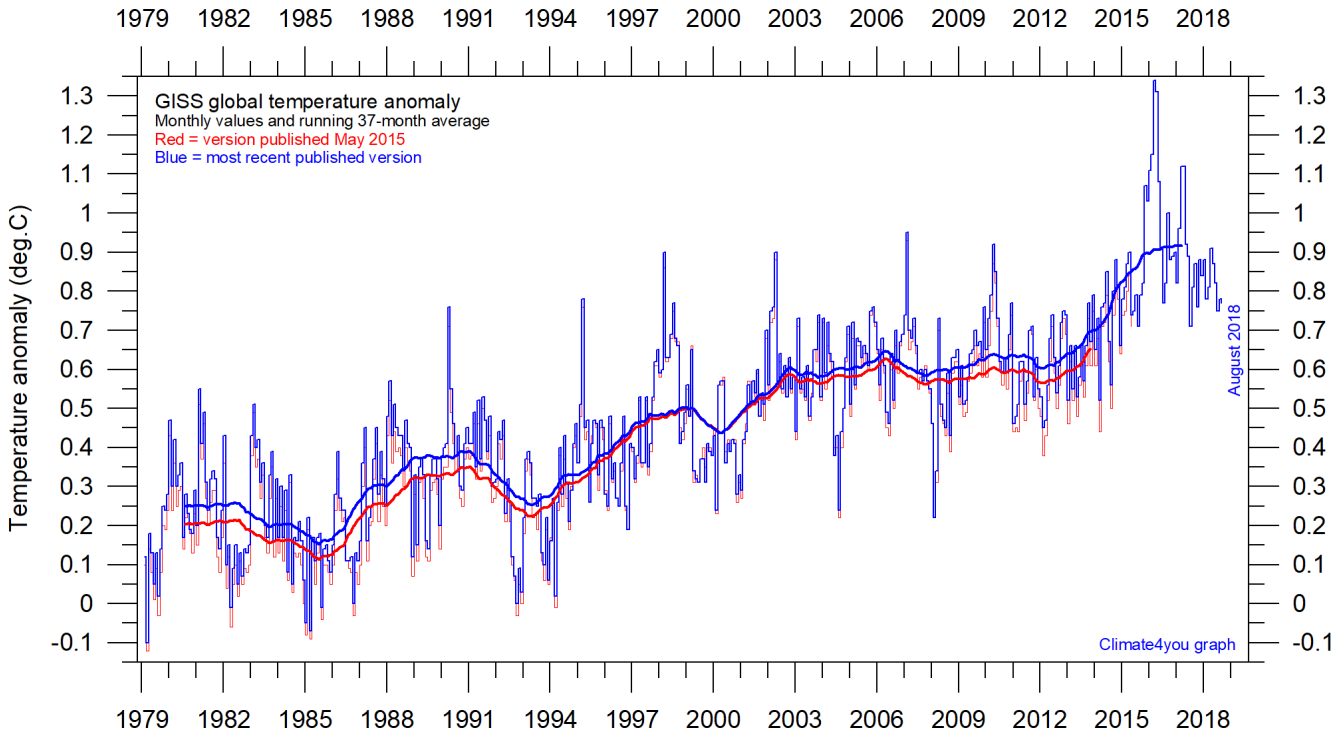

Global monthly average surface air temperature (thin line) since 1979 according to according to the Goddard Institute for Space Studies (GISS), at Columbia University, New York City, USA, using ERSST_v4 ocean surface temperatures. The thick line is the simple running 37-month average.

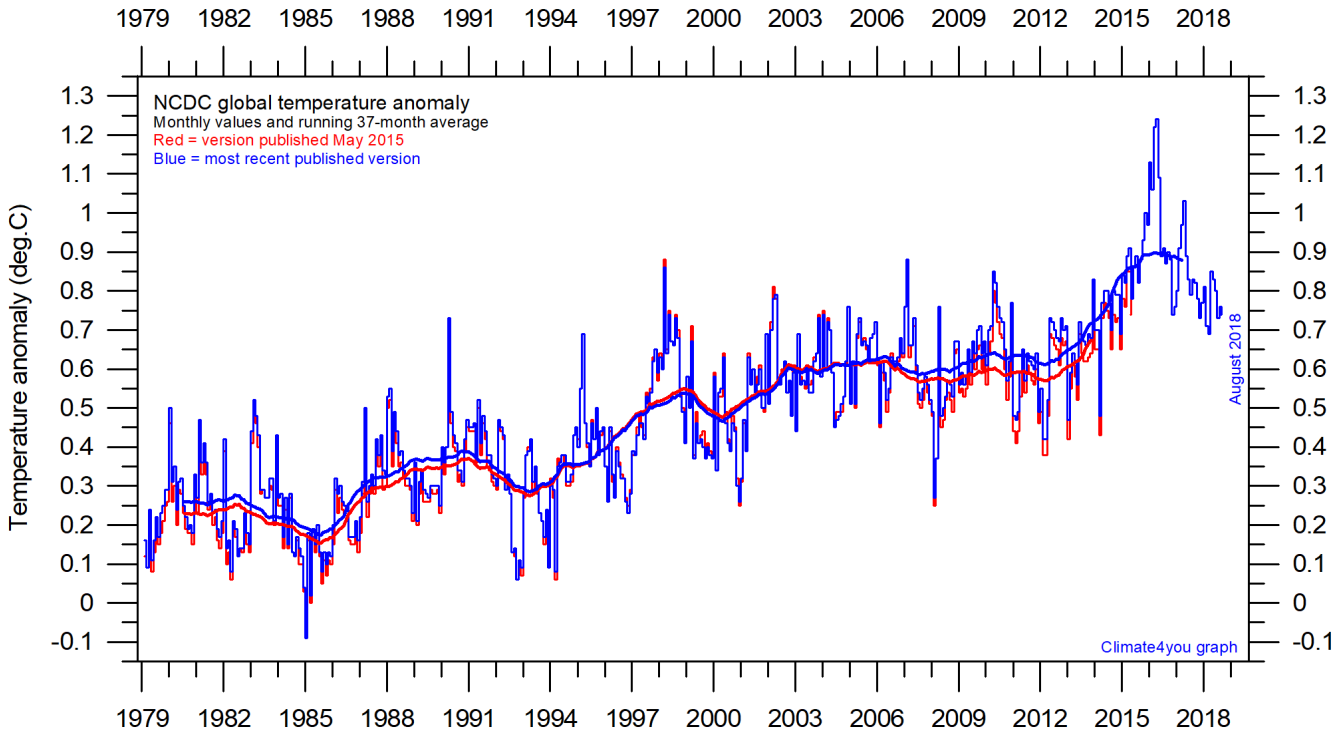

Global monthly average surface air temperature since 1979 according to according to the National Climatic Data Center (NCDC), USA. The thick line is the simple running 37-month average.

A note on data record stability and -quality:

All temperature diagrams shown above have 1979 as starting year. This roughly marks the beginning of the recent period of global warming, after termination of the previous period of global cooling from about 1940. In addition, the year 1979 also represents the starting date for the satellite-based global temperature estimates (UAH and RSS). For the three surface air temperature records (HadCRUT, NCDC and GISS), they begin much earlier (in 1850 and 1880, respectively), as can be inspected on www.climate4you.com.

For all three surface air temperature records, but especially NCDC and GISS, administrative changes to anomaly values are quite often introduced, even for observations many years back in time. Some changes may be due to the delayed addition of new station data, while others probably have their origin in a change of technique to calculate average values. It is clearly impossible to evaluate the validity of such administrative changes for the outside user of these records; it is only possible to note that such changes appear very often (se example diagram next page).

In addition, the three surface records represent a blend of sea surface data collected by moving ships or by other means, plus data from land stations of partly unknown quality and unknown degree of representativeness for their region. Many of the land stations have also moved geographically during their existence, and their instrumentation changed, and they are influenced by changes in their surroundings (vegetation, buildings, etc.).

The satellite temperature records also have their problems, but these are generally of a more technical nature and therefore correctable. In addition, the temperature sampling by satellites is more regular and complete on a global basis than that represented by the surface records. Also important is that the sensors on satellites measure temperature directly by emitted radiation, while most surface temperature measurements are indirect, using electronic resistance.

Everybody interested in climate science should gratefully acknowledge the efforts put into maintaining the different temperature databases referred to in the present newsletter. At the same time, however, it is also important to realise that all temperature records cannot be of equal scientific quality. The simple fact that they to some degree differ shows that they cannot all be correct.

On this background, and for practical reasons, Climate4you operates with three quality classes (1-3) for global temperature records, with 1 representing the highest quality level:

Quality class 1: The satellite records (UAH and RSS).

Quality class 2: The HadCRUT surface record.

Quality class 3: The NCDC and GISS surface records.

The main reason for discriminating between the three surface records is the following:

While both NCDC and GISS often experience quite large administrative changes (see example on p.8), and therefore essentially are unstable temperature records, the changes introduced to HadCRUT are fewer and smaller. For obvious reasons, as the past does not change, any record undergoing continuing changes cannot describe the past correctly all the time.

You can find more on the issue of lack of temporal stability on www.climate4you.com (go to: *Global Temperature*, followed by *Temporal Stability*).

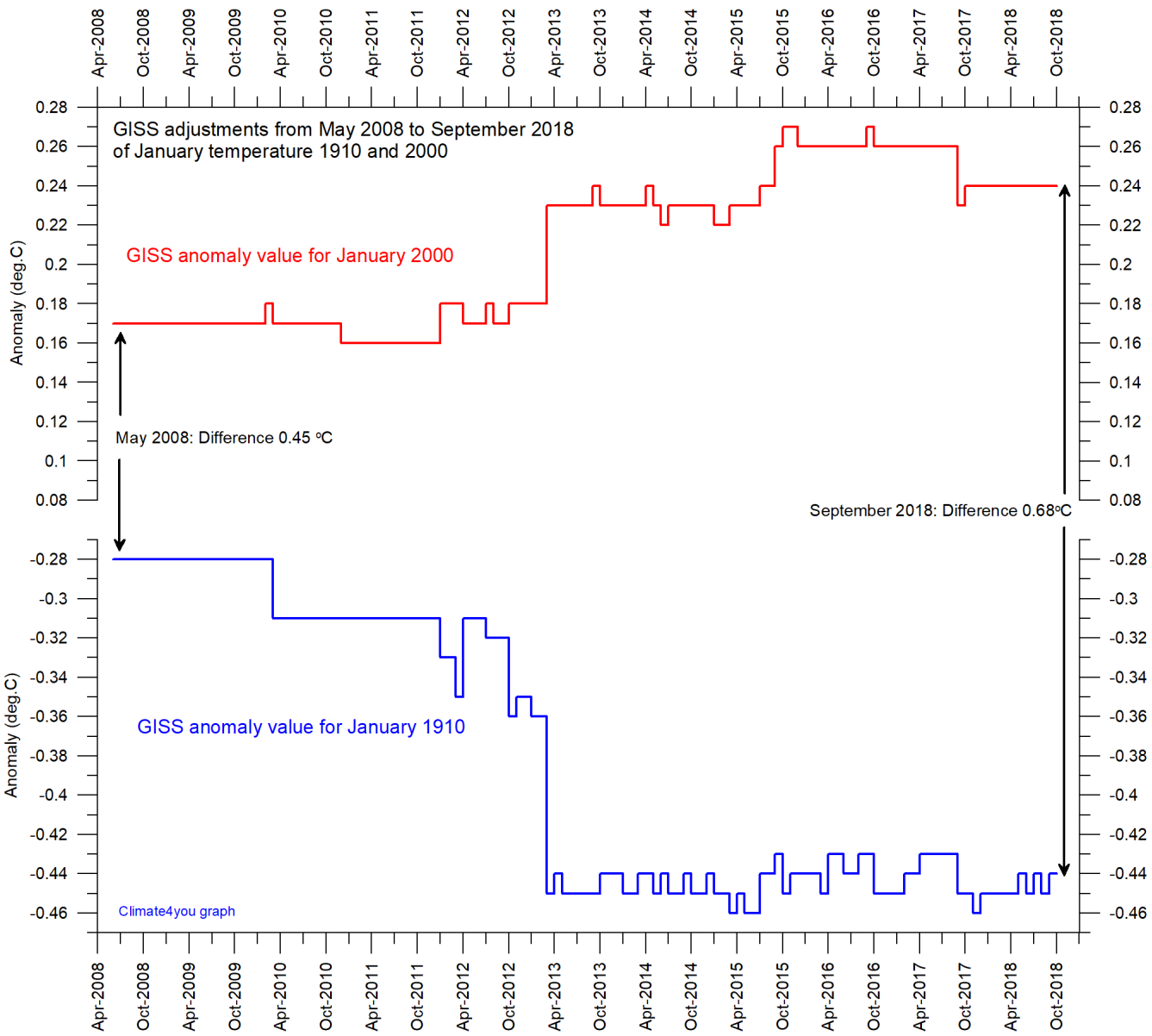

Diagram showing the adjustment made since May 2008 by the Goddard Institute for Space Studies (GISS), USA, in anomaly values for the months January 1910 and January 2000.

Note: The administrative upsurge of the temperature increase from January 1915 to January 2000 has grown from 0.45 (reported May 2008) to 0.68°C (reported September 2018). This represents an about 51% administrative temperature increase over this period, meaning that more than half of the apparent (as reported by GISS) global temperature increase from January 1910 to January 2000 is due to administrative changes of the original data since May 2008.

Comparing global surface air temperature and lower troposphere satellite temperatures; updated to July 2018

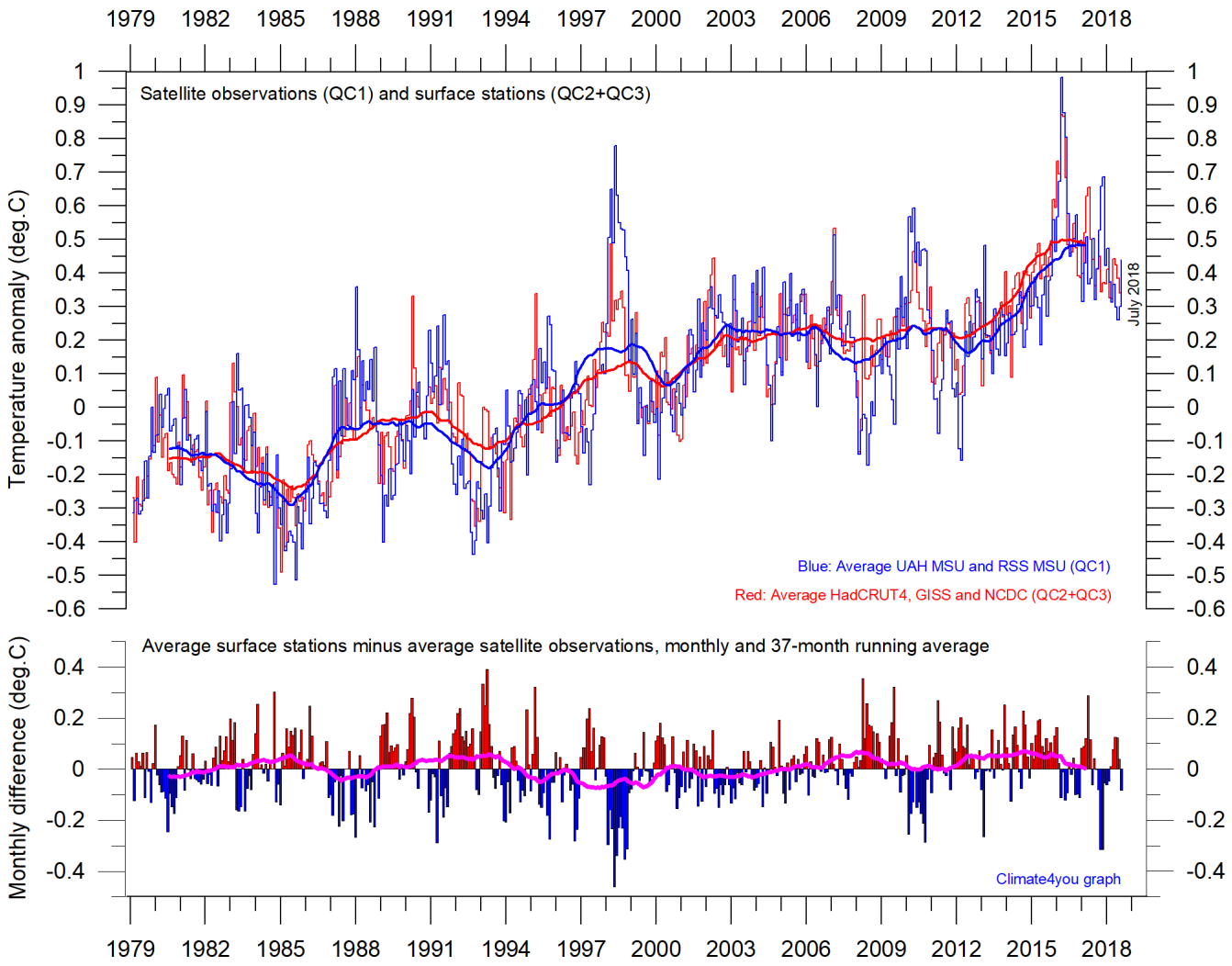

Plot showing the average of monthly global surface air temperature estimates (HadCRUT4, GISS and NCDC) and satellite-based temperature estimates (RSS MSU and UAH MSU). The thin lines indicate the monthly value, while the thick lines represent the simple running 37-month average, nearly corresponding to a running 3-yr average. The lower panel shows the monthly difference between average surface air temperature and satellite temperatures. As the base period differs for the different temperature estimates, they have all been normalised by comparing to the average value of 30 years from January 1979 to December 2008.

NOTE: Since about 2003, the average global surface air temperature has been drifting away in positive direction from the average satellite temperature, meaning that the surface records show warming in relation to the troposphere records. The reason(s) for this is not entirely clear but can presumably at least partly be explained by the recurrent administrative adjustments made to the surface records (see p. 7-8).

Global air temperature linear trends updated to July 2018

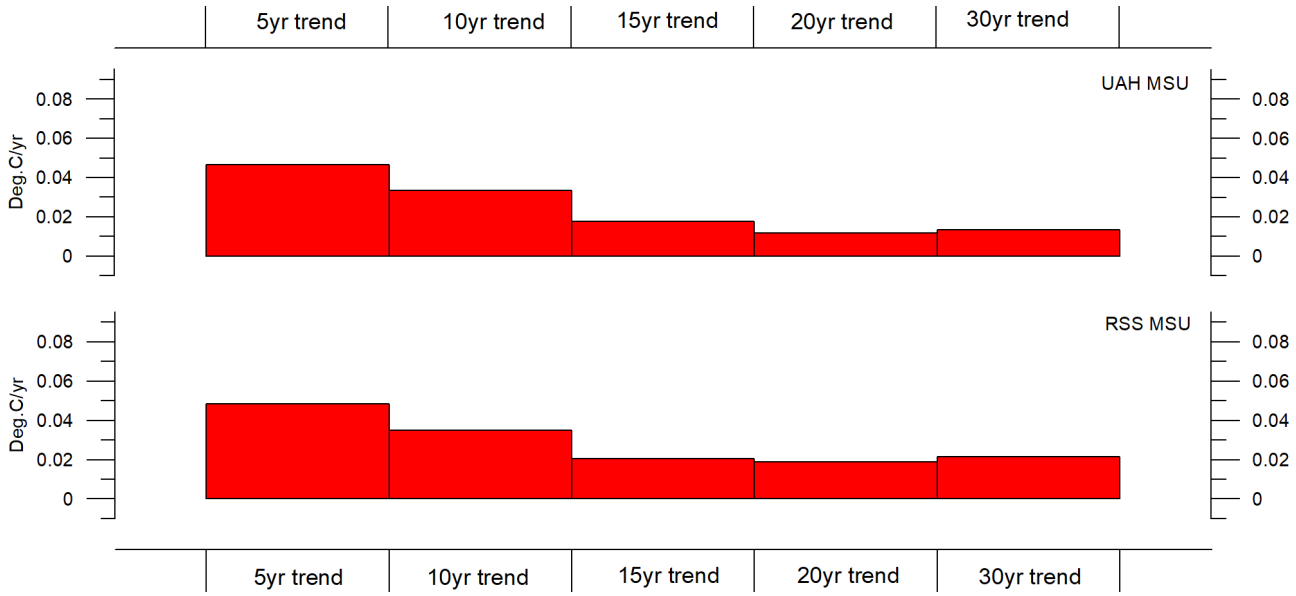

Diagram showing the latest 5, 10, 20 and 30-yr linear annual global temperature trend, calculated as the slope of the linear regression line through the data points, for two satellite-based temperature estimates (UAH MSU and RSS MSU).

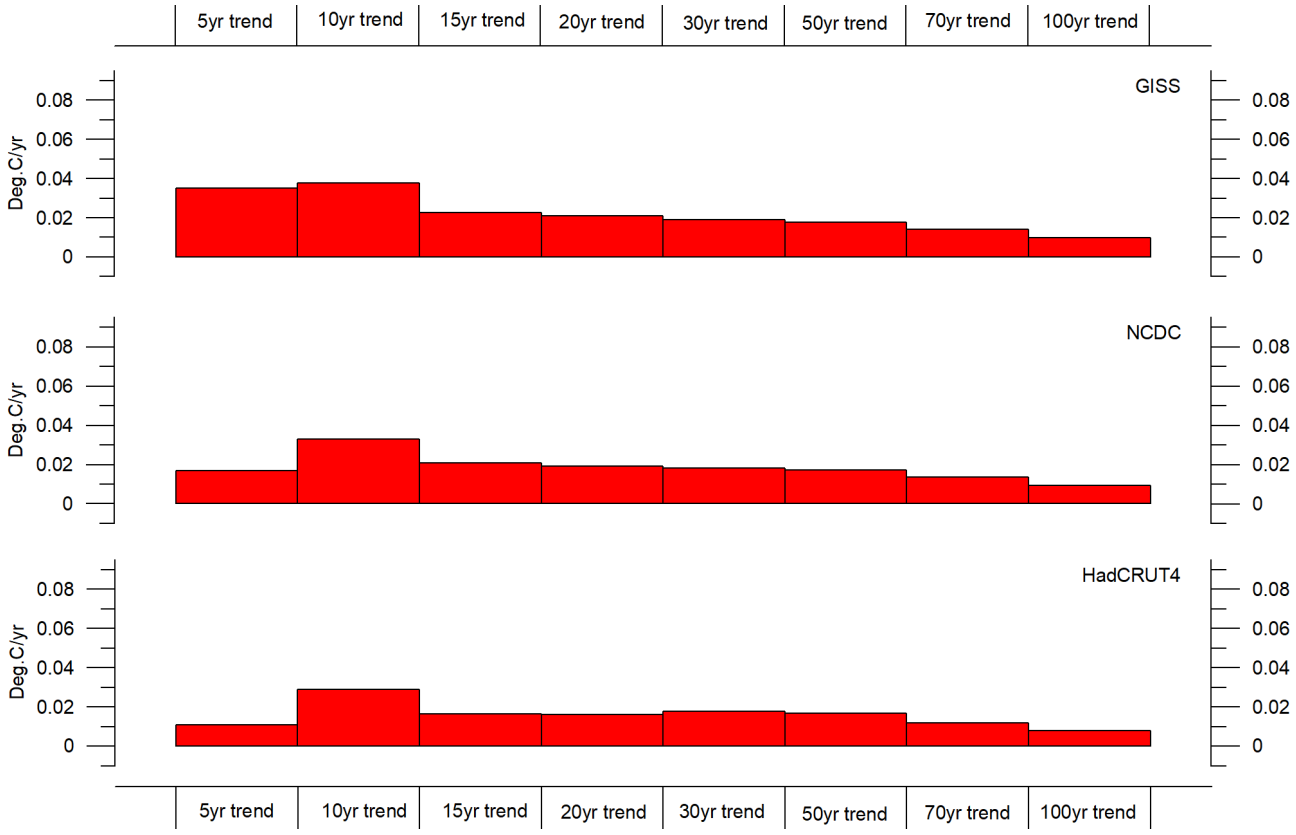

Diagram showing the latest 5, 10, 20, 30, 50, 70 and 100-year linear annual global temperature trend, calculated as the slope of the linear regression line through the data points, for three surface-based temperature estimates (GISS, NCDC and HadCRUT4).

All in one, Quality Class 1, 2 and 3; updated to July 2018

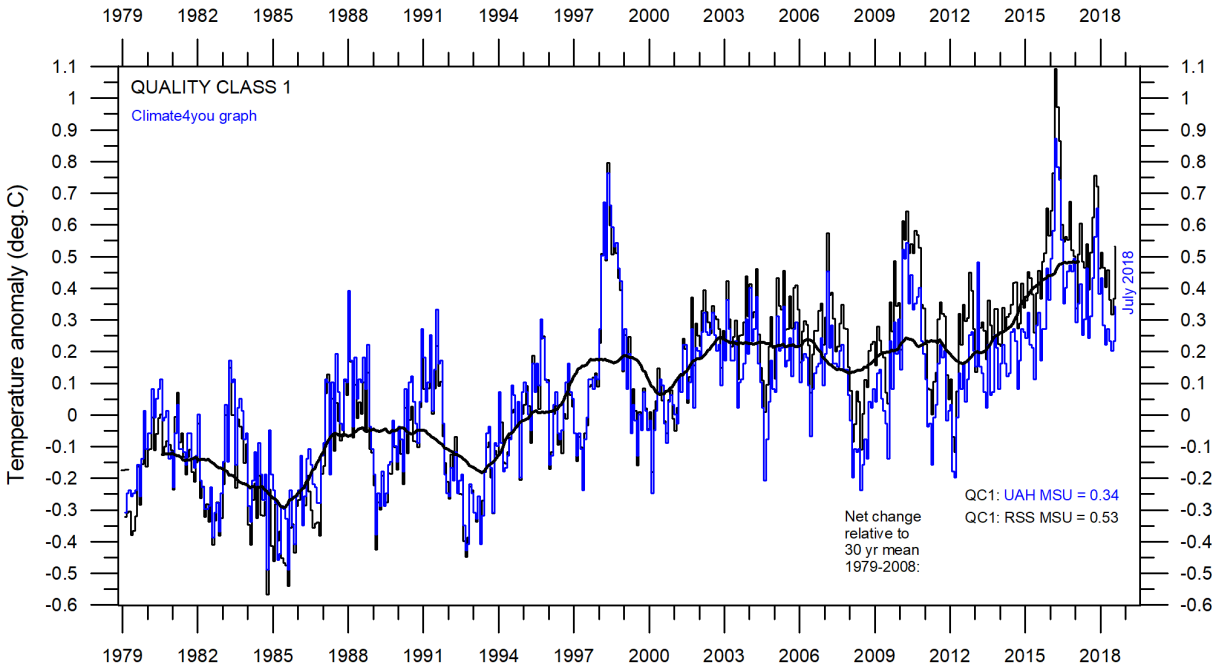

Superimposed plot of Quality Class 1 (UAH and RSS) global monthly temperature estimates. As the base period differs for the individual temperature estimates, they have all been normalised by comparing with the average value of the initial 120 months (30 years) from January 1979 to December 2008. The heavy black line represents the simple running 37 month (c. 3 year) mean of the average of both temperature records. The numbers shown in the lower right corner represent the temperature anomaly relative to the individual 1979-2008 averages.

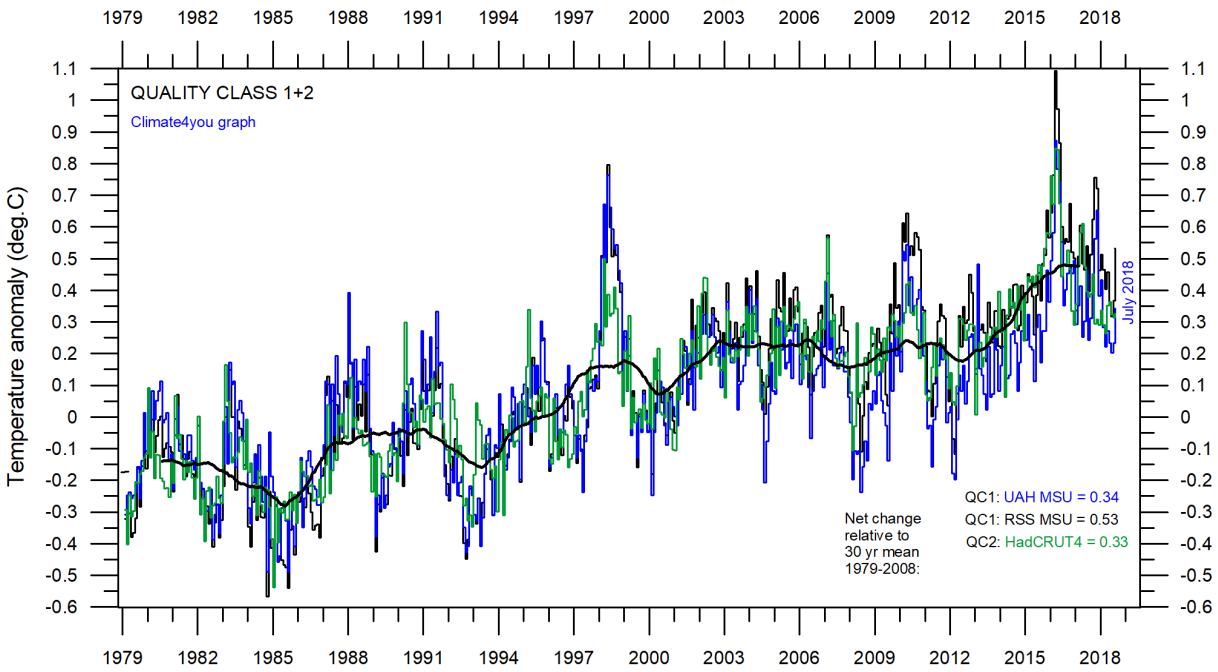

Superimposed plot of Quality Class 1 and 2 (UAH, RSS and HadCRUT4) global monthly temperature estimates. As the base period differs for the individual temperature estimates, they have all been normalised by comparing with the average value of the initial 120 months (30 years) from January 1979 to December 2008. The heavy black line represents the simple running 37 month (c. 3 year) mean of the average of all three temperature records. The numbers shown in the lower right corner represent the temperature anomaly relative to the individual 1979-2008 averages.

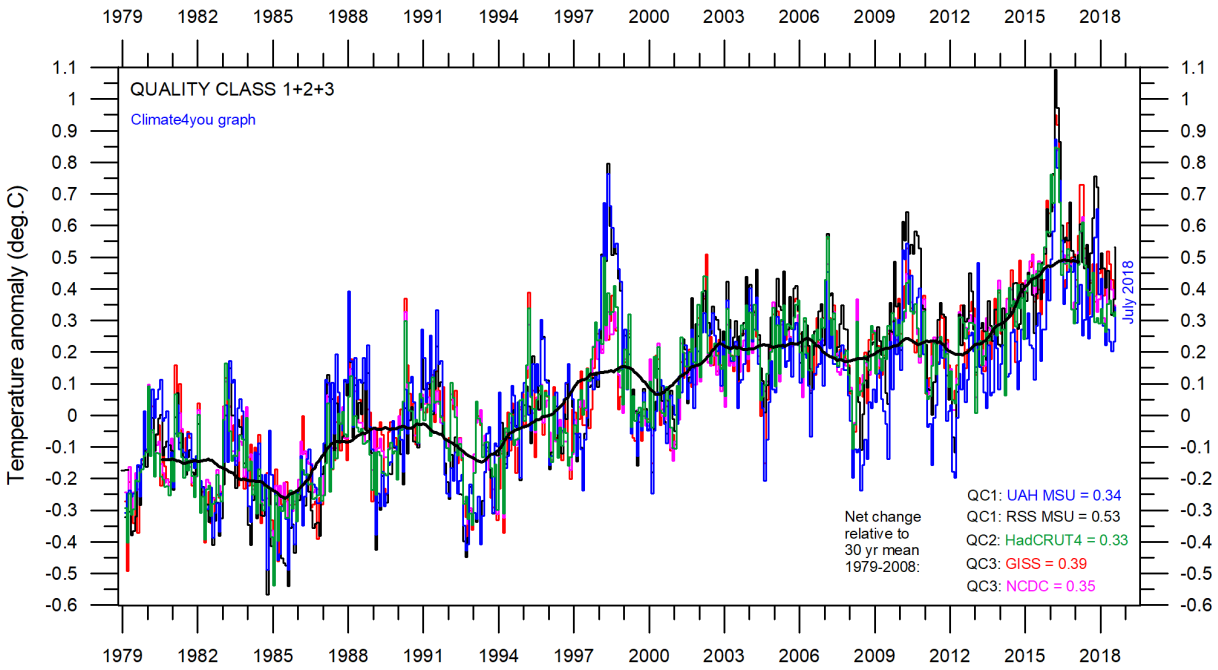

Superimposed plot of Quality Class 1, 2 and 3 global monthly temperature estimates (UAH, RSS, HadCRUT4, GISS and NCDC). As the base period differs for the individual temperature estimates, they have all been normalised by comparing with the average value of the initial 120 months (30 years) from January 1979 to December 2008. The heavy black line represents the simple running 37 month (c. 3 year) mean of the average of all five temperature records. The numbers shown in the lower right corner represent the temperature anomaly relative to the individual 1979-2008 averages.

Please see notes on page 7 relating to the above three quality classes.

It should be kept in mind that satellite- and surface-based temperature estimates are derived from different types of measurements, and that comparing them directly as done in the diagram above therefore may be somewhat problematical. However, as both types of estimate often are discussed together, the above diagram may nevertheless be of some interest. In fact, the different types of temperature estimates appear to agree as to the overall temperature variations on a 2-3-year scale, although on a shorter time scale there are often considerable differences between the individual records. However, since about 2003 the surface records are slowly drifting towards higher temperatures than the combined satellite record (see p. 9).

The average of all five global temperature estimates presently shows an overall stagnation, at least since 2002-2003. There has been no significant increase in global air temperature since 1998, which however was affected by the oceanographic El Niño event. Also, the recent (2015-16) El Niño event may well represent a relatively short-lived spike on a longer development. The coming years will show if this is the case or not. Neither has there been a temperature decrease since about 2002-2003.

The present temperature stagnation does not exclude the possibility that global temperatures will begin to increase again later. On the other hand, it also remains a possibility that Earth just now is passing an overall temperature peak, and that global temperatures will begin to decrease during the coming years. Again, time will show which of these possibilities is correct.

Global sea surface temperature, updated to August 2018

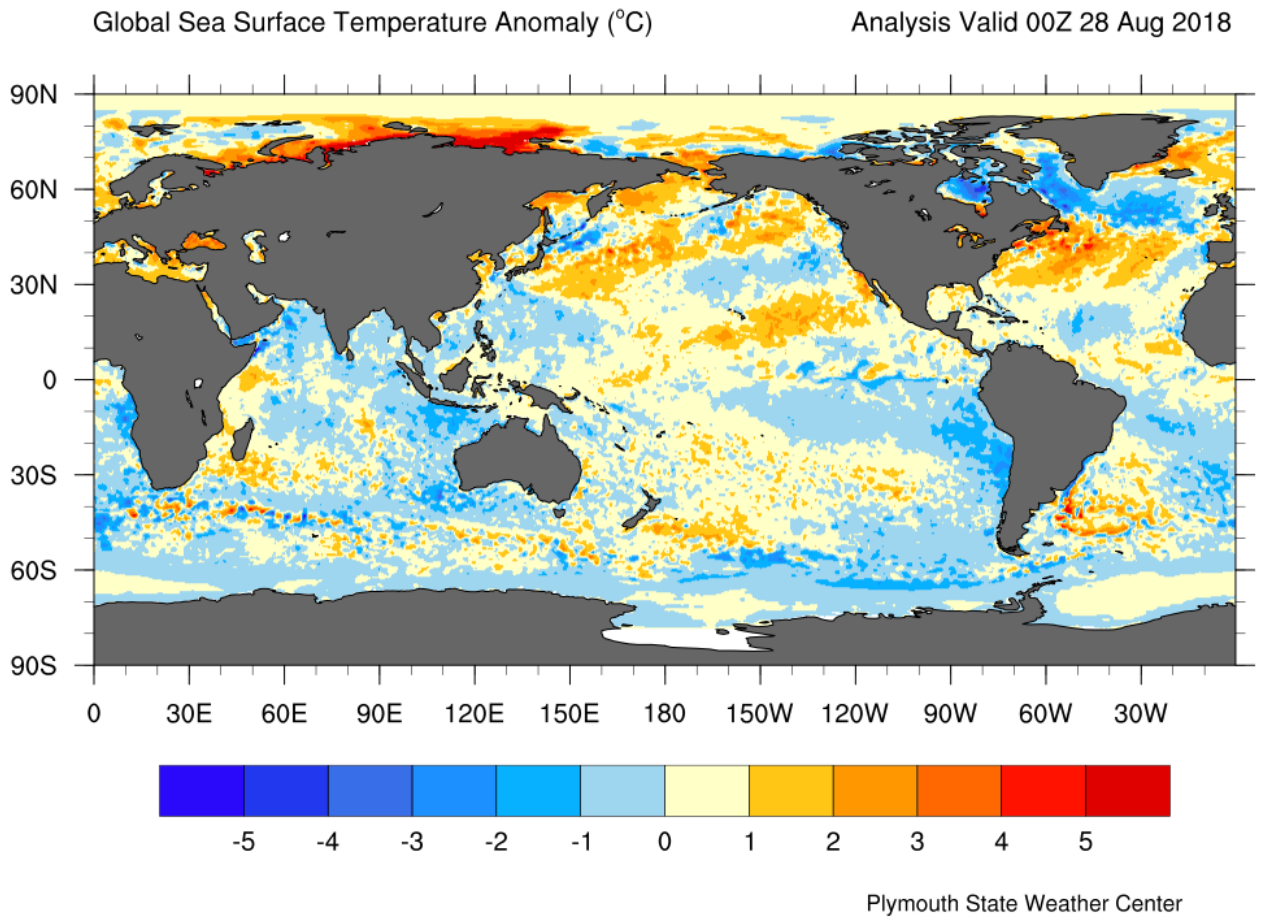

Sea surface temperature anomaly on 28 August 2018. Map source: Plymouth State Weather Center. Reference period: 1977-1991.

Because of the large surface areas near Equator, the temperature of the surface water in these regions is especially important for the global atmospheric temperature (p. 4-6).

Relatively cold water in August 2018 dominates much of the oceans near the Equator. In addition, parts of the North Atlantic are cooling. Presumably, all this will be influencing global air temperatures in the months to come.

However, the significance of any short-term cooling or warming reflected in air temperatures should not be overstated. Whenever Earth experiences cold La Niña or warm El Niño episodes (Pacific Ocean) major heat exchanges takes place between the Pacific Ocean and the atmosphere above, eventually showing up in estimates of the global air temperature.

However, this does not reflect similar changes in the total heat content of the atmosphere-ocean system. In fact, global net changes can be small and such heat exchanges may mainly reflect redistribution of energy between ocean and atmosphere. What matters is the overall temperature development when seen over several years.

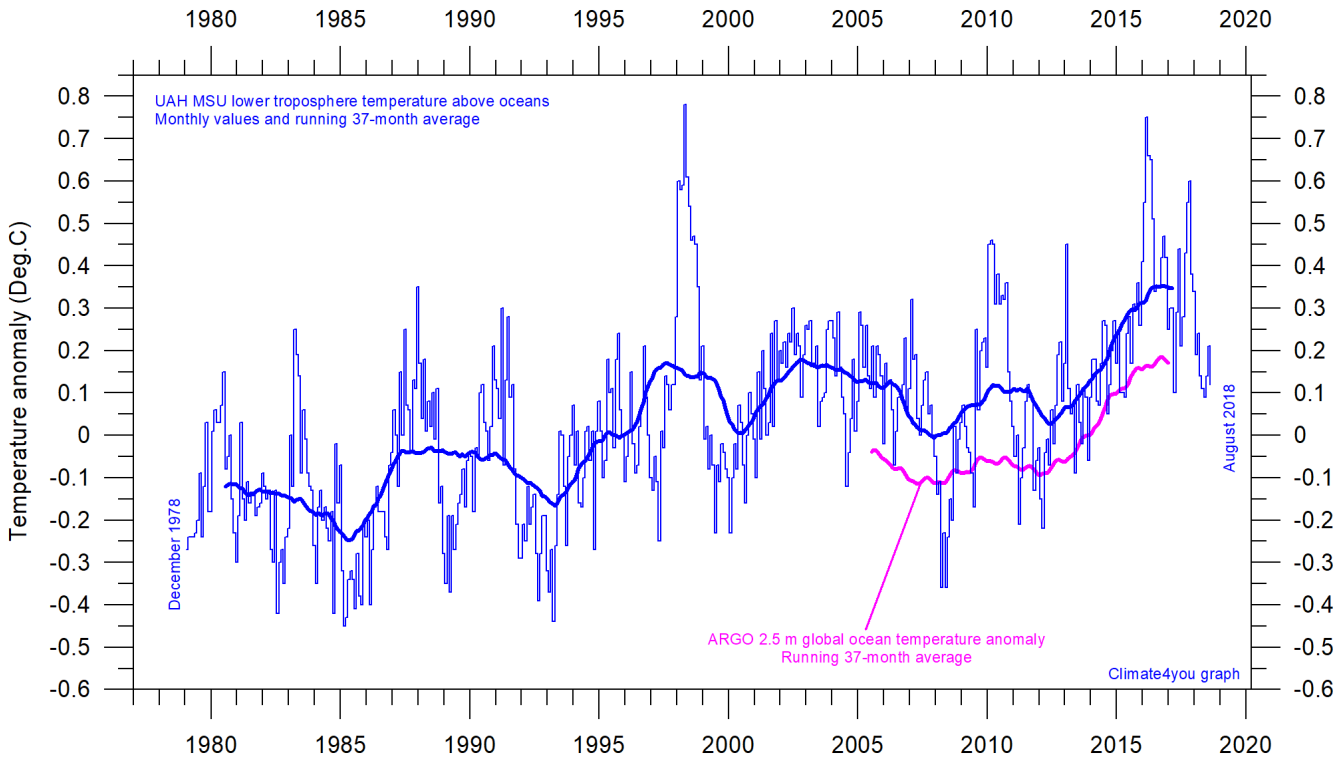

Global monthly average lower troposphere temperature over oceans (thin line) since 1979 according to University of Alabama at Huntsville, USA. The thick line is the simple running 37-month average. Insert: Argo global ocean temperature anomaly from floats.

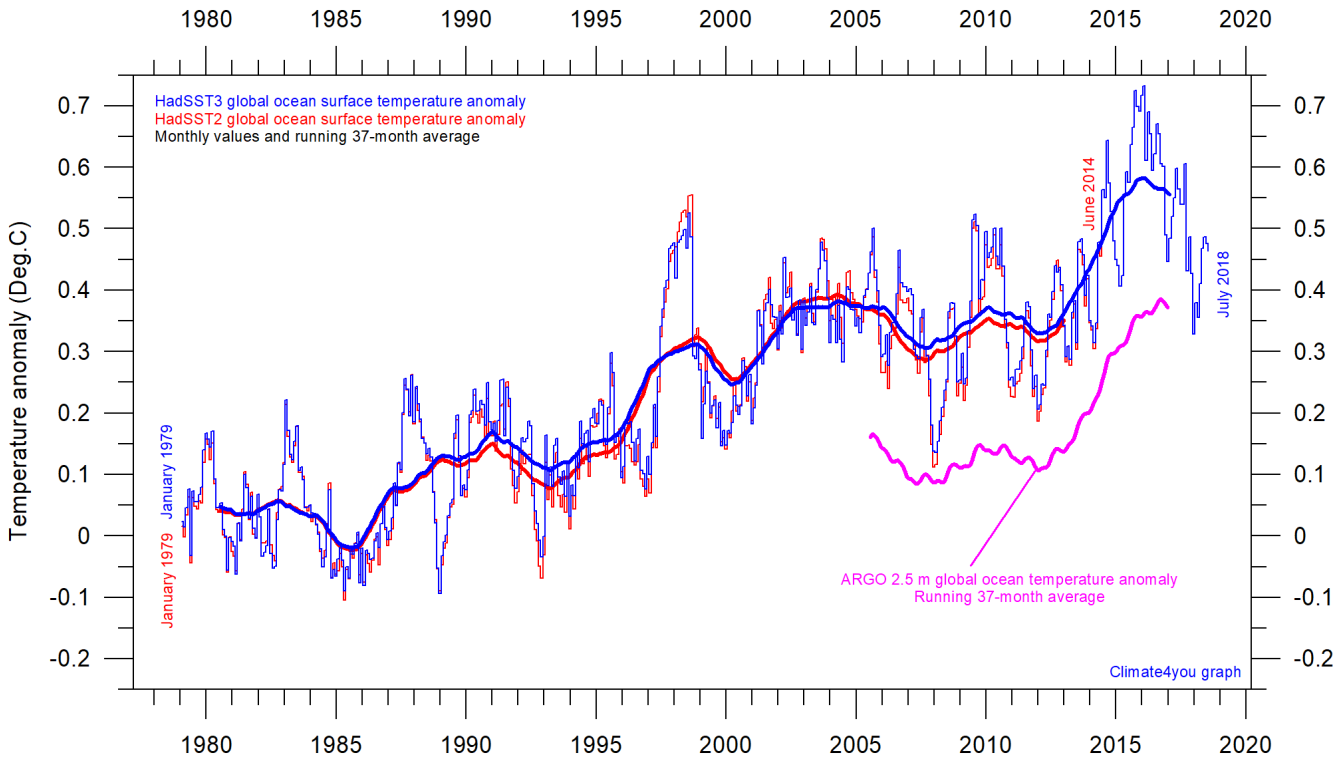

Global monthly average sea surface temperature since 1979 according to University of East Anglia's Climatic Research Unit (CRU), UK. Base period: 1961-1990. The thick line is the simple running 37-month average. Insert: Argo global ocean temperature anomaly from floats.

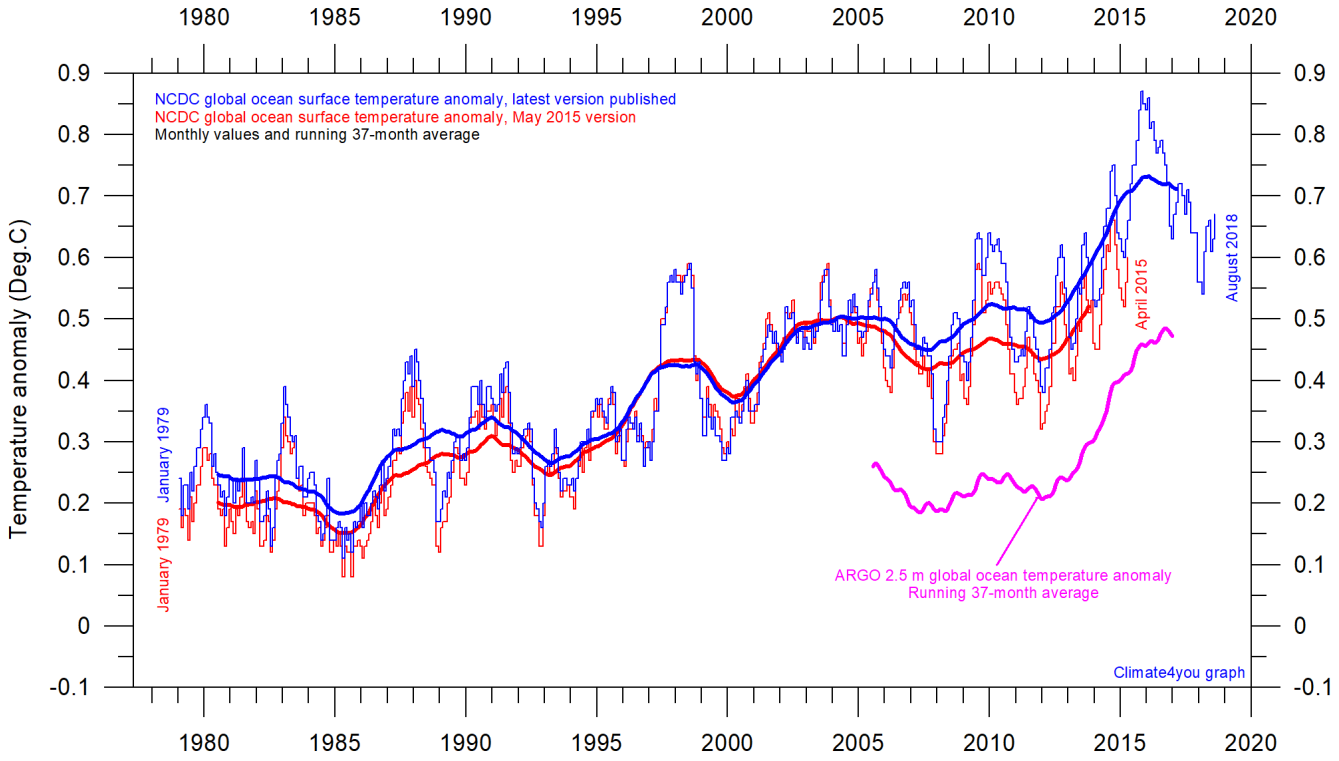

Global monthly average sea surface temperature since 1979 according to the National Climatic Data Center (NCDC), USA. Base period: 1901-2000. The thick line is the simple running 37-month average. Insert: Argo global ocean temperature anomaly from floats.

15

June 18, 2015: *NCDC has introduced several rather large administrative changes to their sea surface temperature record. The overall result is to produce a record giving the impression of a continuous temperature increase, also in the 21st century. As the oceans cover about 71% of the entire surface of planet Earth, the effect of this administrative change is clearly seen in the NCDC record for global surface air temperature (p. 6).*

Ocean temperature in uppermost 100 m, updated to June 2018

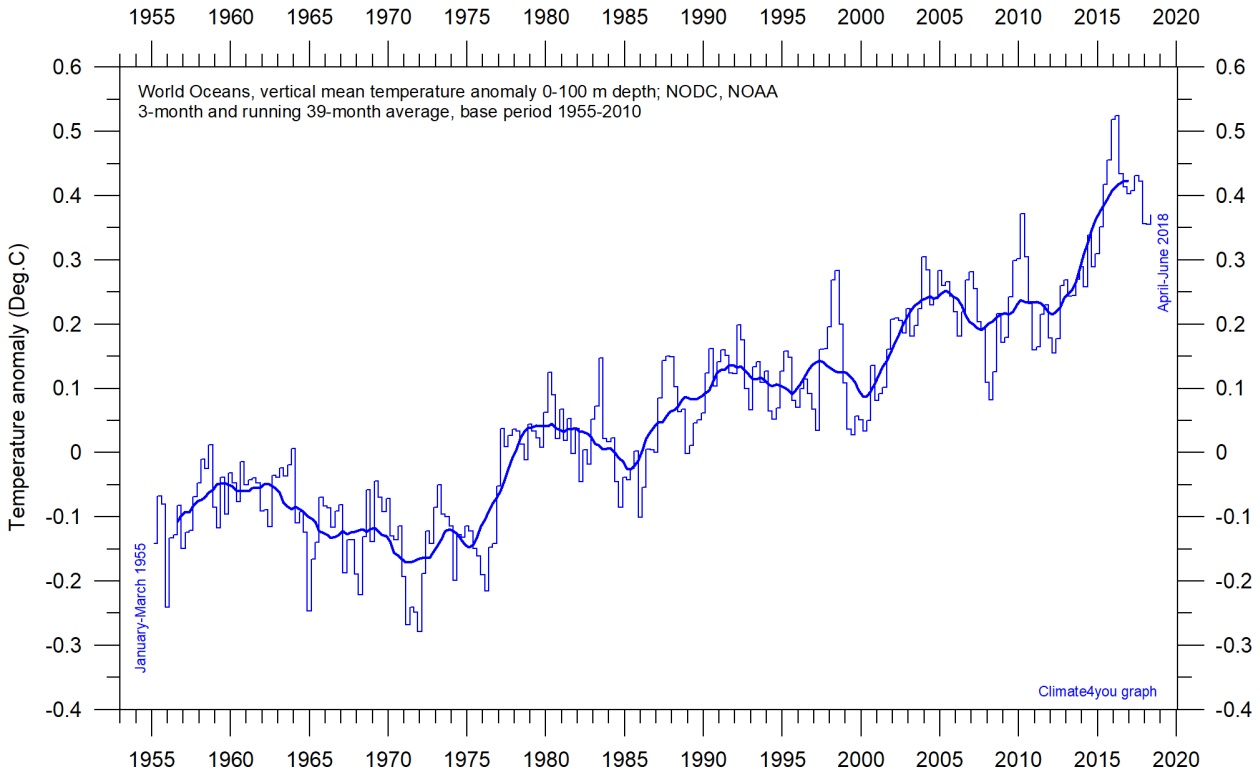

World Oceans vertical average temperature 0-100 m depth since 1955. The thin line indicates 3-month values, and the thick line represents the simple running 39-month (c. 3 year) average. Data source: NOAA National Oceanographic Data Center (NODC). Base period 1955-2010.

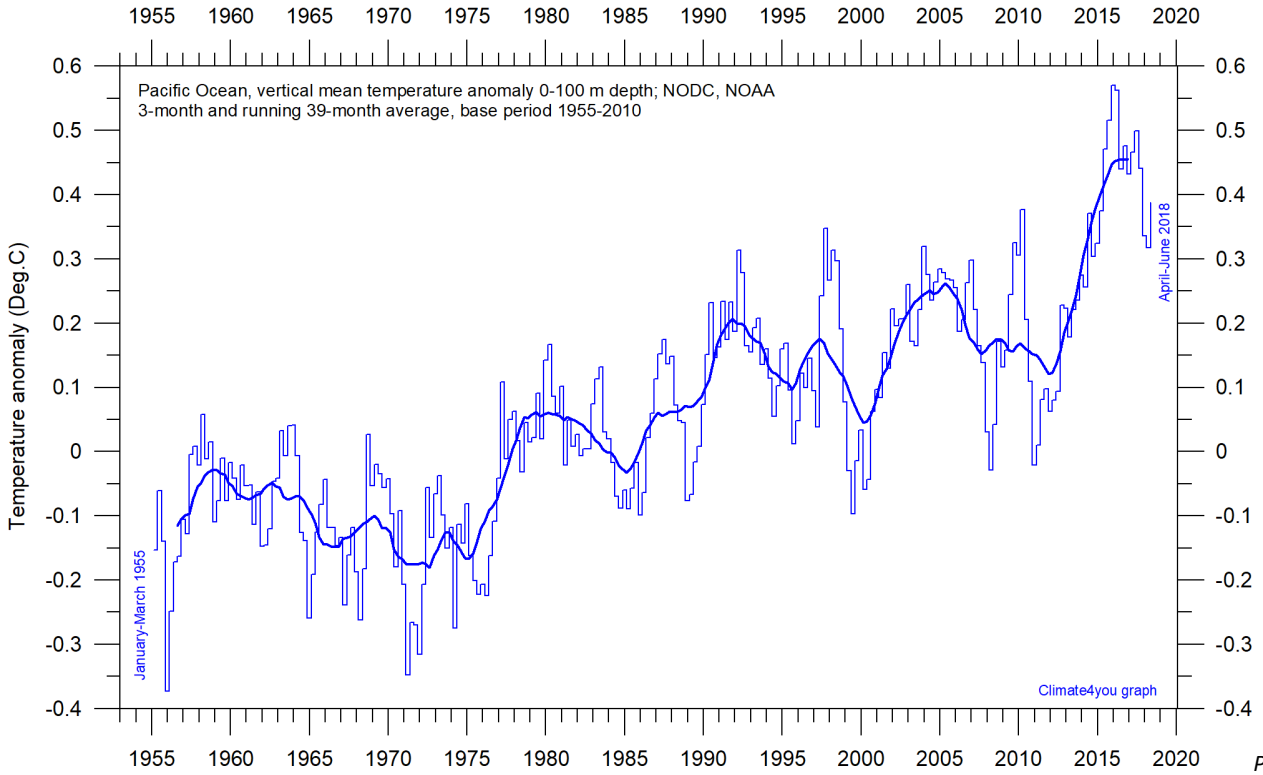

Pacific Ocean vertical average temperature 0-100 m depth since 1955. The thin line indicate 3-month values, and the thick line represents the simple running 39-month (c. 3 year) average. Data source: NOAA National Oceanographic Data Center (NODC). Base period 1955-2010.

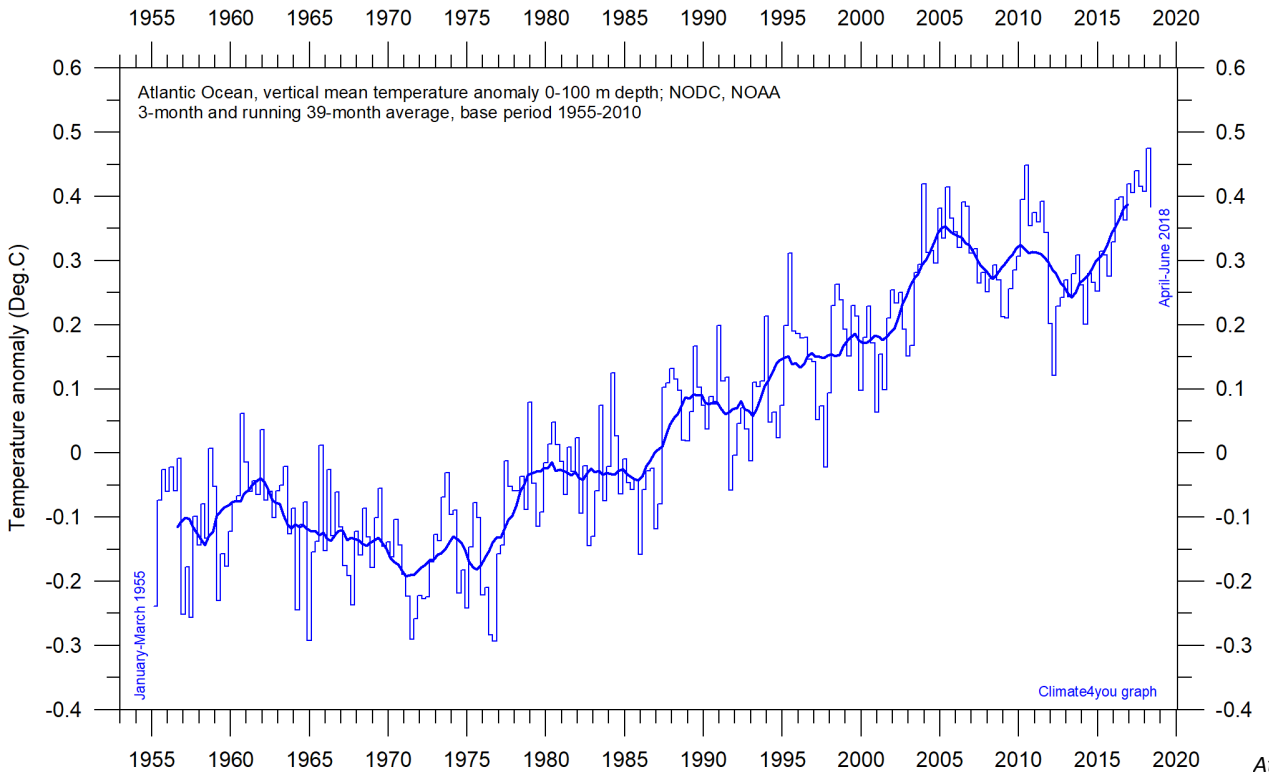

Ocean vertical average temperature 0-100 m depth since 1955. The thin line indicate 3-month values, and the thick line represents the simple running 39-month (c. 3 year) average. Data source: NOAA National Oceanographic Data Center (NODC). Base period 1955-2010.

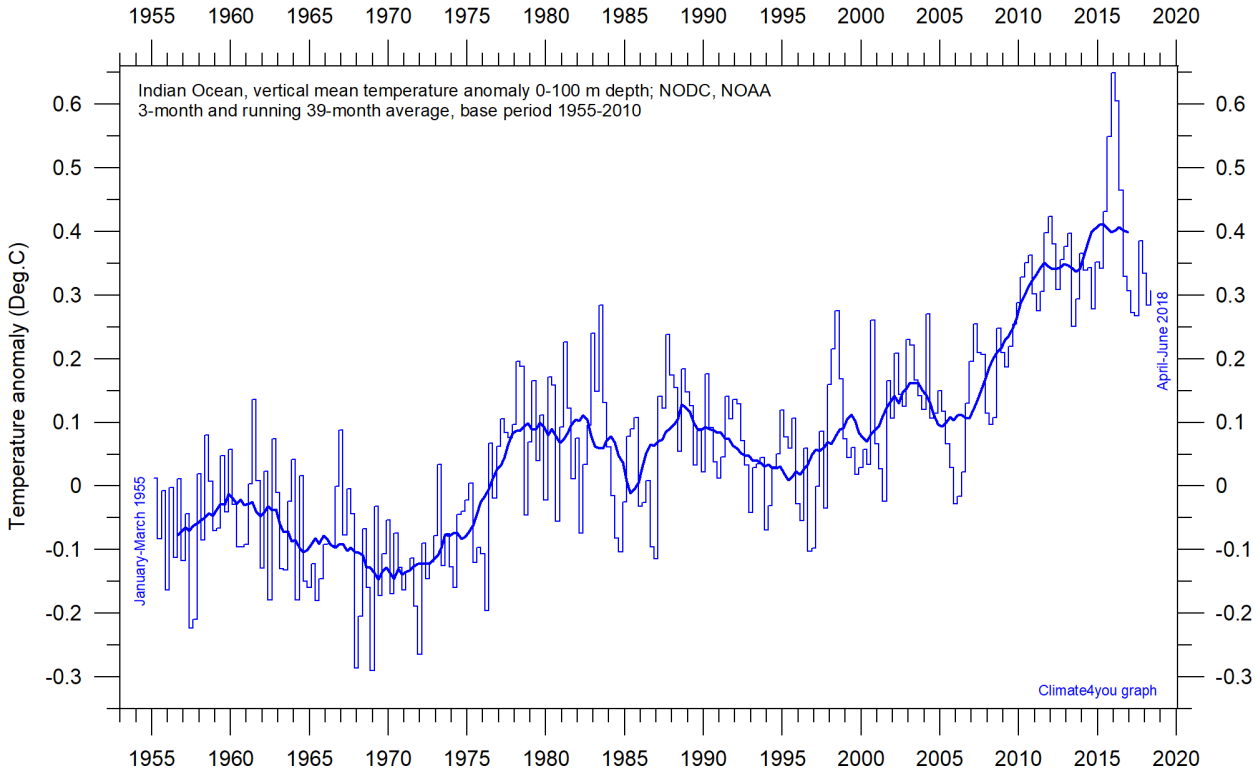

Indian Ocean vertical average temperature 0-100 m depth since 1955. The thin line indicate 3-month values, and the thick line represents the simple running 39-month (c. 3 year) average. Data source: NOAA National Oceanographic Data Center (NODC). Base period 1955-2010.

North Atlantic heat content uppermost 700 m, updated to December 2017

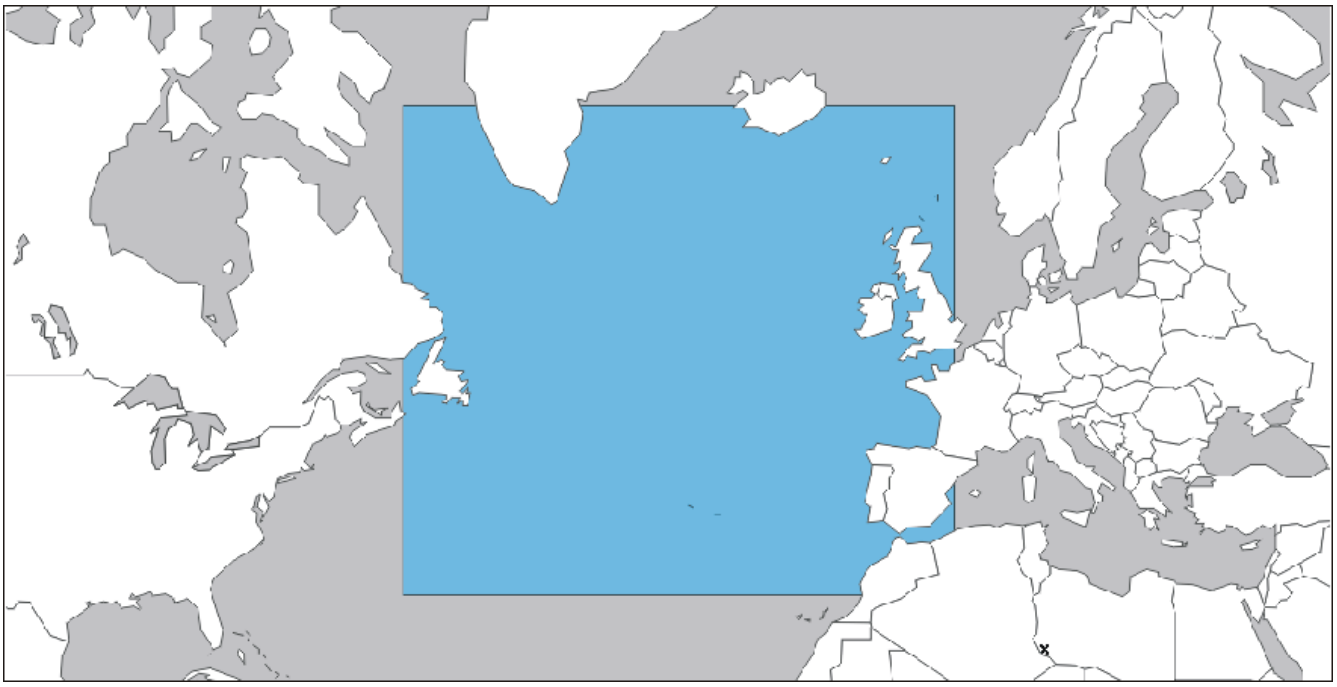

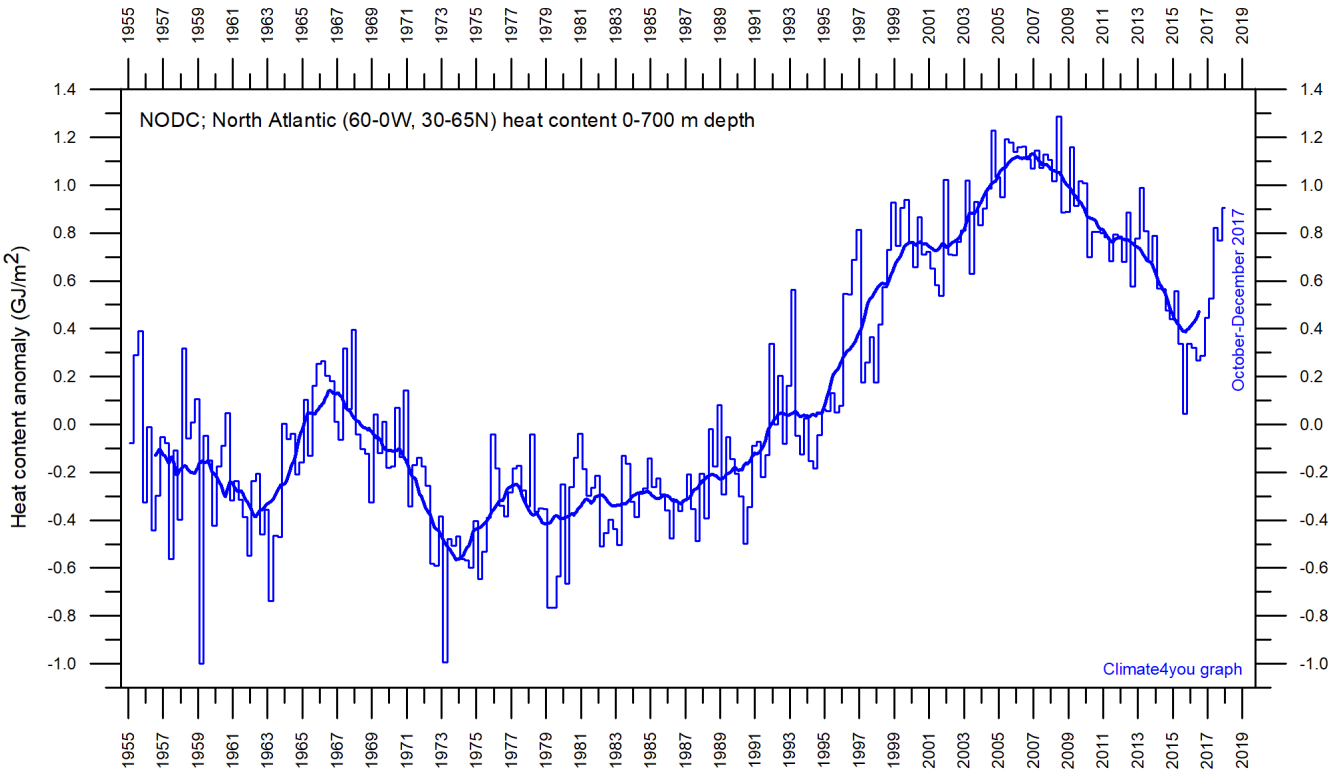

Global monthly heat content anomaly (GJ/m2) in the uppermost 700 m of the North Atlantic (60-0W, 30-65N; see map above) *ocean since January 1955. The thin line indicates monthly values, and the thick line represents the simple running 37-month (c. 3 year) average. Data source: National Oceanographic Data Center (NODC).*

North Atlantic temperatures 0-800 m depth along 59°N, 30-0W, updated to June 2018

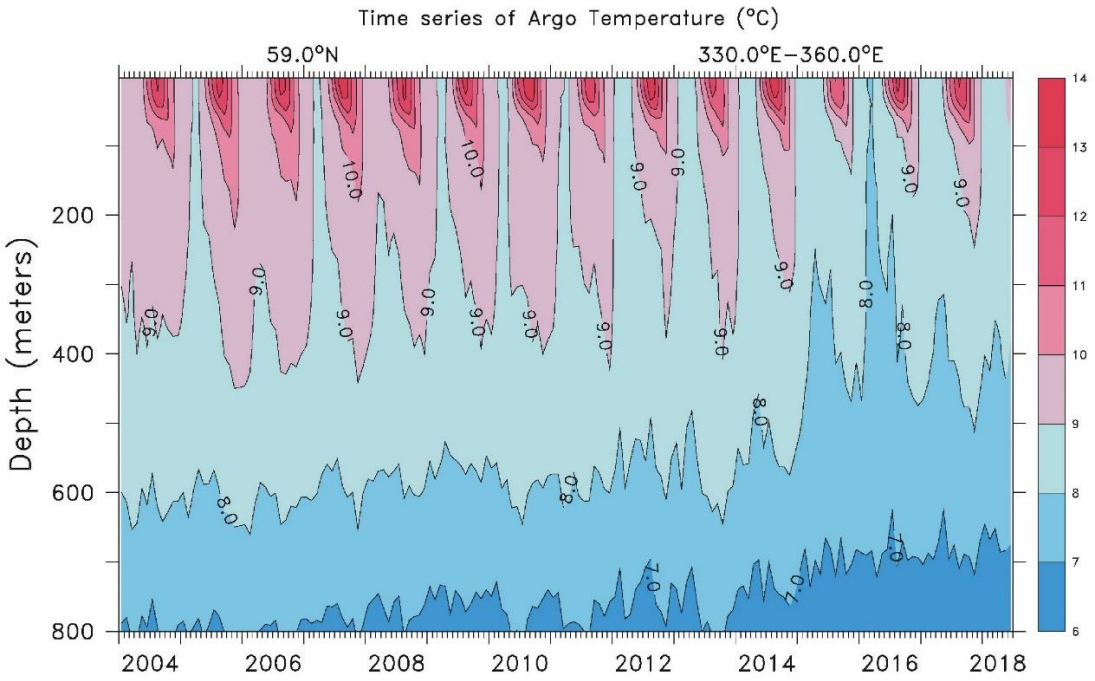

Time series depth-temperature diagram along 59 N across the North Atlantic Current from 30°W to 0°W, from surface to 800 m depth. Source: Global Marine Argo Atlas. See also the diagram below.

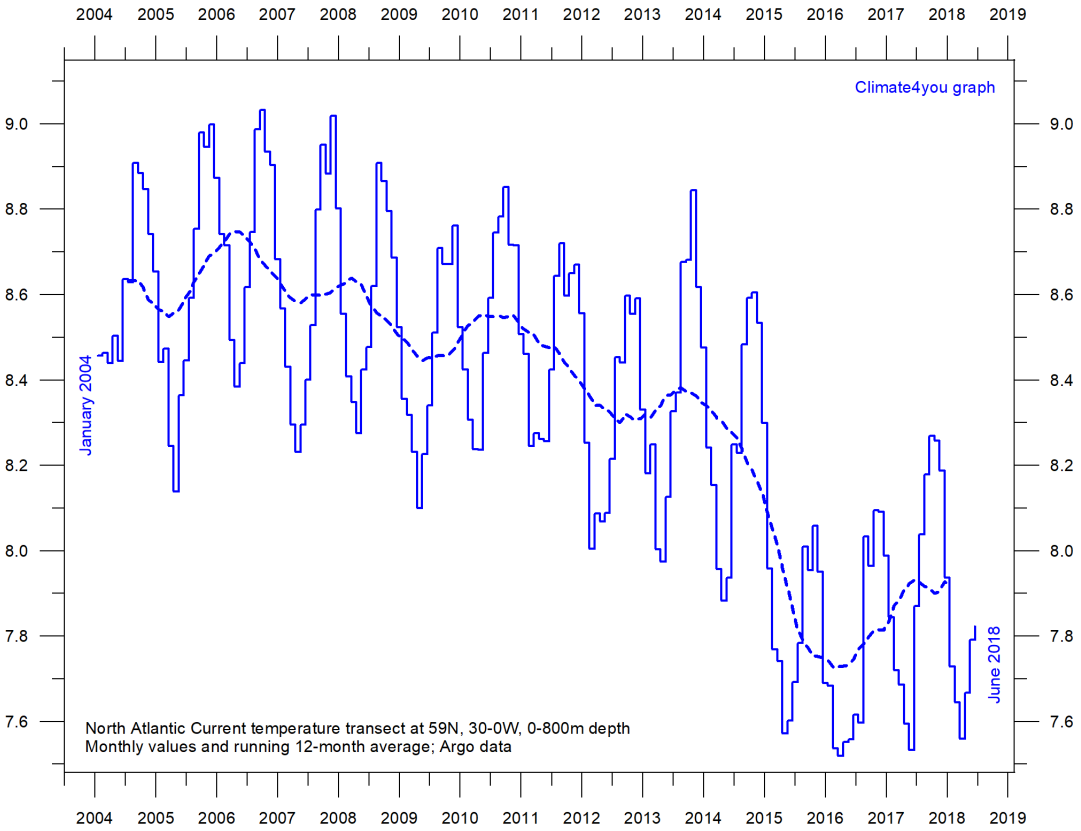

Average temperature along 59 N, 30-0W, 0-800m depth, corresponding to the main part of the North Atlantic Current, using Argo-data. Source: Global Marine Argo Atlas. Additional information can be found in: Roemmich, D. and J. Gilson, 2009. The 2004-2008 mean and annual cycle of temperature, salinity, and steric height in the global ocean from the Argo Program. Progress in Oceanography, 82, 81-100.

Global ocean temperature 0-1900 m depth summary, updated to June 2018

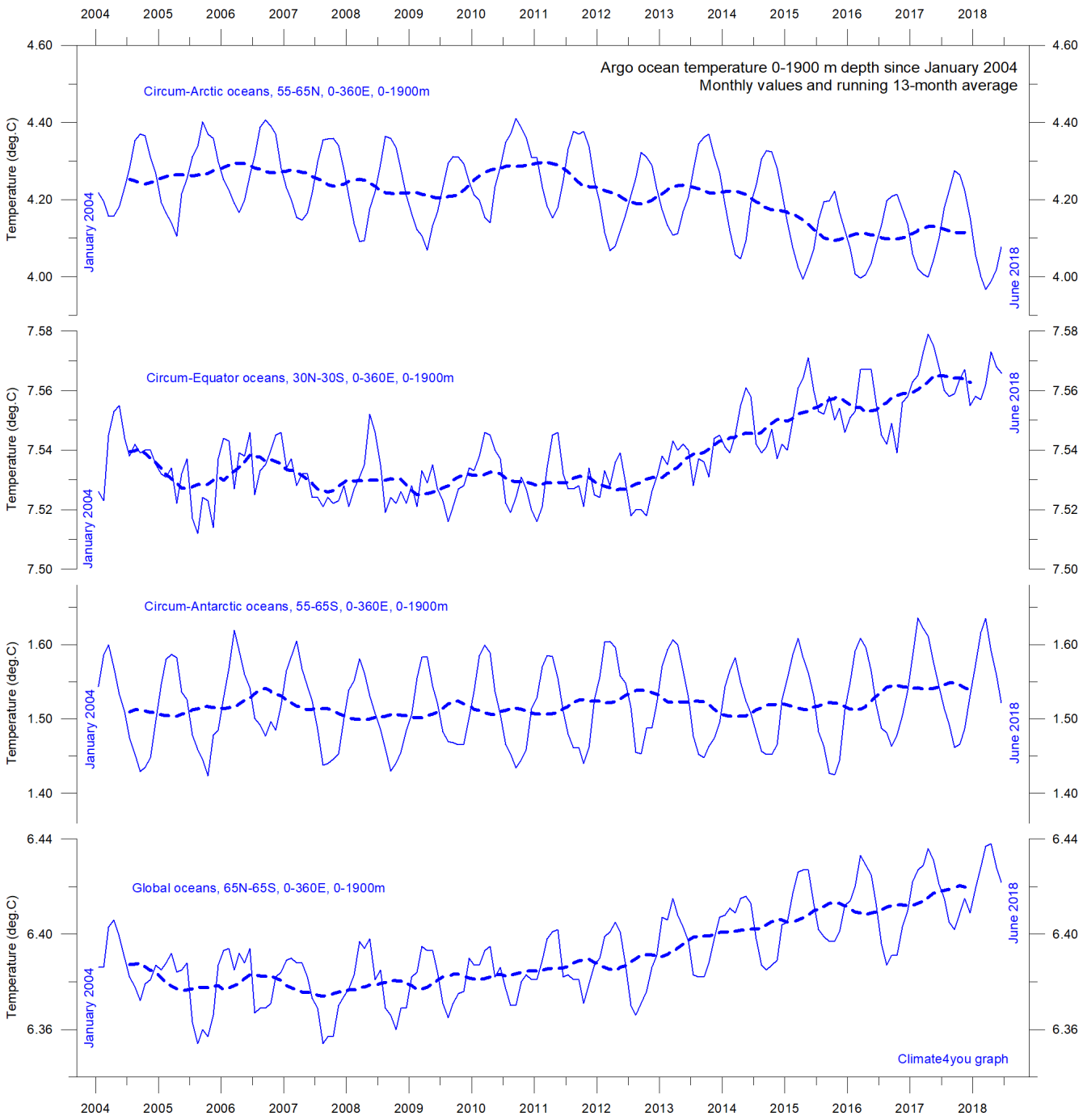

Summary of average temperature in uppermost 1900 m in different parts of the global oceans, using Argo-data. Source: Global Marine Argo Atlas. Additional information can be found in: Roemmich, D. and J. Gilson, 2009. The 2004-2008 mean and annual cycle of temperature, salinity, and steric height in the global ocean from the Argo Program. Progress in Oceanography, 82, 81-100.

Global ocean net temperature change since 2004 at different depths, updated to June 2018

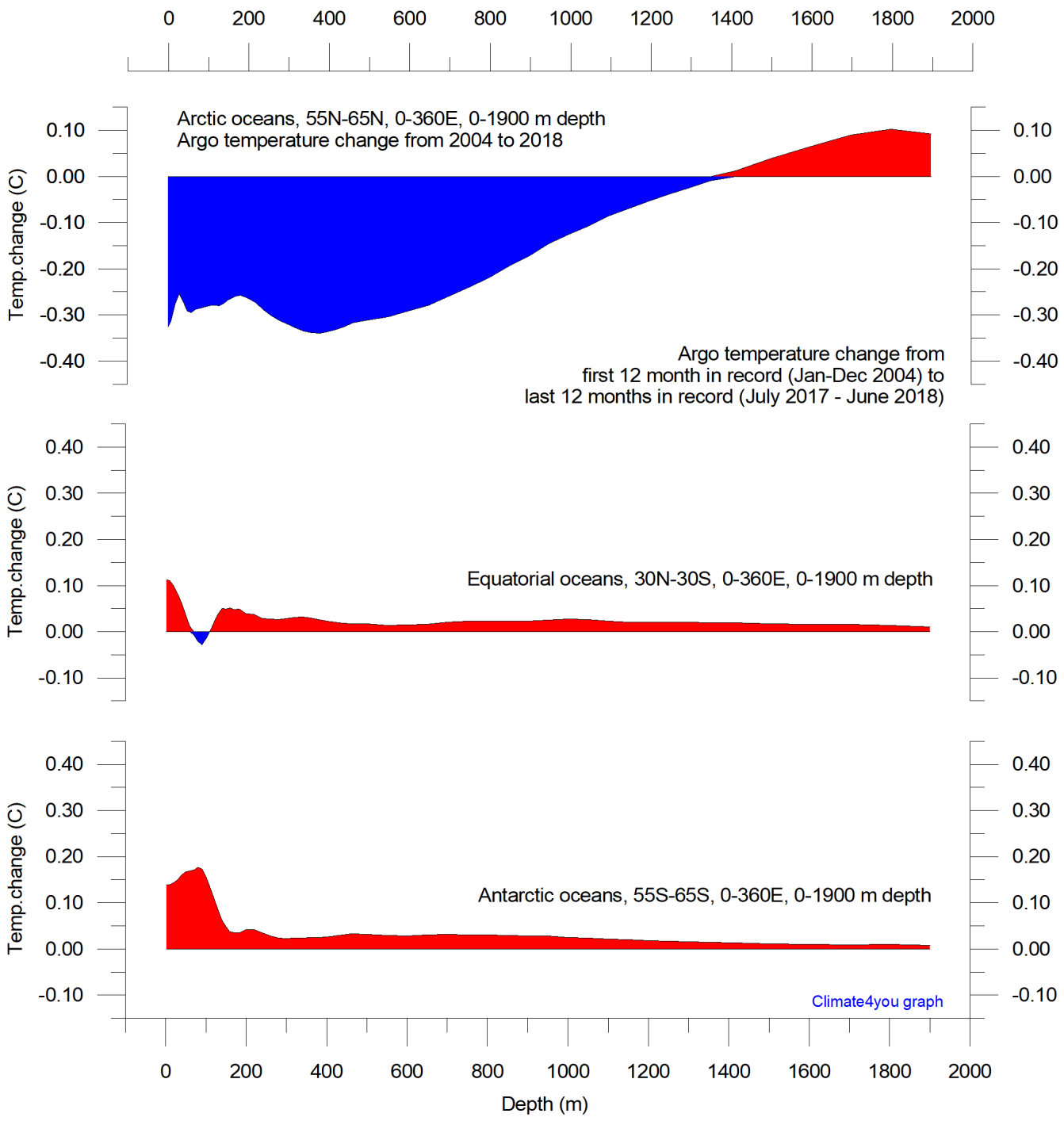

Net temperature change since 2004 from surface to 1900 m depth in different parts of the global oceans, using Argo-data. Source: Global Marine Argo Atlas. Additional information can be found in: Roemmich, D. and J. Gilson, 2009. The 2004-2008 mean and annual cycle of temperature, salinity, and steric height in the global ocean from the Argo Program. Progress in Oceanography, 82, 81-100. Please note that due to the spherical form of Earth, northern and southern latitudes represent only small ocean volumes, compared to latitudes near the Equator.

La Niña and El Niño episodes, updated to August 2018

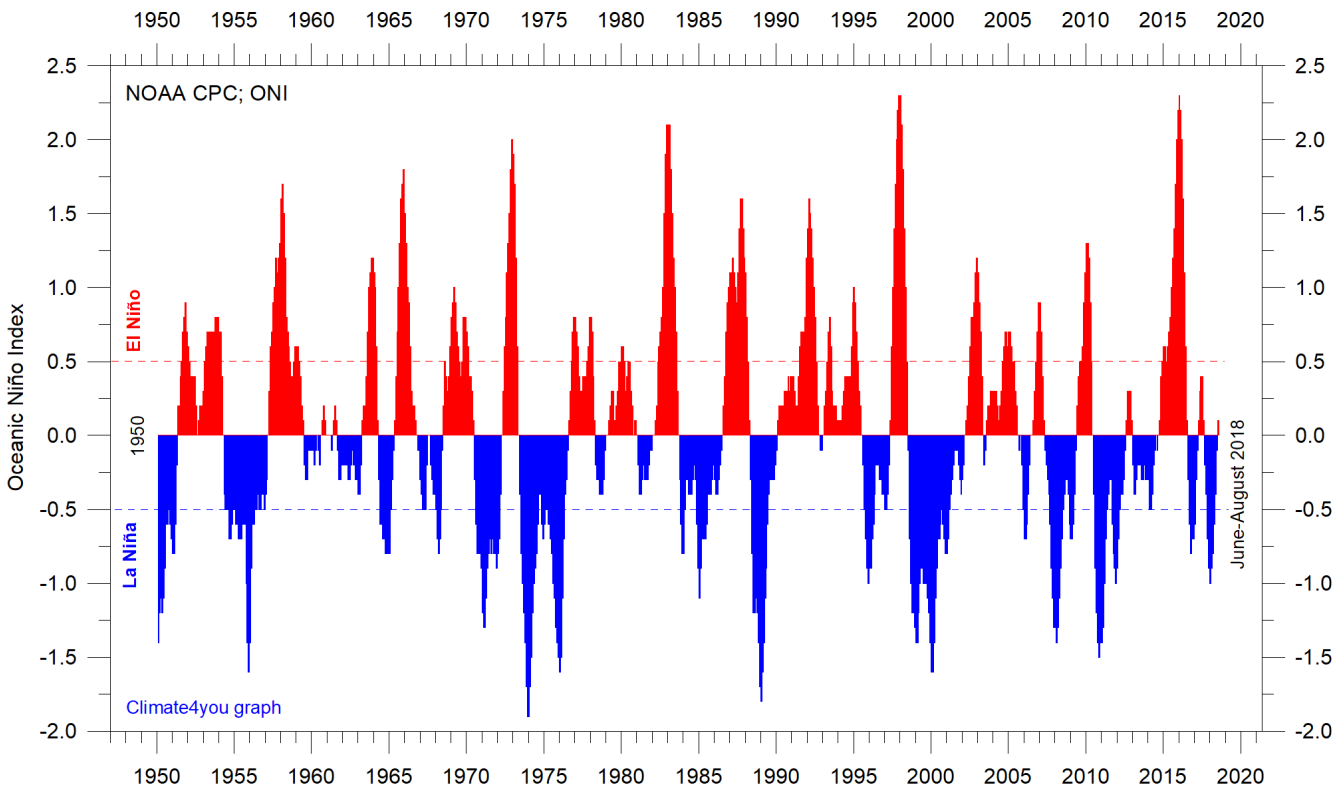

Warm (>+0.5°C) and cold (<0.5°C) episodes for the Oceanic Niño Index (ONI), defined as 3 month running mean of ERSSTv4 SST anomalies in the Niño 3.4 region (5°N-5°S, 120°-170°W)]. For historical purposes cold and warm episodes are defined when the threshold is met for a minimum of 5 consecutive over-lapping seasons. Anomalies are centred on 30-yr base periods updated every 5 years.

Troposphere and stratosphere temperatures from satellites, updated to August 2018

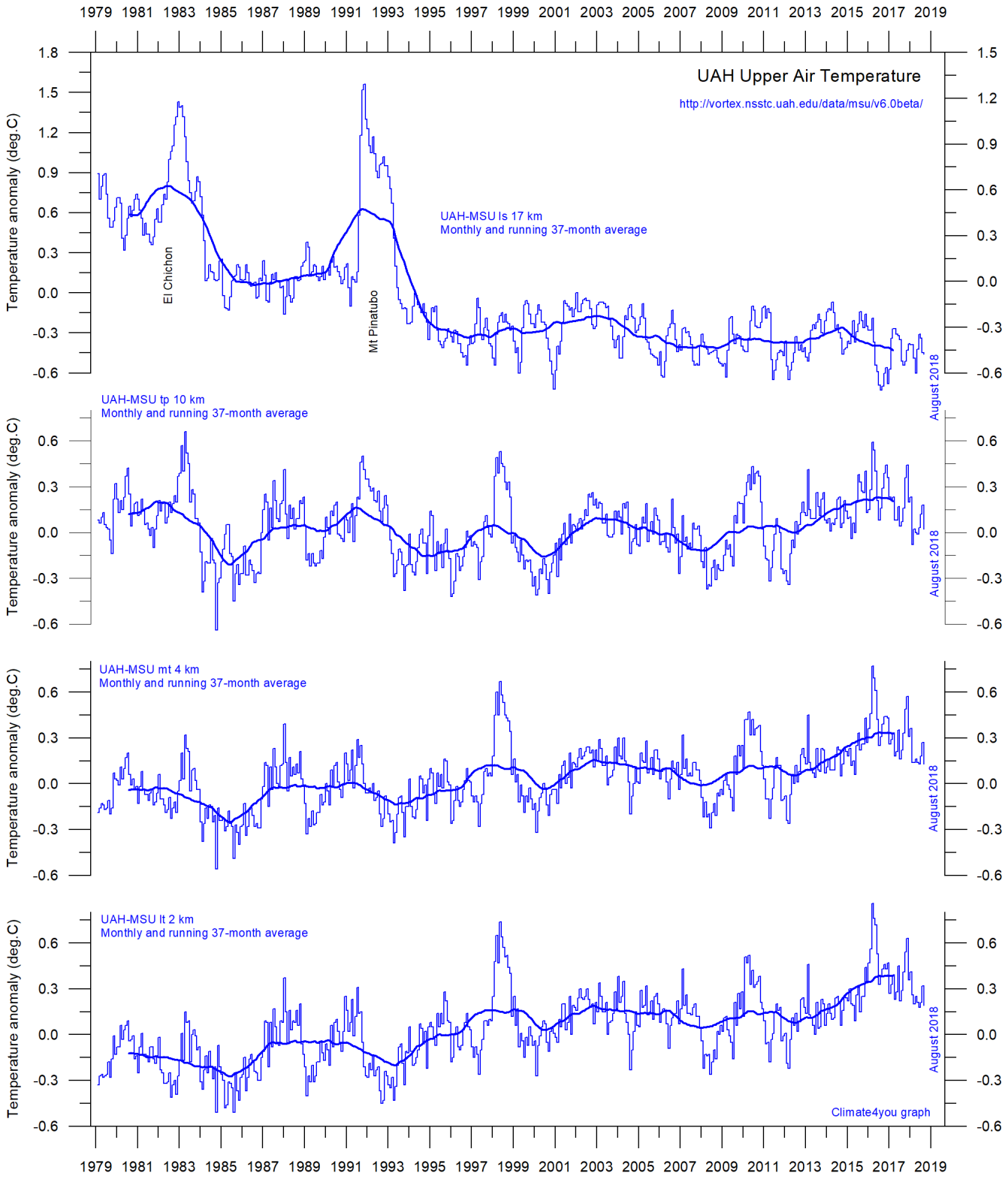

Global monthly average temperature in different according to University of Alabama at Huntsville, USA. The thin lines represent the monthly average, and the thick line the simple running 37-month average, nearly corresponding to a running 3-year average.

Zonal lower troposphere temperatures from satellites, updated to August 2018

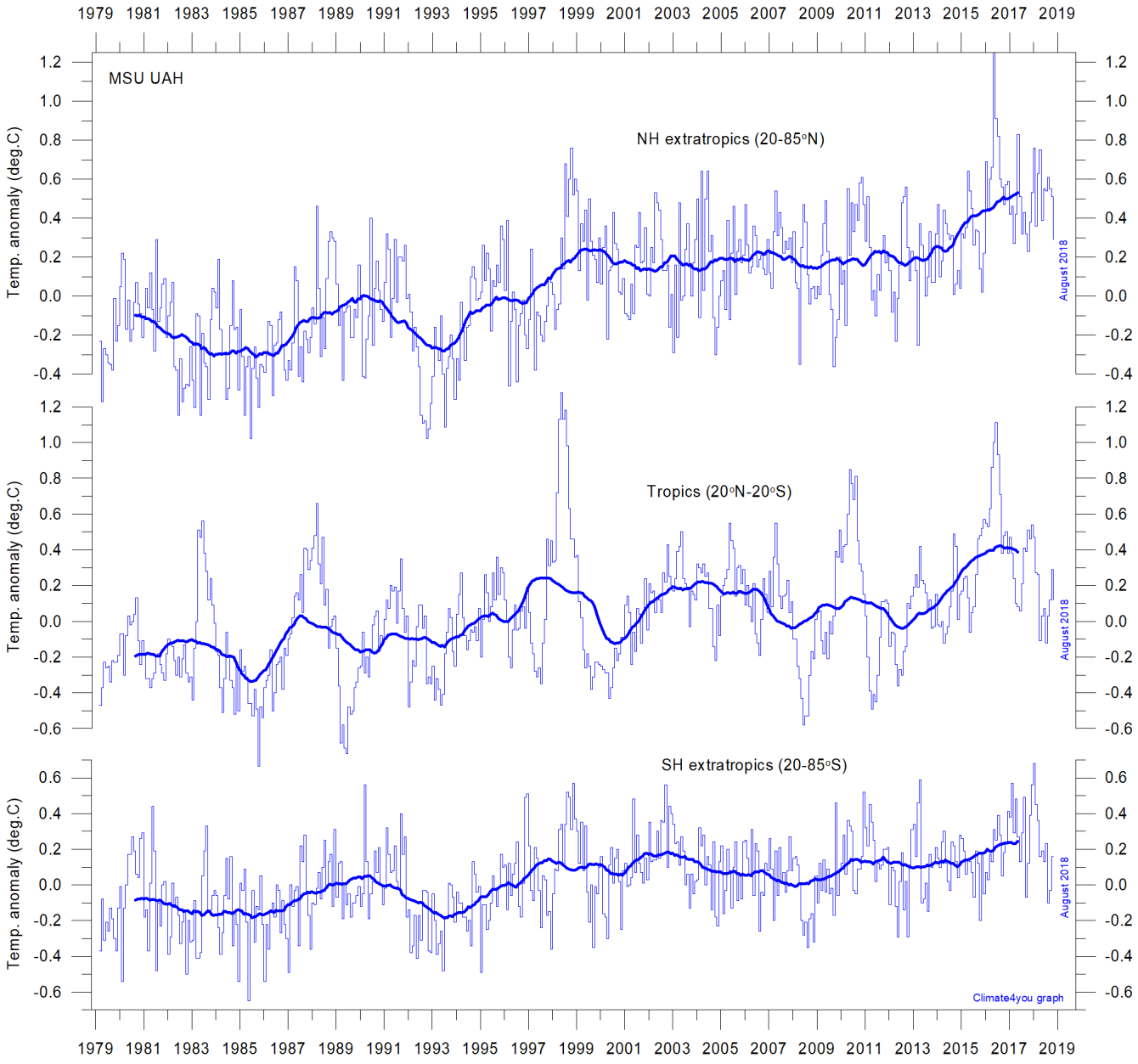

Global monthly average lower troposphere temperature since 1979 for the tropics and the northern and southern extratropics, according to University of Alabama at Huntsville, USA. Thin lines show the monthly temperature. Thick lines represent the simple running 37-month average, nearly corresponding to a running 3-year average. Reference period 1981-2010.

Arctic and Antarctic lower troposphere temperature, updated to August 2018

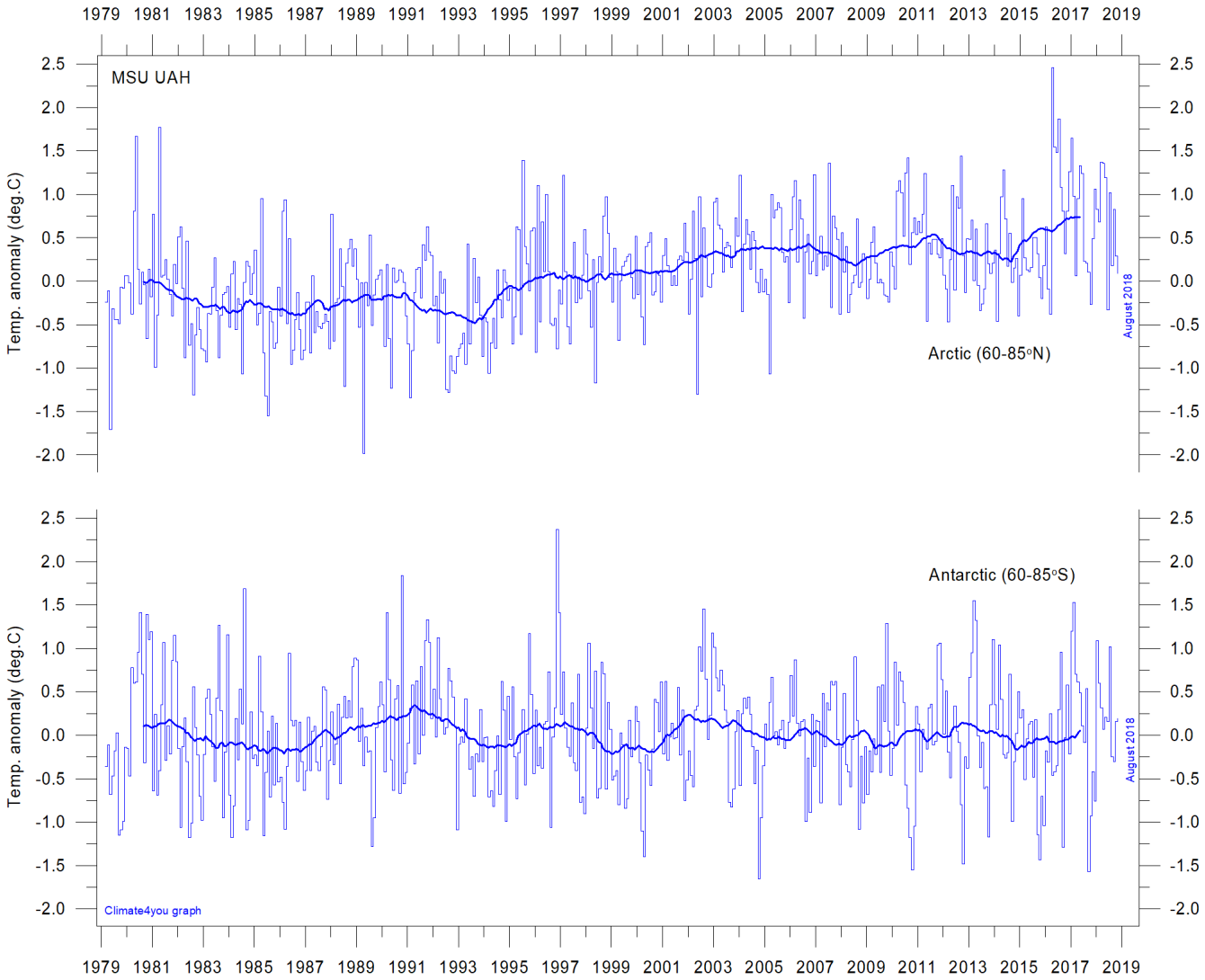

Global monthly average lower troposphere temperature since 1979 for the North Pole and South Pole regions, based on satellite observations (University of Alabama at Huntsville, USA). Thin lines show the monthly temperature. The thick line is the simple running 37-month average, nearly corresponding to a running 3-year average. Reference period 1981-2010.

Temperature over land versus over oceans, updated to August 2018

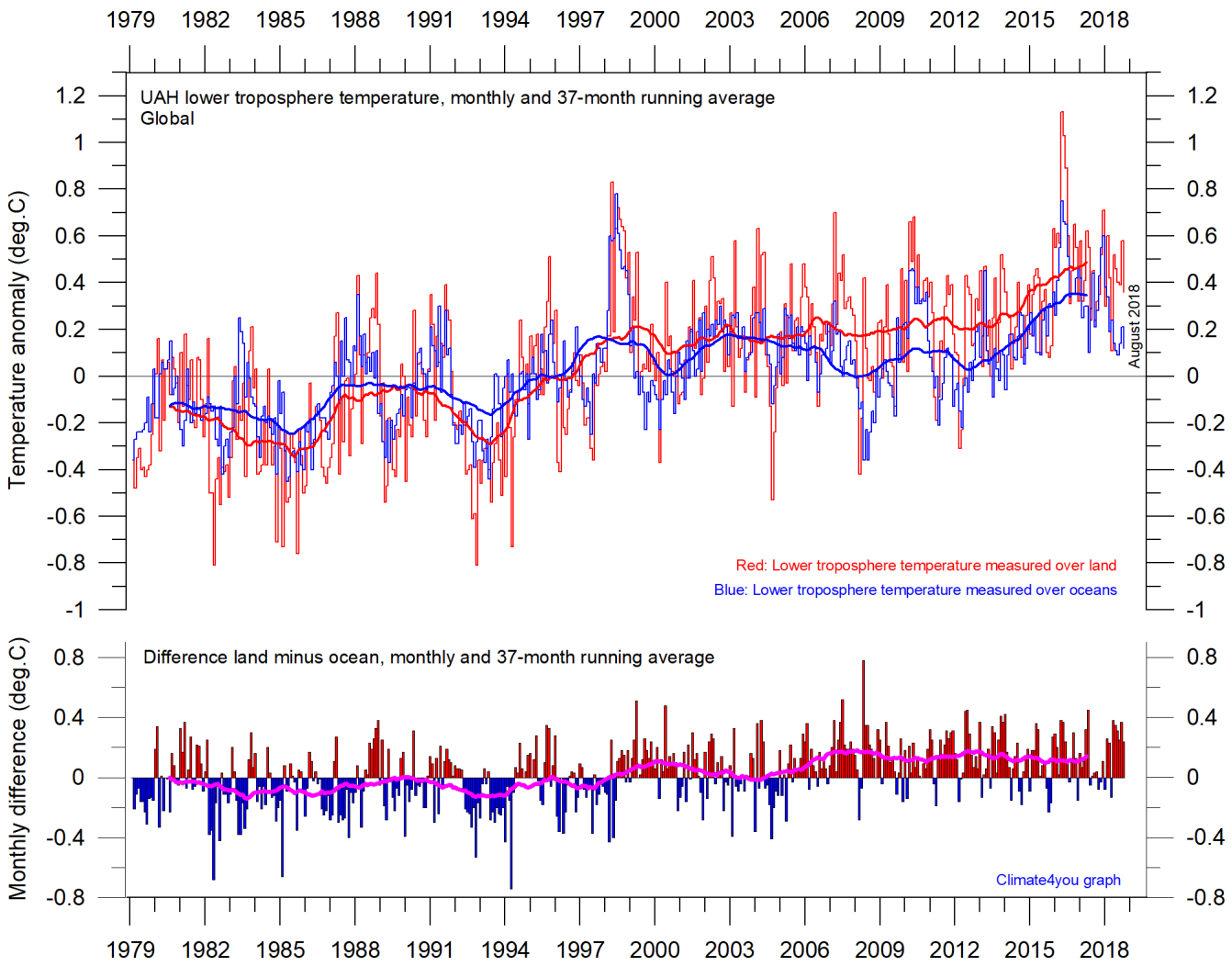

Global monthly average lower troposphere temperature since 1979 measured over land and oceans, respectively, according to University of Alabama at Huntsville, USA. Thick lines are the simple running 37-month average, nearly corresponding to a running 3-year average. Reference period 1981-2010.

Arctic and Antarctic surface air temperature, updated to July 2018

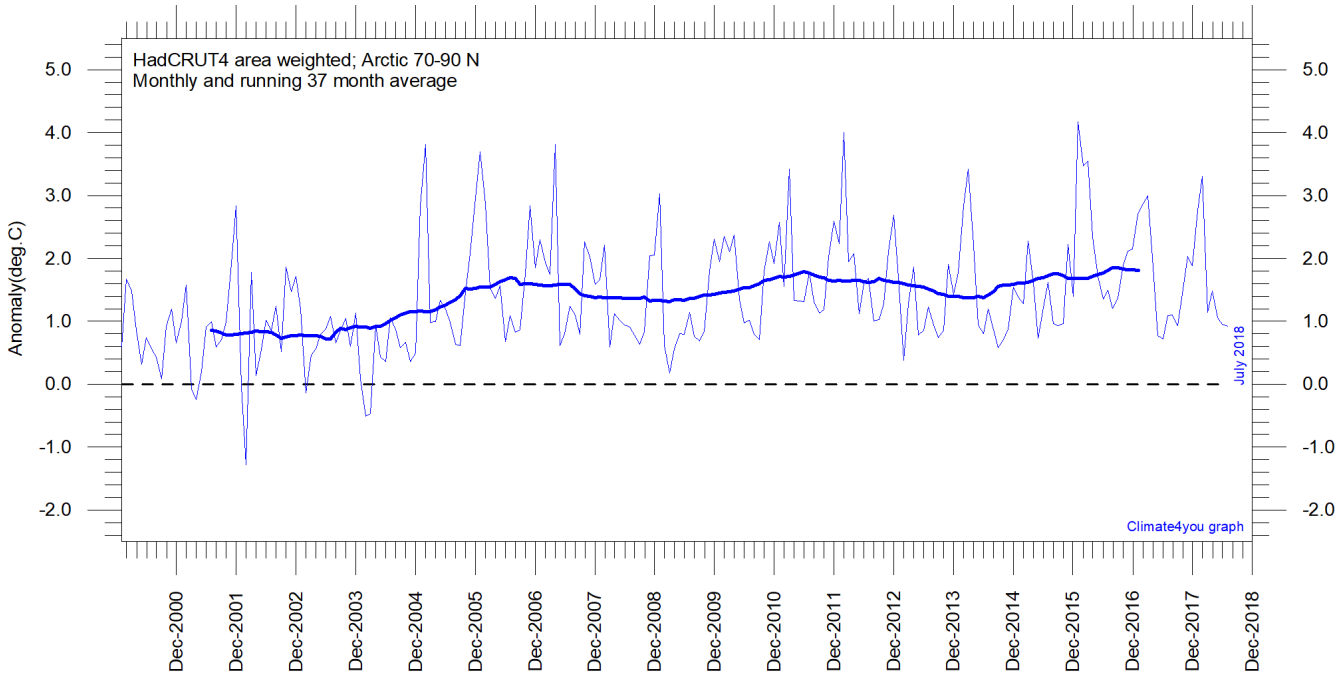

Diagram showing area weighted Arctic (70-90°N) monthly surface air temperature anomalies (HadCRUT4) since January 2000, in relation to the WMO normal period 1961-1990. The thin line shows the monthly temperature anomaly, while the thicker line shows the running 37-month (c. 3 year) average.

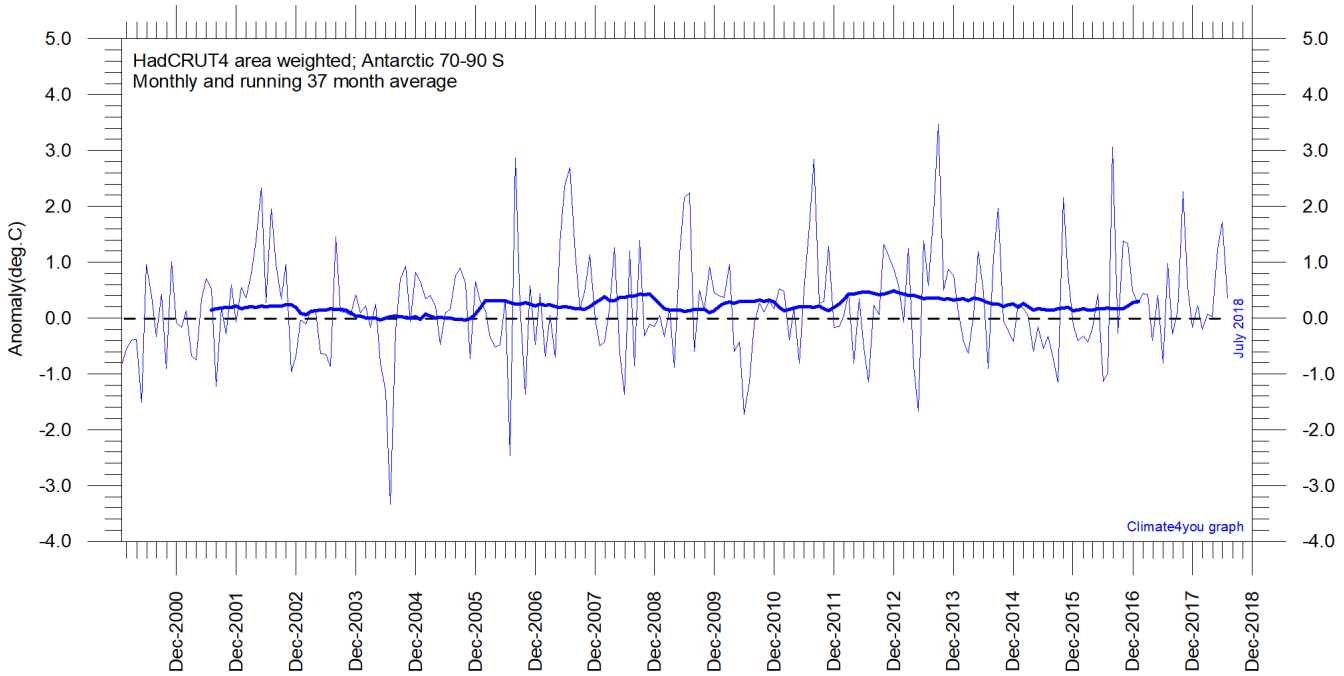

Diagram showing area weighted Antarctic (70-90°N) monthly surface air temperature anomalies (HadCRUT4) since January 2000, in relation to the WMO normal period 1961-1990. The thin line shows the monthly temperature anomaly, while the thicker line shows the running 37-month (c. 3 year) average.

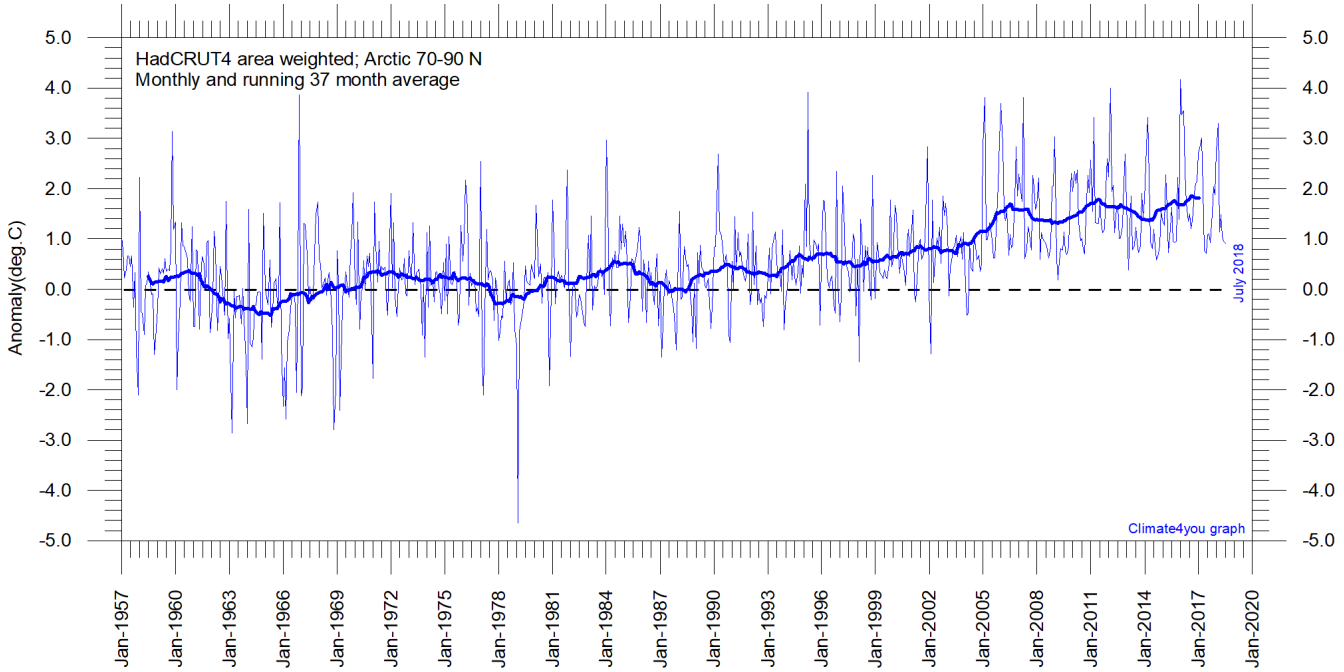

Diagram showing area weighted Arctic (70-90°N) monthly surface air temperature anomalies (HadCRUT4) since January 1957, in relation to the WMO normal period 1961-1990. The thin line shows the monthly temperature anomaly, while the thicker line shows the running 37-month (c. 3 year) average.

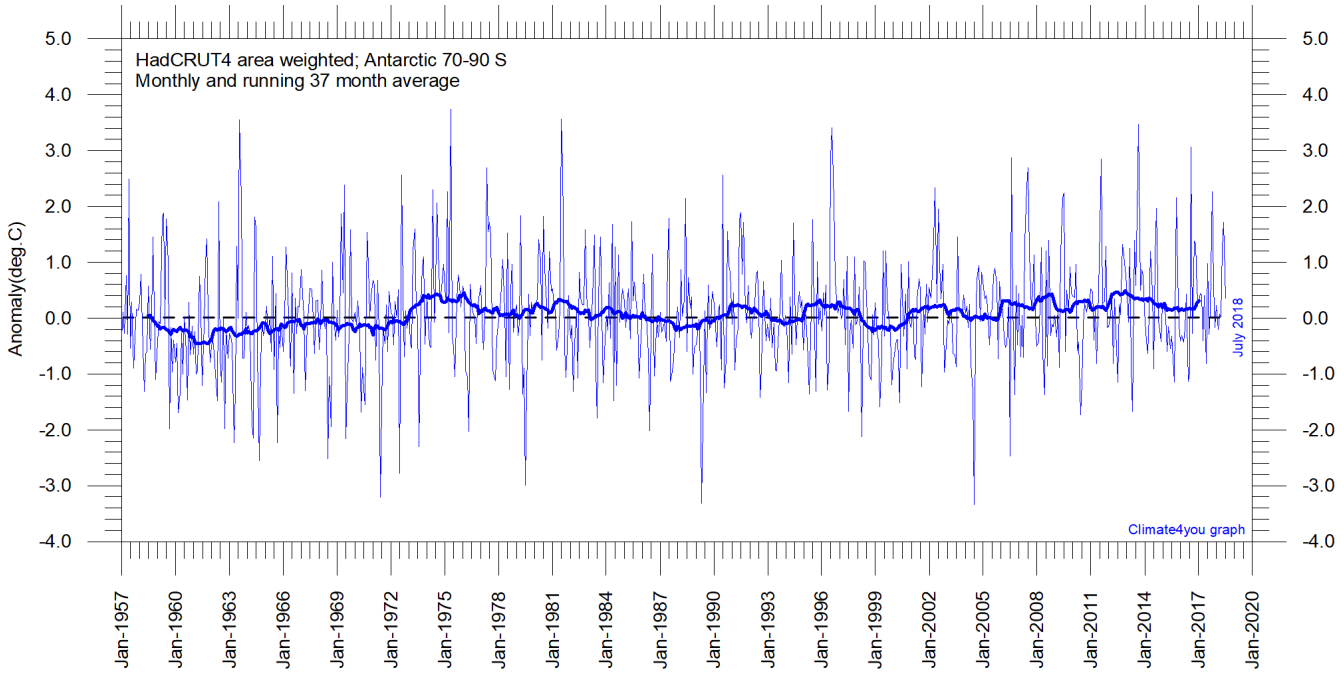

Diagram showing area weighted Antarctic (70-90°N) monthly surface air temperature anomalies (HadCRUT4) since January 1957, in relation to the WMO normal period 1961-1990. The thin line shows the monthly temperature anomaly, while the thicker line shows the running 37-month (c. 3 year) average.

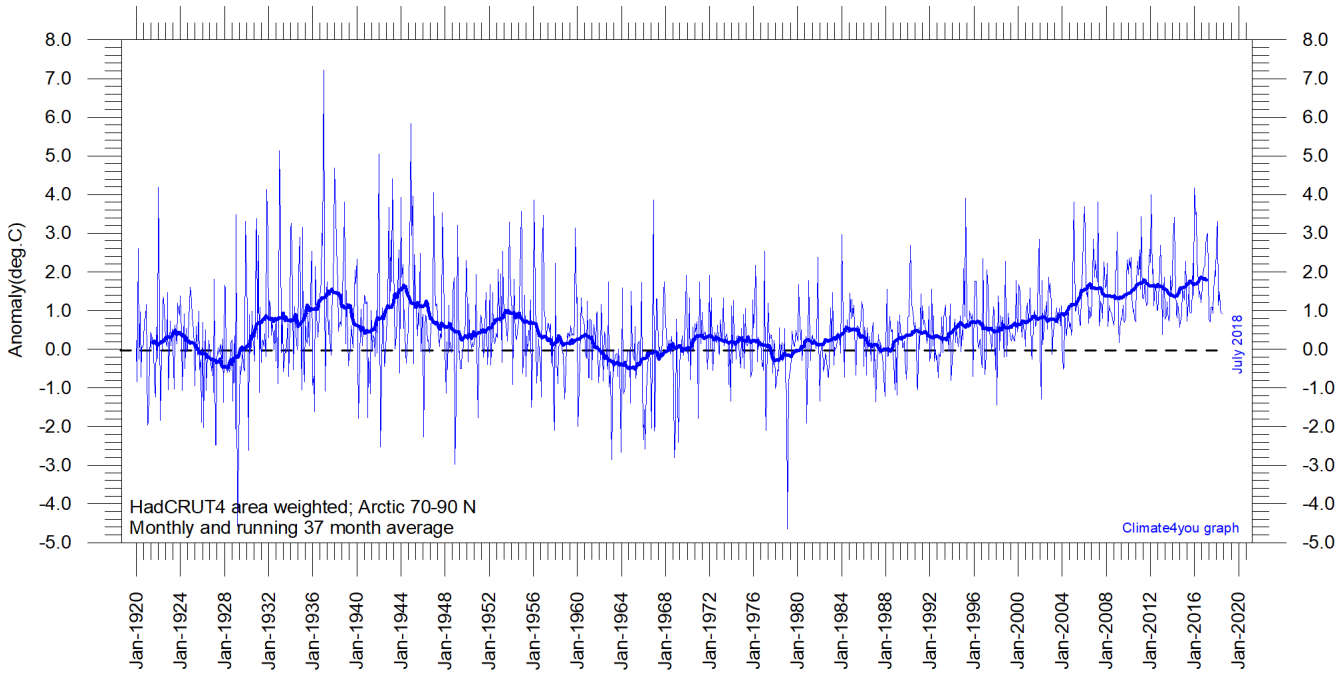

Diagram showing area-weighted Arctic (70-90°N) monthly surface air temperature anomalies (HadCRUT4) since January 1920, in relation to the WMO normal period 1961-1990. The thin line shows the monthly temperature anomaly, while the thicker line shows the running 37-month (c. 3 year) average.

Because of the relatively small number of Arctic stations before 1930, month-to-month variations in the early part of the Arctic temperature record 1920-2018 are larger than later (diagram above).

The period from about 1930 saw the establishment of many new Arctic meteorological stations, first in Russia and Siberia, and following the 2nd World War, also in North America. The period since 2005 is warm, about as warm as the period 1930-1940.

As the HadCRUT4 data series has improved high latitude coverage data coverage (compared to the HadCRUT3 series), the individual 5°x5° grid cells has been weighted according to their surface area. This contrasts with Gillet et al. 2008 which calculated a simple average, with no consideration of the effect of latitude on the surface area represented by the individual 5°x5° grid cells.

Literature:

Gillett, N.P., Stone, D.A., Stott, P.A., Nozawa, T., Karpechko, A.Y.U., Hegerl, G.C., Wehner, M.F. and Jones, P.D. 2008. Attribution of polar warming to human influence. *Nature Geoscience* 1, 750-754.

Arctic and Antarctic sea ice, updated to August 2018

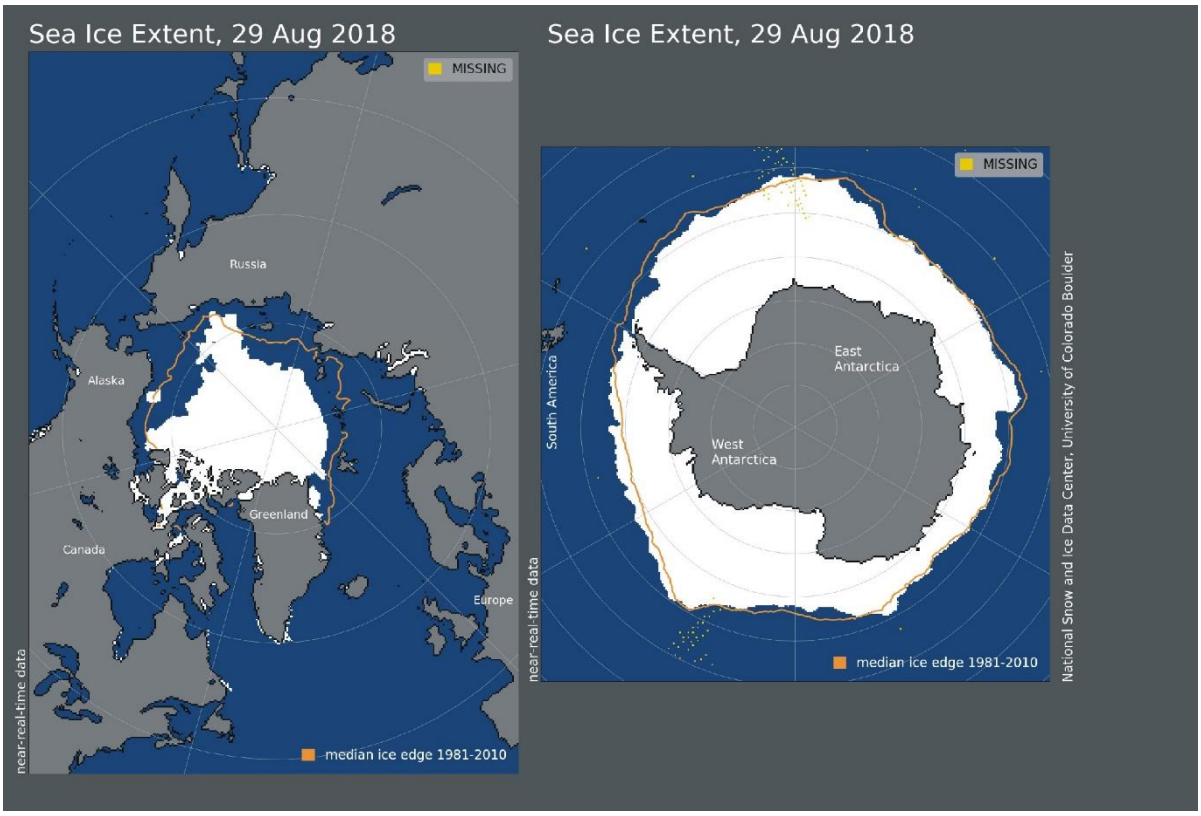

Sea ice extent 29 August 2018. The median limit of sea ice (orange line) is defined as 15% sea ice cover, according to the average of satellite observations 1981-2010 (both years included). Sea ice may therefore well be encountered outside and open water areas inside the limit shown in the diagrams above. Map source: National Snow and Ice Data Center (NSIDC).

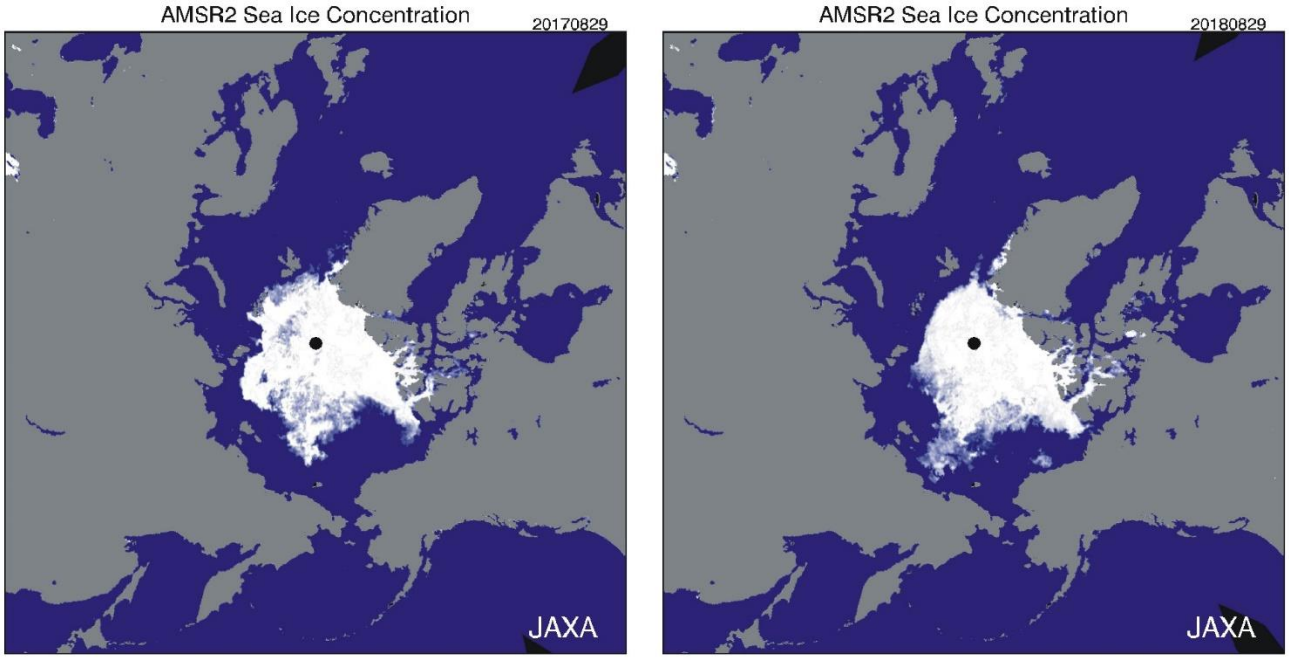

Diagrams showing Arctic sea ice extent and concentration 29 August 2017 (left) and 2018 (right), according to the Japan Aerospace Exploration Agency (JAXA).

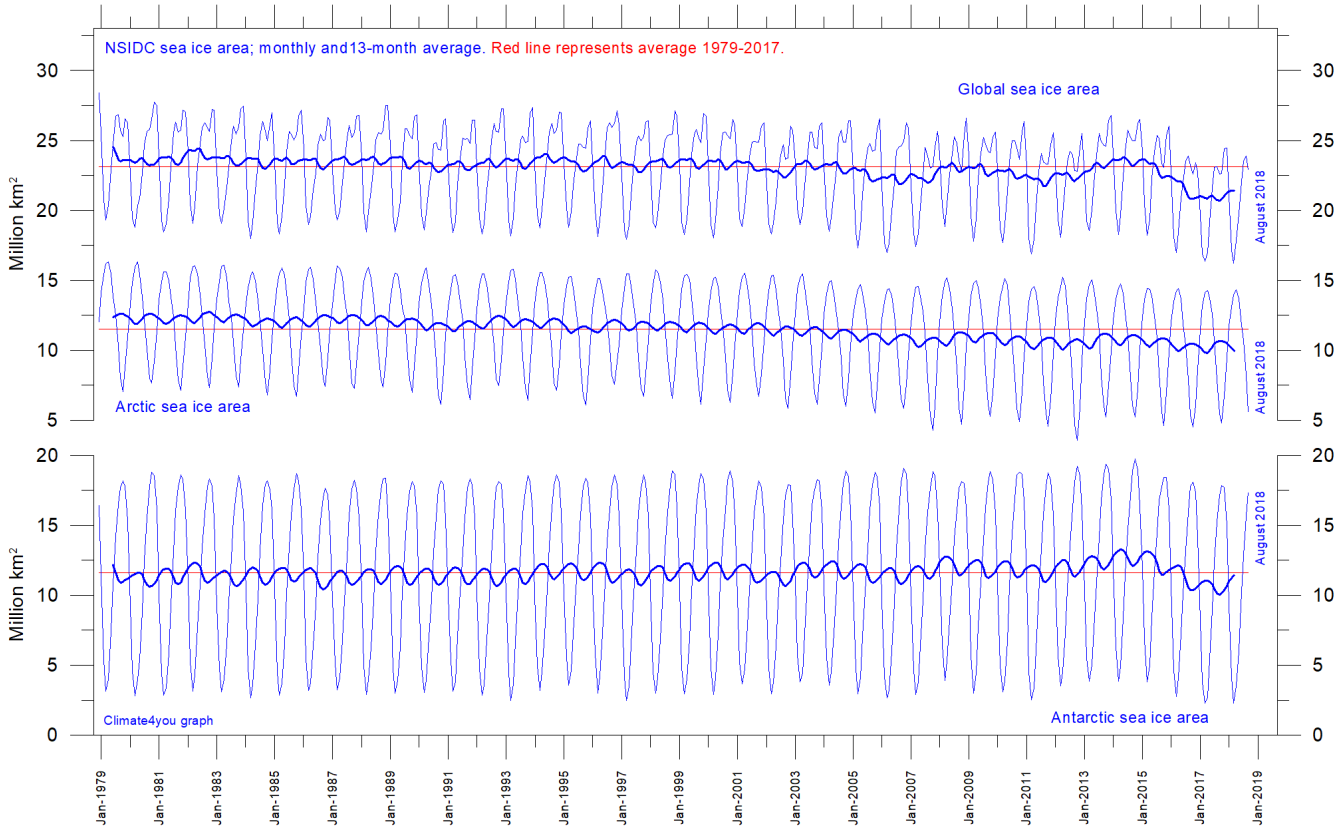

Graphs showing monthly Antarctic, Arctic and global sea ice extent since November 1978, according to the National Snow and Ice data Center (NSIDC).

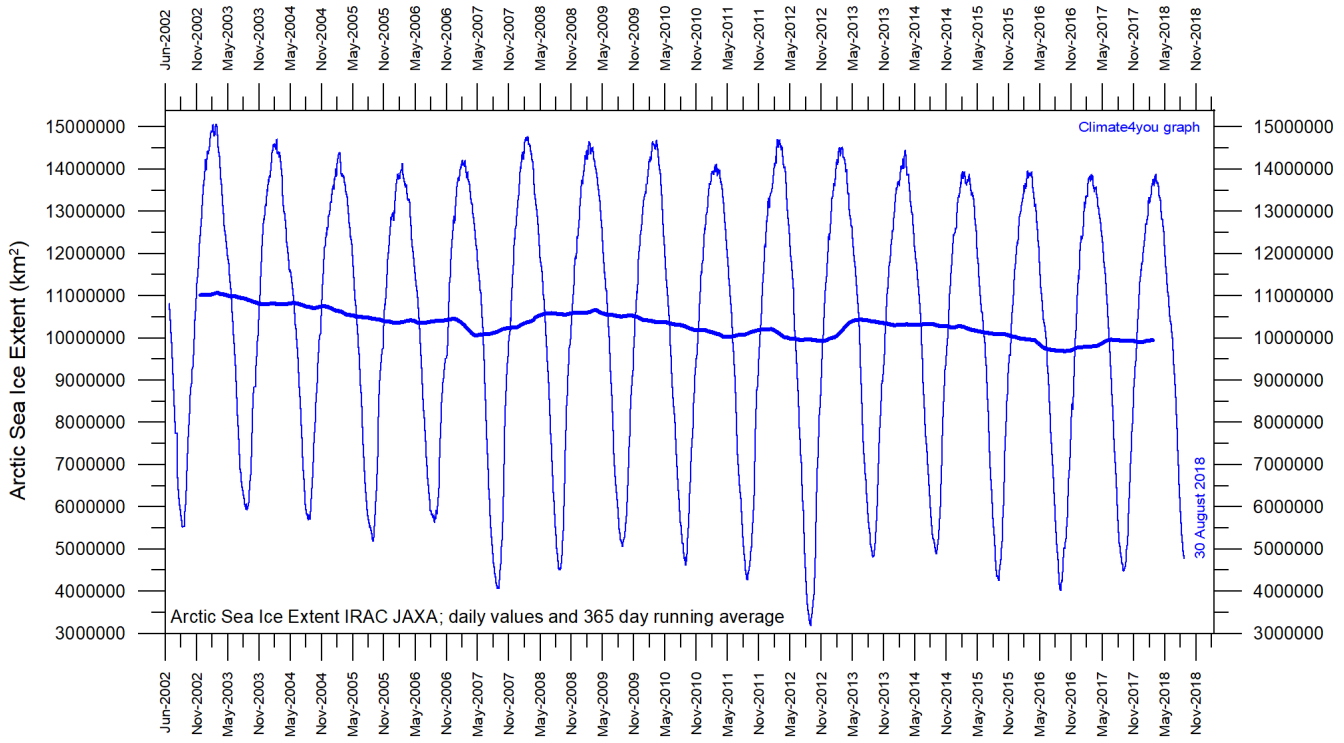

Diagram showing daily Arctic sea ice extent since June 2002, to 30 August 2018, by courtesy of Japan Aerospace Exploration Agency (JAXA).

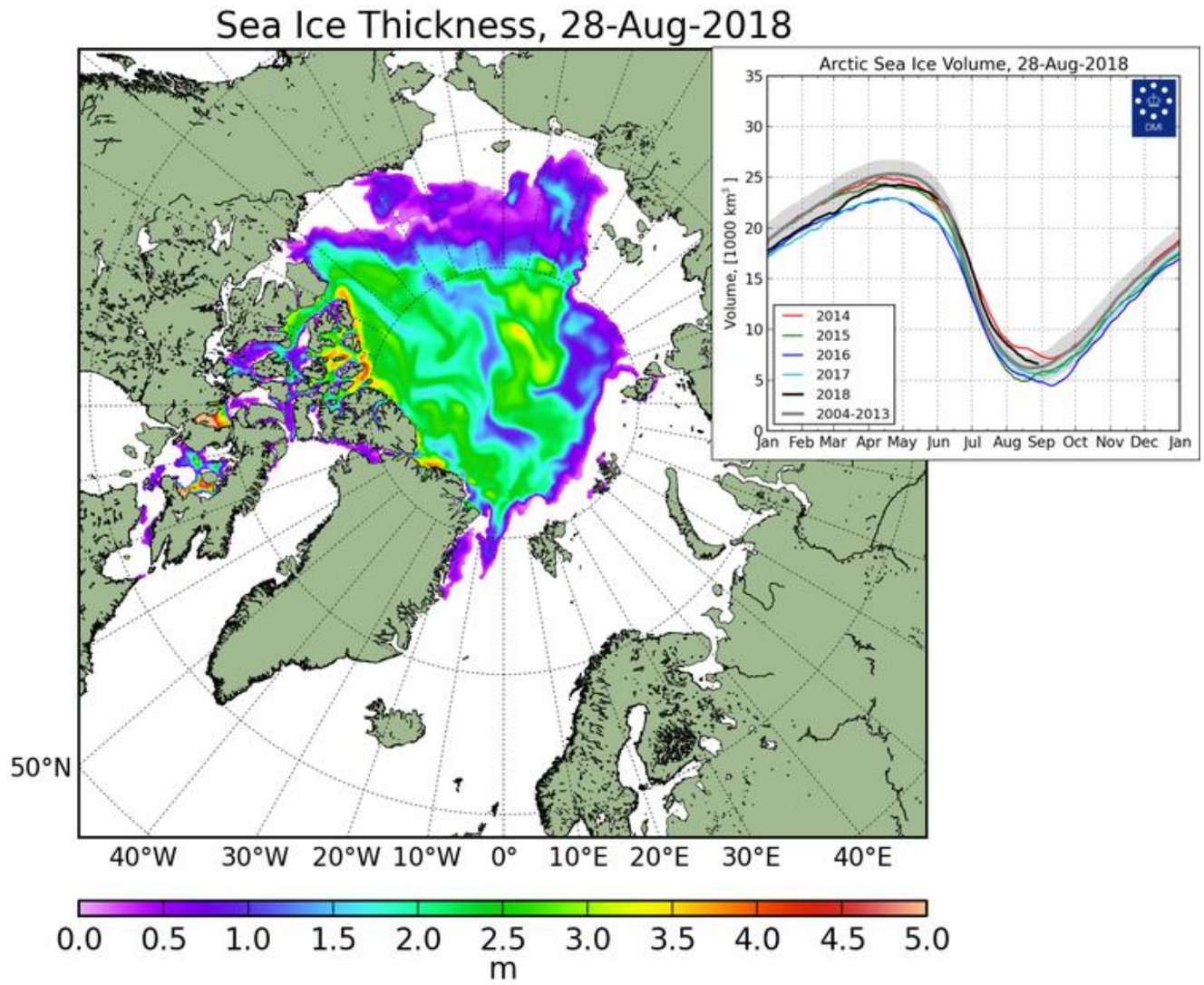

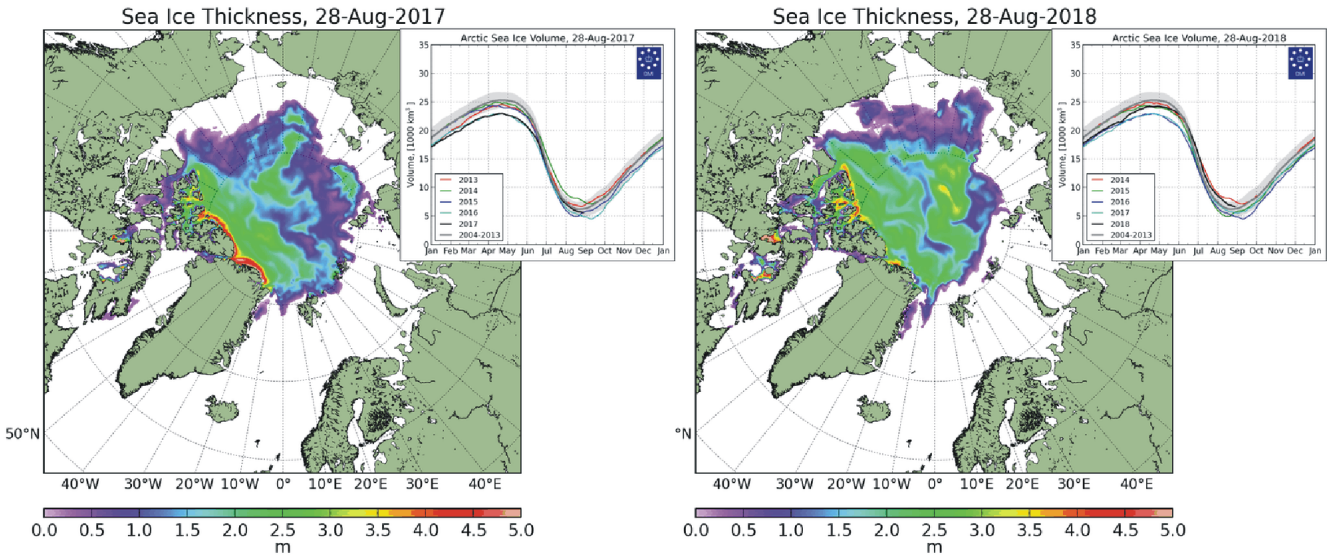

Diagrams showing Arctic sea ice extent and thickness 28 August 2017 (left) and 2018 (right and above) and the seasonal cycles of the calculated total arctic sea ice volume, according to [The Danish Meteorological Institute (DMI)](). The mean sea ice volume and standard deviation for the period 2004-2013 are shown by grey shading.

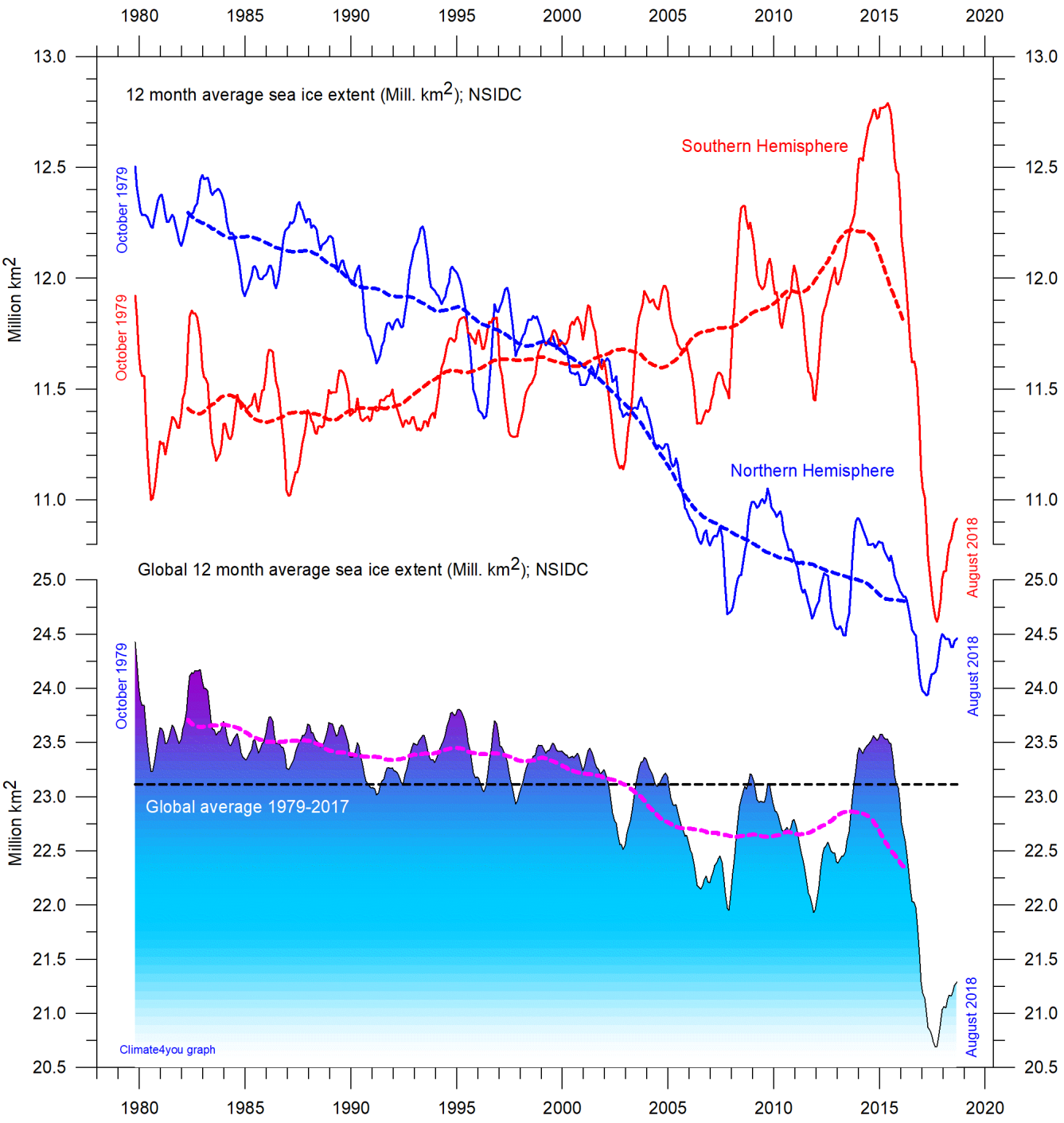

12 month running average sea ice extension, global and in both hemispheres since 1979, the satellite-era. The October 1979 value represents the monthly 12-month average of November 1978 - October 1979, the November 1979 value represents the average of December 1978 - November 1979, etc. The stippled lines represent a 61-month (ca. 5 years) average. Data source: National Snow and Ice Data Center (NSIDC).

Sea level in general

Global (or eustatic) sea-level change is measured relative to an idealised reference level, the geoid, which is a mathematical model of planet Earth's surface (Carter et al. 2014). Global sea-level is a function of the volume of the ocean basins and the volume of water they contain. Changes in global sea-level are caused by – but not limited to - four main mechanisms:

1. Changes in local and regional air pressure and wind, and tidal changes introduced by the Moon.
2. Changes in ocean basin volume by tectonic (geological) forces.
3. Changes in ocean water density caused by variations in currents, water temperature and salinity.
4. Changes in the volume of water caused by changes in the mass balance of terrestrial glaciers.

In addition to these there are other mechanisms influencing sea-level; such as storage of ground water, storage in lakes and rivers, evaporation, etc.

Mechanism 1 is controlling sea-level at many sites on a time scale from months to several years. As an example, many coastal stations show a pronounced annual variation reflecting seasonal changes in air pressures and wind speed. Longer-term climatic changes playing out over decades or centuries will also affect measurements of sea-level changes. Hansen et al. (2011, 2015) provide excellent analyses of sea-level changes caused by recurrent changes of the orbit of the Moon and other phenomena.

Mechanism 2 – with the important exception of earthquakes and tsunamis - typically operates over long (geological) time scales, and is not significant on human time scales. It may relate to variations in the sea-floor spreading rate, causing volume changes in mid-ocean mountain ridges, and to the slowly changing configuration of land and oceans. Another effect may be the slow rise of basins due to isostatic offloading by deglaciation after an ice age. The floor of the Baltic Sea and the Hudson Bay are presently rising, causing a slow net transfer of water from these basins into the adjoining oceans. Slow changes of very big glaciers (ice sheets) and movements in the mantle will affect the gravity field and thereby the vertical position of the ocean surface. Any increase of the total water mass as well as sediment deposition into oceans increase the load on their bottom, generating sinking by viscoelastic flow in the mantle below. The mantle flow is directed towards the surrounding land areas, which will rise, thereby partly compensating for the initial sea level increase induced by the increased water mass in the ocean.

Mechanism 3 (temperature-driven expansion) only affects the uppermost part of the oceans on human time scales. Usually, temperature-driven changes in density are more important than salinity-driven changes. Seawater is characterised by a relatively small coefficient of expansion, but the effect should however not be overlooked, especially when interpreting satellite altimetry data. Temperature-driven expansion of a column of seawater will not affect the total mass of water within the column considered and will therefore not affect the potential at the top of the water column. Temperature-driven ocean water expansion will therefore not in itself lead to lateral displacement of water, but only lift the ocean surface locally. Near the coast, where people are living, the depth of water approaches zero, so no temperature-driven expansion will take place here (Mörner 2015). Mechanism 3 is for that reason not important for coastal regions.

Mechanism 4 (changes in glacier mass balance) is an important driver for global sea-level changes along coasts, for human time scales. Volume changes of floating glaciers – ice shelves – has no influence on the global sea-level, just like volume changes of floating sea ice has no influence. Only the mass-balance of grounded or land-based glaciers is important for the global sea-level along coasts.

Summing up: Mechanism 1 and 4 are the most important for understanding sea-level changes along coasts.

References:

Carter R.M., de Lange W., Hansen, J.M., Humlum O., Idso C., Kear, D., Legates, D., Mörner, N.A., Ollier C., Singer F. & Soon W. 2014. Commentary and Analysis on the Whitehead& Associates 2014 NSW Sea-Level Report. Policy Brief, NIPCC, 24. September 2014, 44 pp. http://climatechangereconsidered.org/wp-content/uploads/2014/09/NIPCC-Report-on-NSW-Coastal-SL-9z-corrected.pdf

Hansen, J.-M., Aagaard, T. and Binderup, M. 2011. Absolute sea levels and isostatic changes of the eastern North Sea to central Baltic region during the last 900 years. Boreas, 10.1111/j.1502-3885.2011.00229.x. ISSN 0300–9483.

Hansen, J.-M., Aagaard, T. and Huijpers, A. 2015. Sea-Level Forcing by Synchronization of 56- and 74-YearOscillations with the Moon's Nodal Tide on the Northwest European Shelf (Eastern North Sea to Central Baltic Sea). Journ. Coastal Research, 16 pp.

Mörner, Nils-Axel 2015. Sea Level Changes as recorded in nature itself. Journal of Engineering Research and Applications, Vol.5, 1, 124-129.

Global sea level from satellite altimetry, updated to January 2018

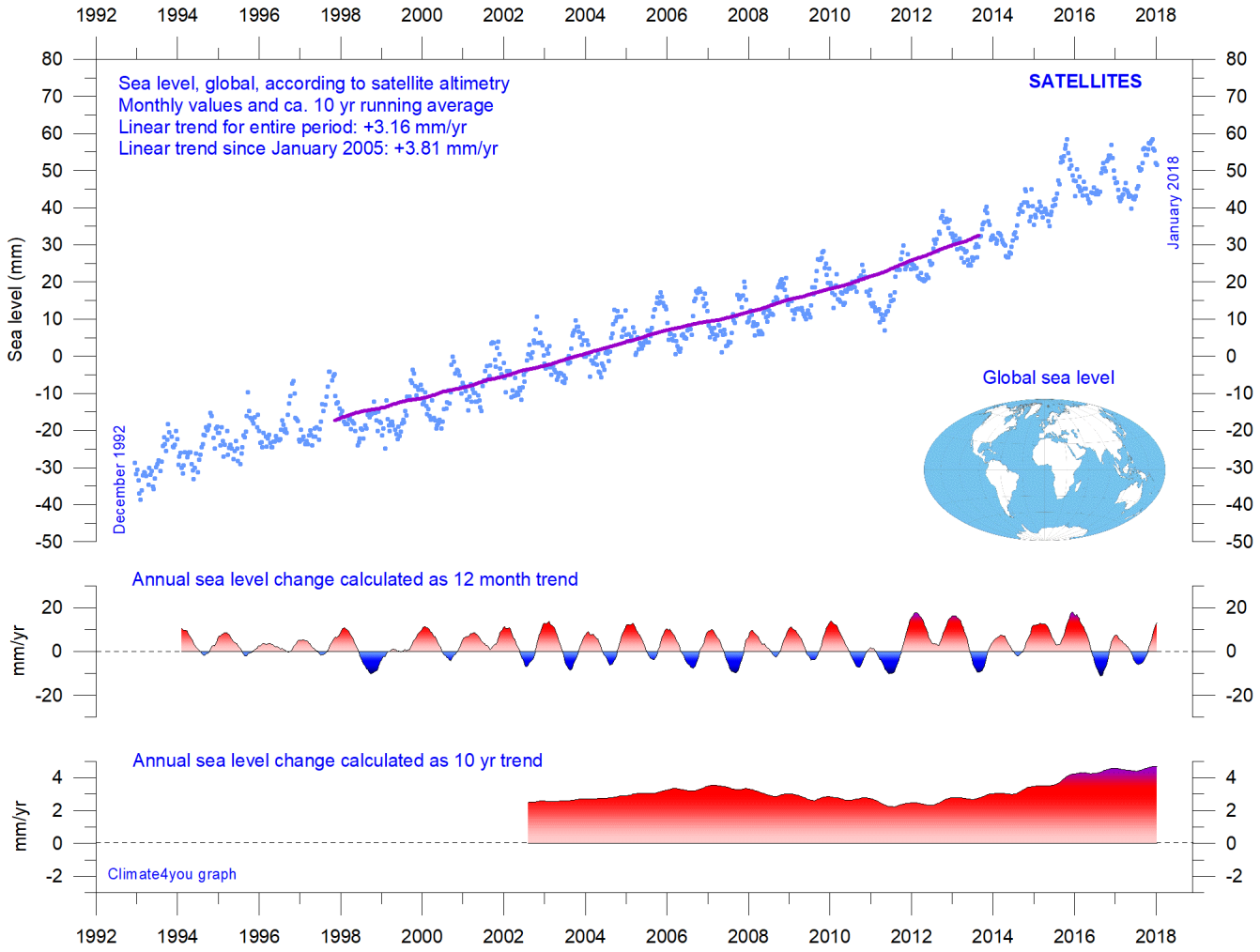

Global sea level since December 1992 according to the Colorado Center for Astrodynamics Research at University of Colorado at Boulder. The blue dots are the individual observations, and the purple line represents the running 121-month (ca. 10 year) average. The two lower panels show the annual sea level change, calculated for 1 and 10-year time windows, respectively. These values are plotted at the end of the interval considered. Data from the TOPEX/Poseidon mission have been used before 2002, and data from the Jason-1 mission (satellite launched December 2001) after 2002.

Global sea level from tide-gauges, updated to December 2017

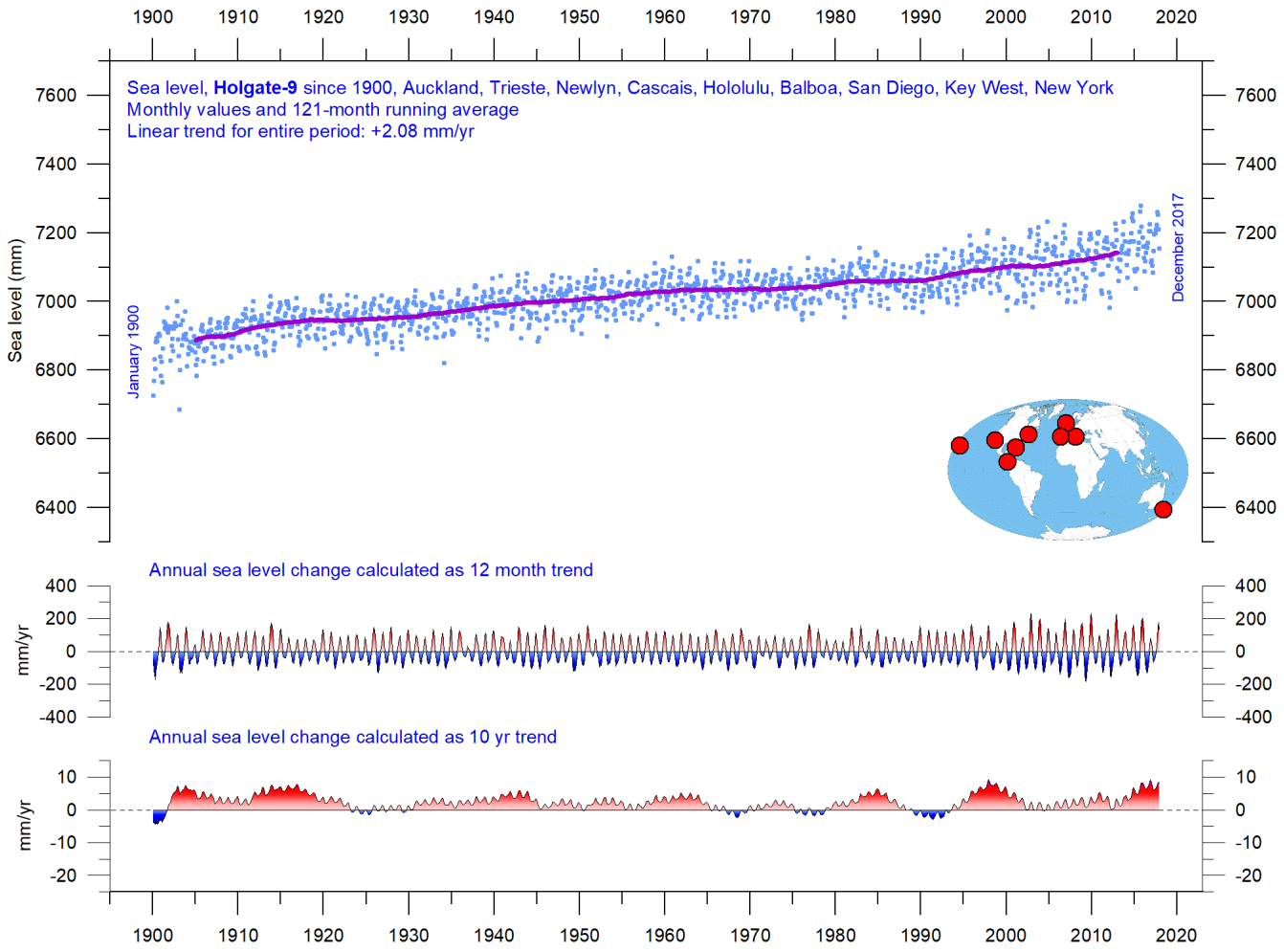

Holgate-9 monthly tide gauge data from PSMSL Data Explorer. Holgate (2007) suggested the nine stations listed in the diagram to capture the variability found in a larger number of stations over the last half century studied previously. For that reason, average values of the Holgate-9 group of tide gauge stations are interesting to follow. The blue dots are the individual average monthly observations, and the purple line represents the running 121-month (ca. 10 year) average. The two lower panels show the annual sea level change, calculated for 1 and 10-year windows, respectively. These values are plotted at the end of the interval considered.

Reference:

Holgate, S.J. 2007. On the decadal rates of sea level change during the twentieth century. Geophys. Res. Letters, 34, L01602, doi:10.1029/2006GL028492

Northern Hemisphere weekly and seasonal snow cover, updated to August 2018

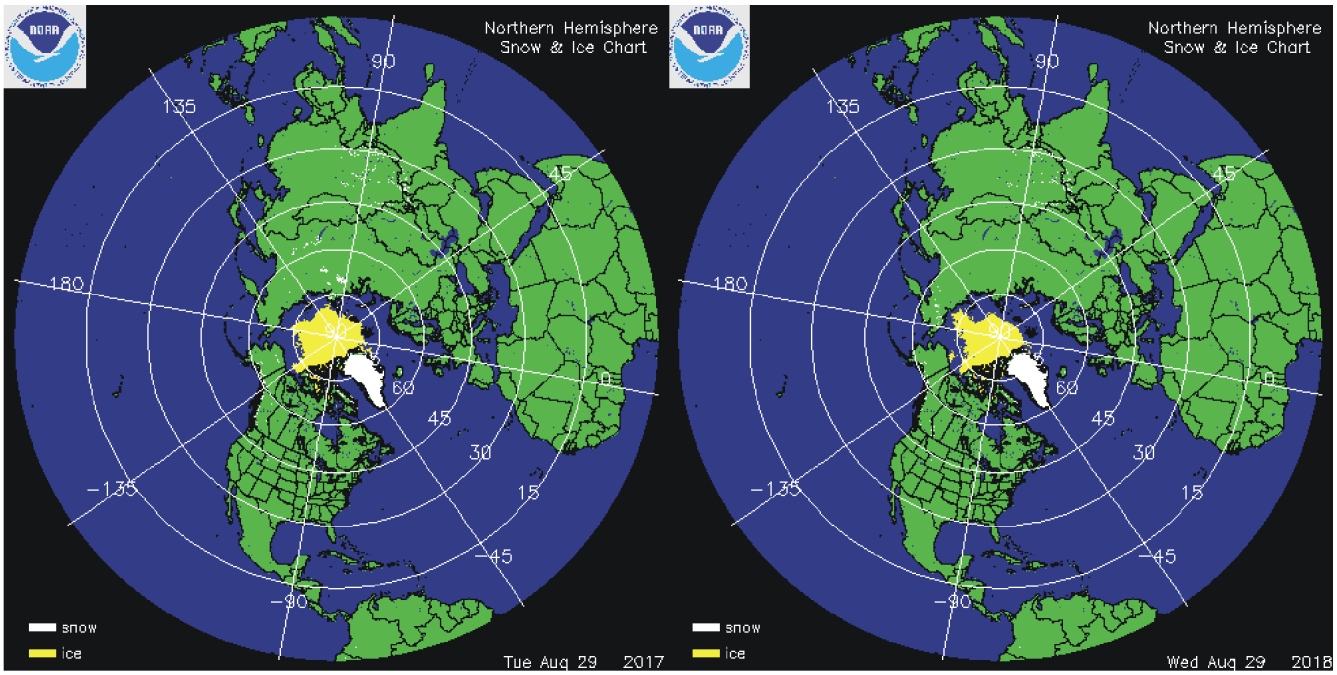

Northern hemisphere snow cover (white) and sea ice (yellow) 29 July 2017 (left) and 2018 (right). Map source: National Ice Center (NIC).

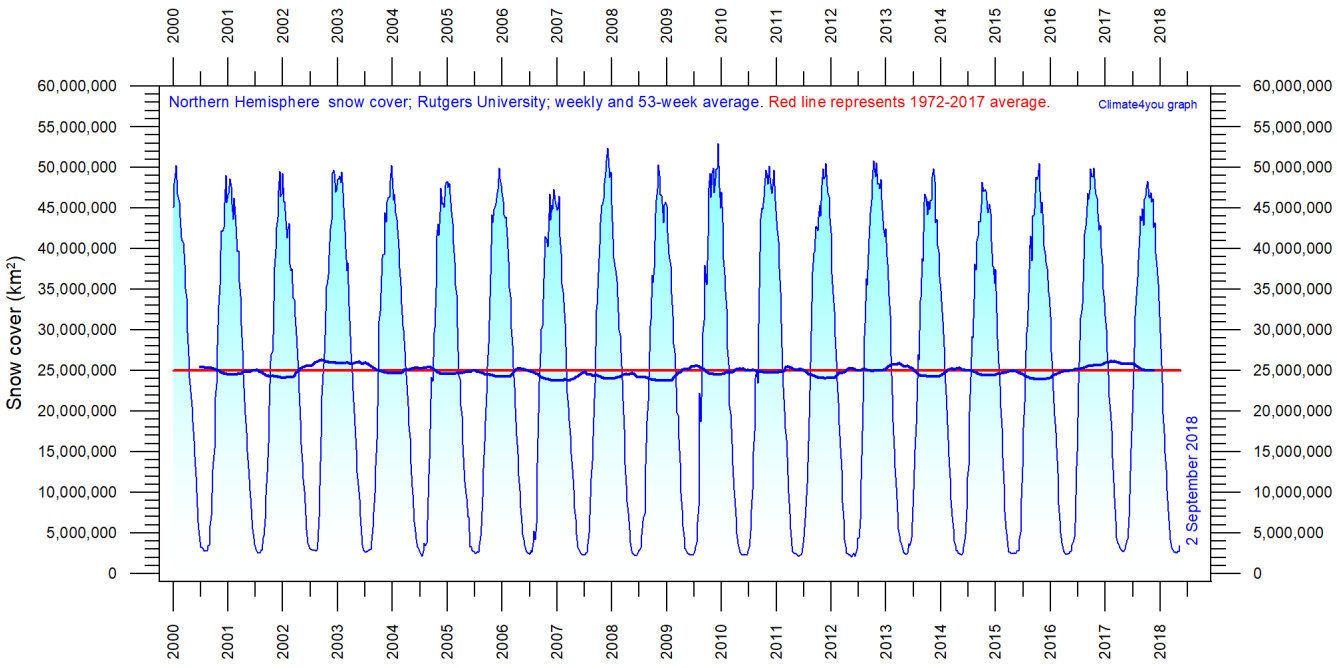

Northern hemisphere weekly snow cover since January 2000 according to Rutgers University Global Snow Laboratory. The thin blue line is the weekly data, and the thick blue line is the running 53-week average (approximately 1 year). The horizontal red line is the 1972-2017 average.

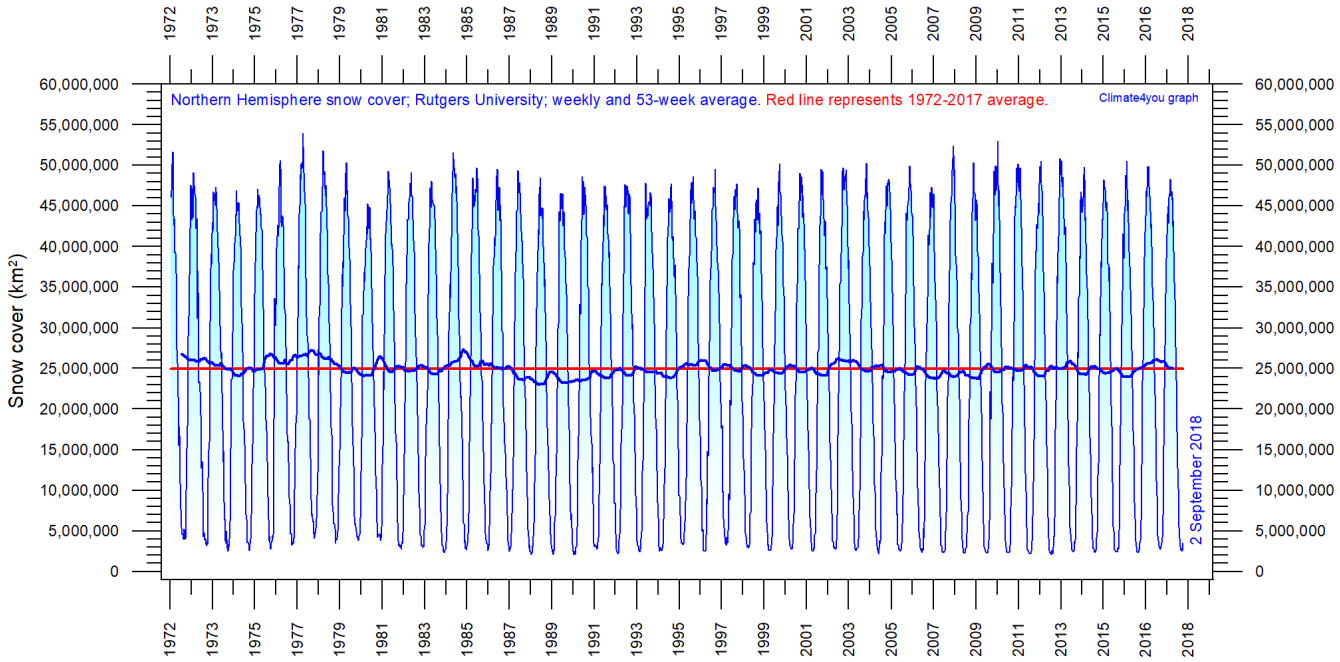

Northern hemisphere weekly snow cover since January 1972 according to Rutgers University Global Snow Laboratory. The thin blue line is the weekly data, and the thick blue line is the running 53-week average (approximately 1 year). The horizontal red line is the 1972-2017 average.

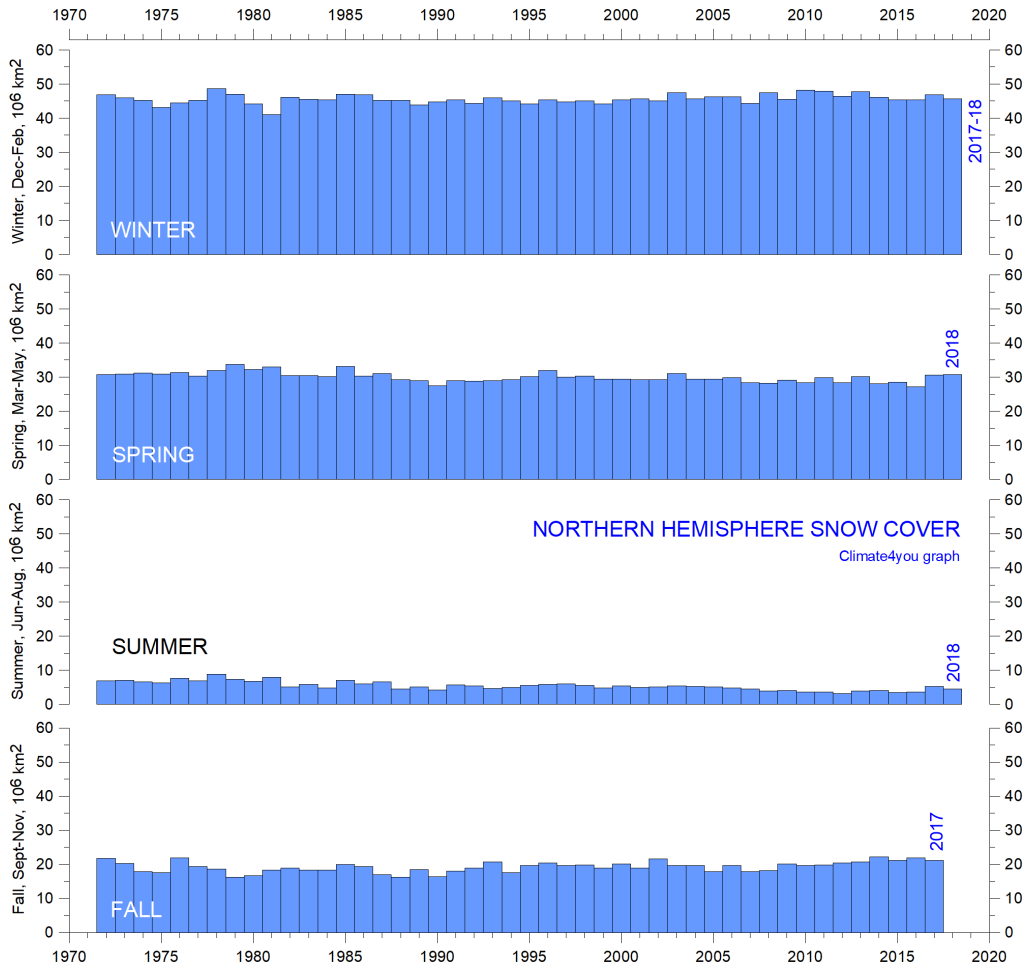

Northern hemisphere seasonal snow cover since January 1972 according to Rutgers University Global Snow Laboratory.

Atmospheric specific humidity, updated to August 2018

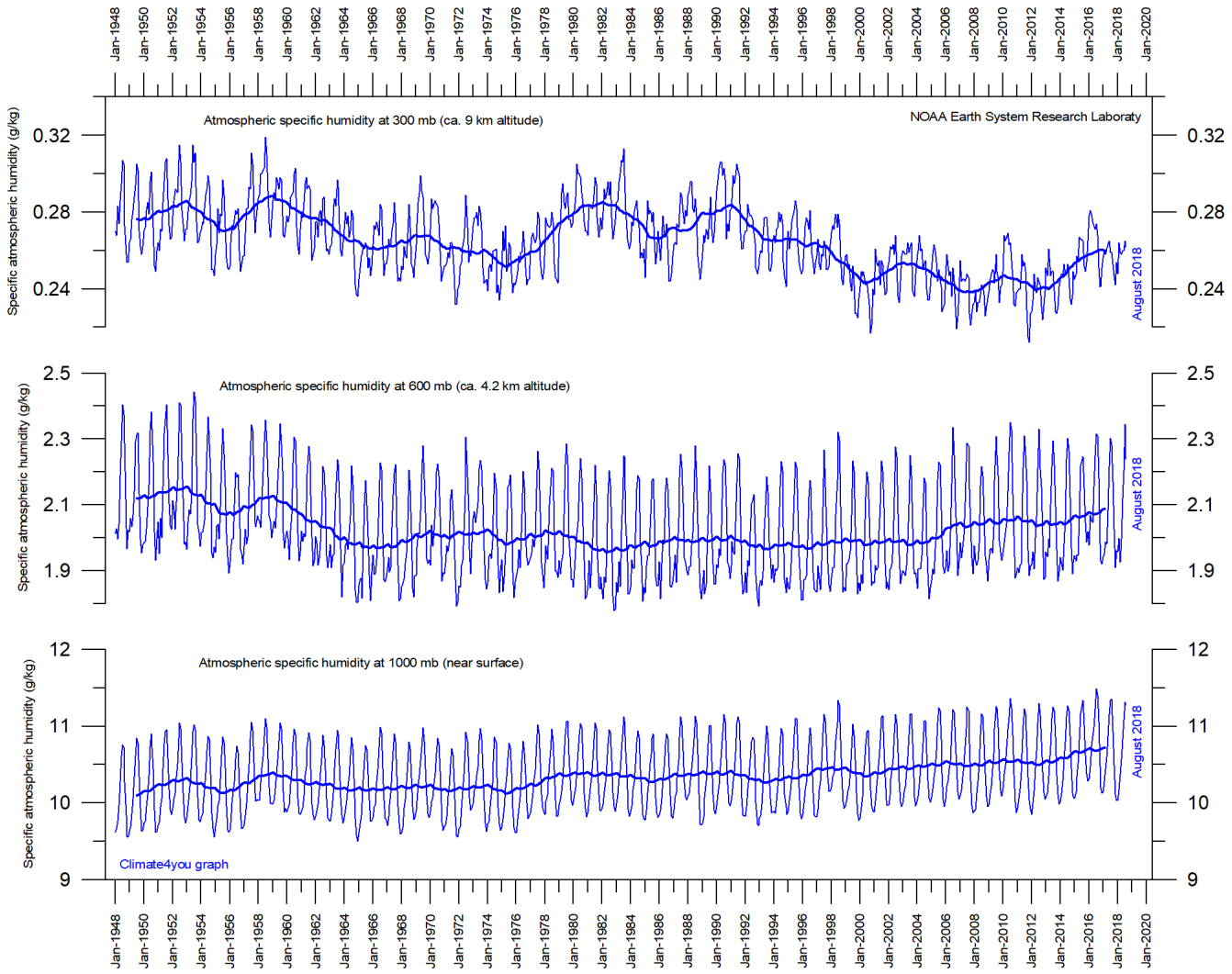

Specific atmospheric humidity (g/kg) at three different altitudes in the lower part of the atmosphere (the Troposphere) since January 1948 (Kalnay et al. 1996). The thin blue lines show monthly values, while the thick blue lines show the running 37-month average (about 3 years). Data source: Earth System Research Laboratory (NOAA).

Atmospheric CO_2, updated to August 2018

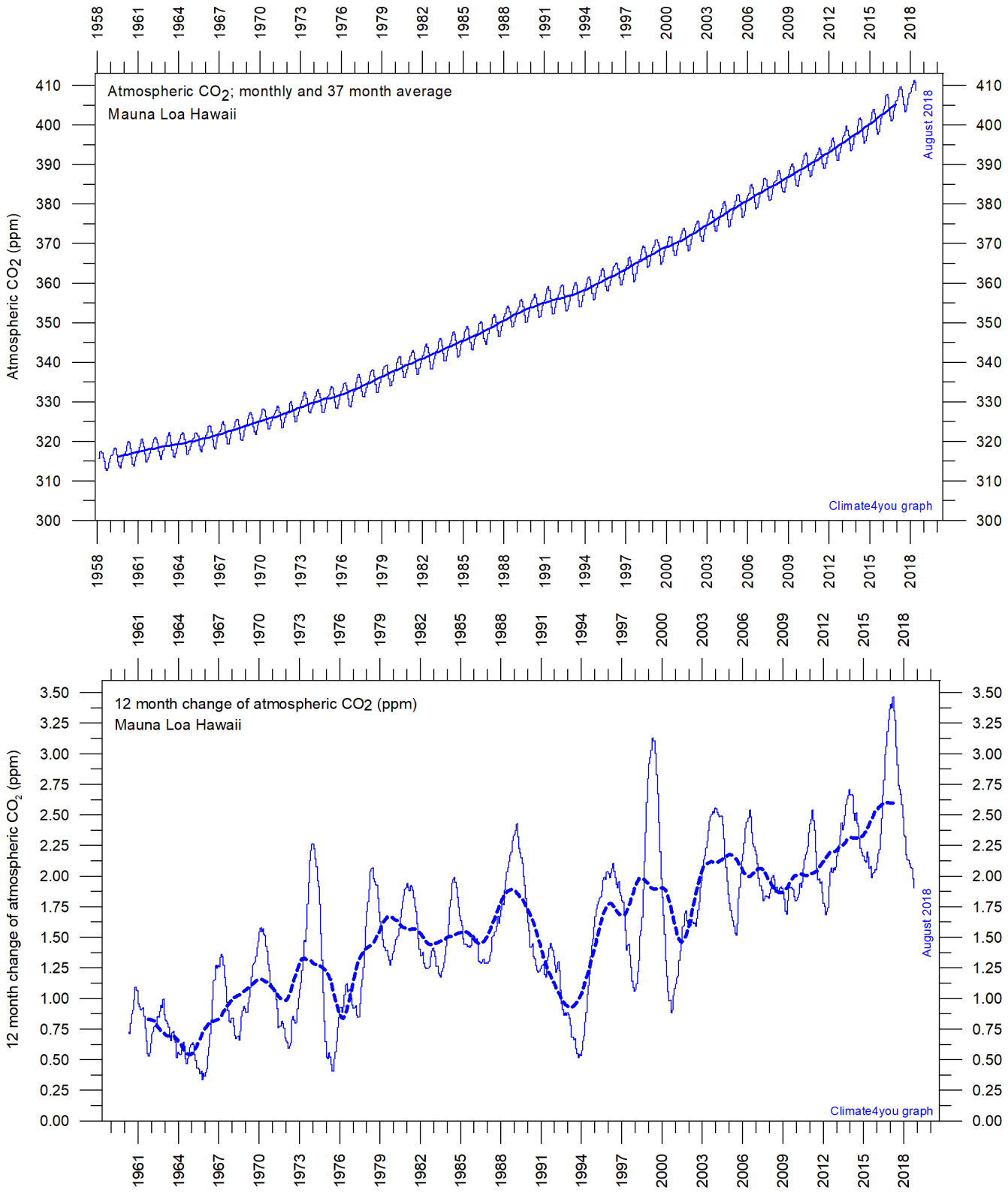

Monthly amount of atmospheric CO_2 (upper diagram) and annual growth rate (lower diagram); average last 12 months minus average preceding 12 months, thin line) of atmospheric CO_2 since 1959, according to data provided by the Mauna Loa Observatory, Hawaii, USA. The thick, stippled line is the simple running 37-observation average, nearly corresponding to a running 3-year average.

The phase relation between atmospheric CO_2 and global temperature, updated to July 2018

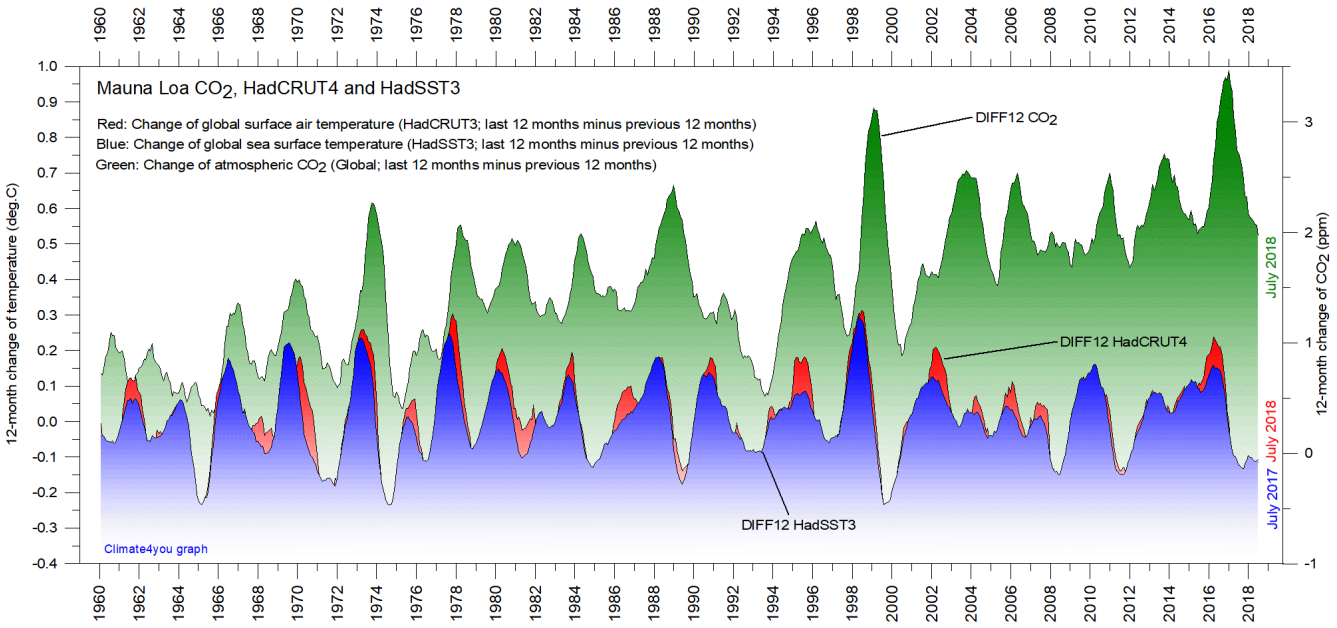

12-month change of global atmospheric CO_2 concentration (Mauna Loa; green), global sea surface temperature (HadSST3; blue) and global surface air temperature (HadCRUT4; red dotted). All graphs are showing monthly values of DIFF12, the difference between the average of the last 12 month and the average for the previous 12 months for each data series.

References:

Humlum, O., Stordahl, K. and Solheim, J-E. 2012. The phase relation between atmospheric carbon dioxide and global temperature. Global and Planetary Change, August 30, 2012. http://www.sciencedirect.com/science/article/pii/S0921818112001658?v=s5

Global air temperature and atmospheric CO_2, updated to August 2018

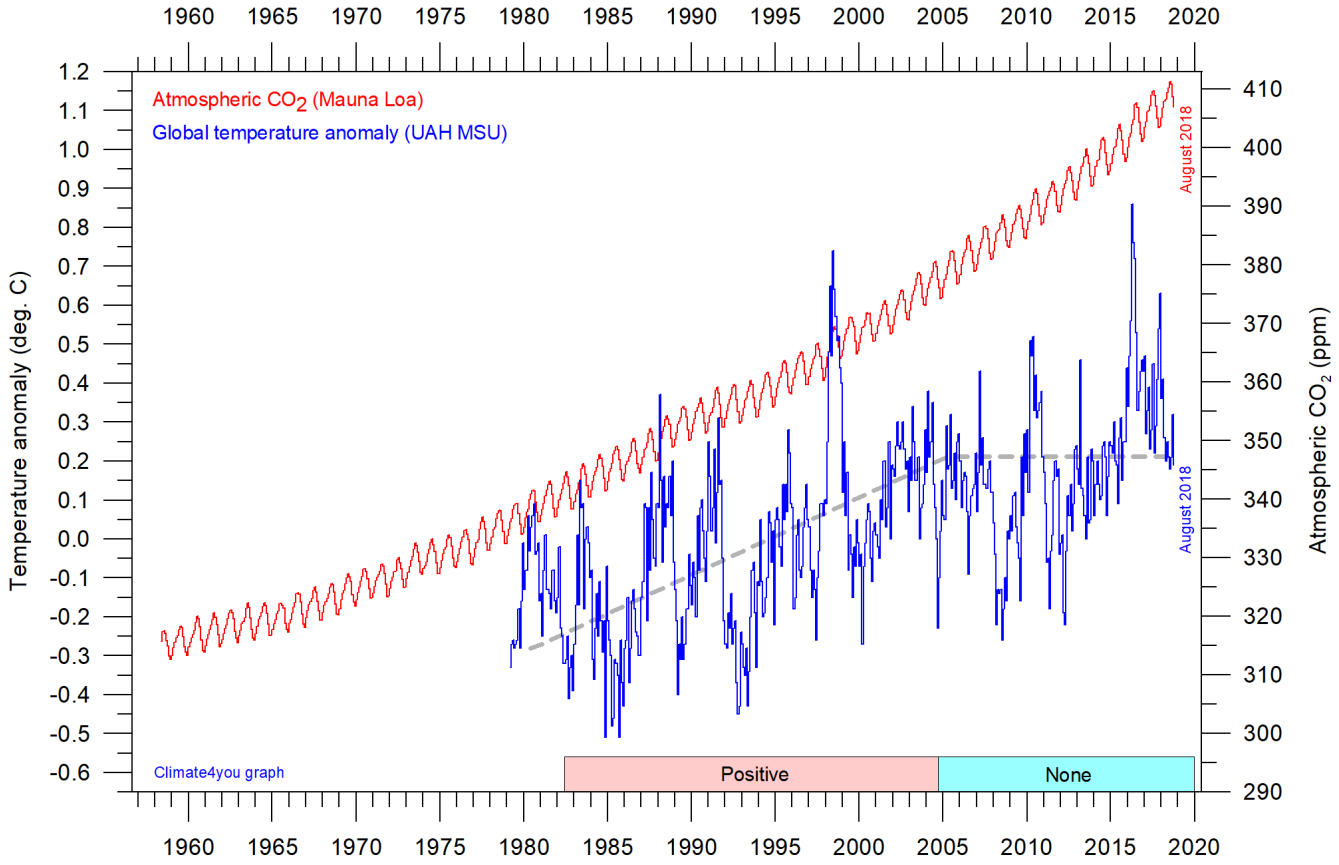

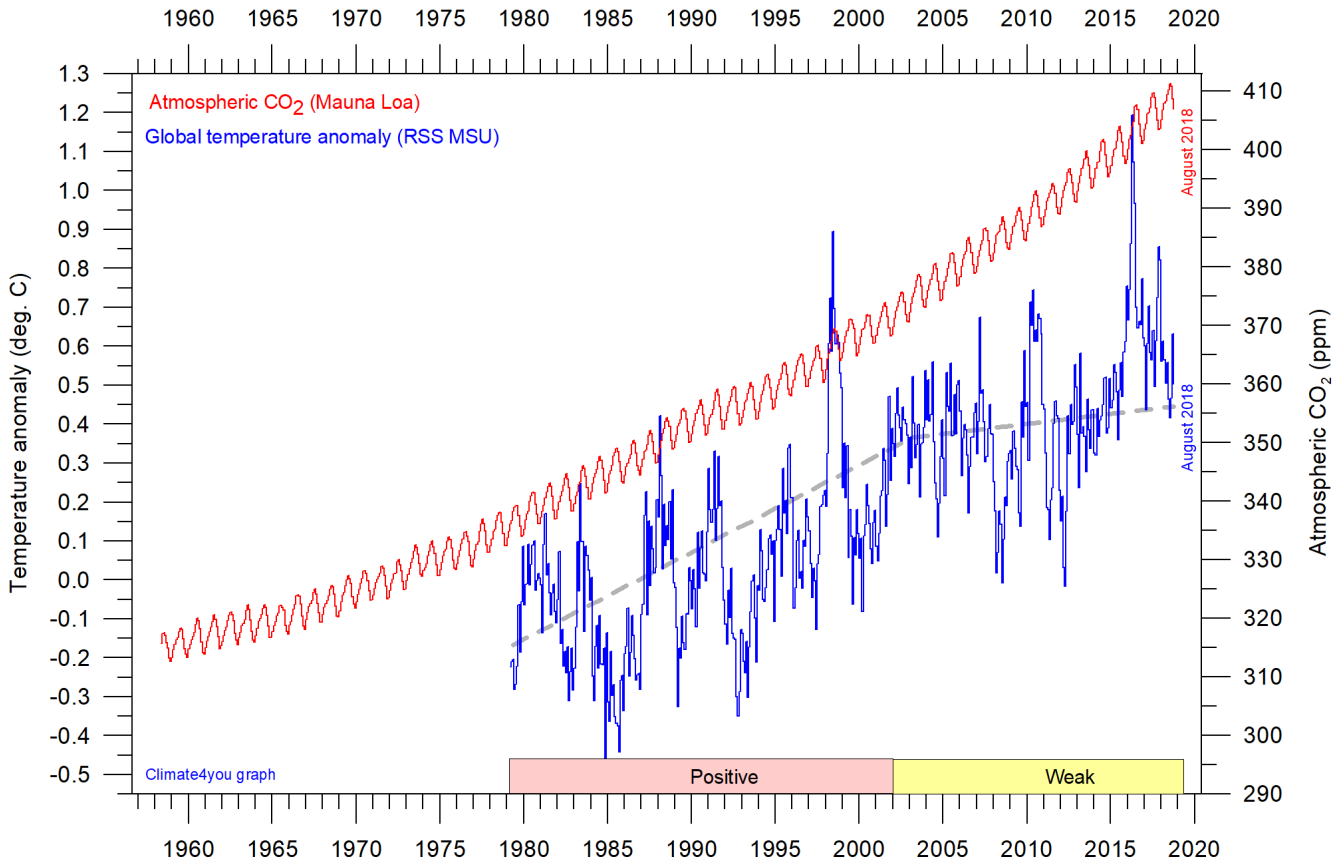

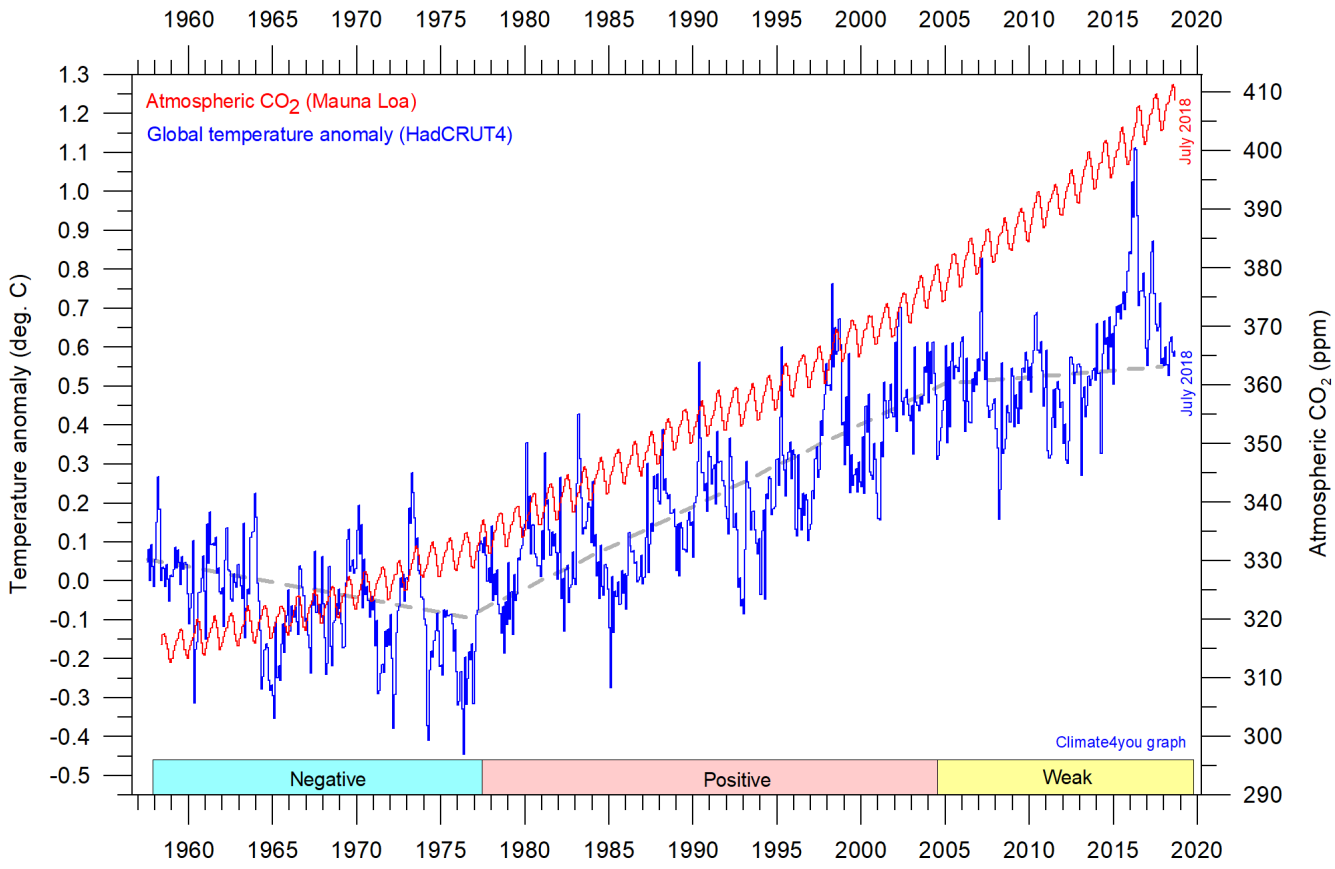
Atmospheric CO2 (Mauna Loa)
Global temperature anomaly (HadCRUT4)
July 2018
July 2018
Climate4you graph
Negative
Positive
Weak
Temperature anomaly (deg. C)
Atmospheric CO2 (ppm)
1960 1965 1970 1975 1980 1985 1990 1995 2000 2005 2010 2015 2020
1.3 1.2 1.1 1.0 0.9 0.8 0.7 0.6 0.5 0.4 0.3 0.2 0.1 0.0 -0.1 -0.2 -0.3 -0.4 -0.5
410 400 390 380 370 360 350 340 330 320 310 300 290

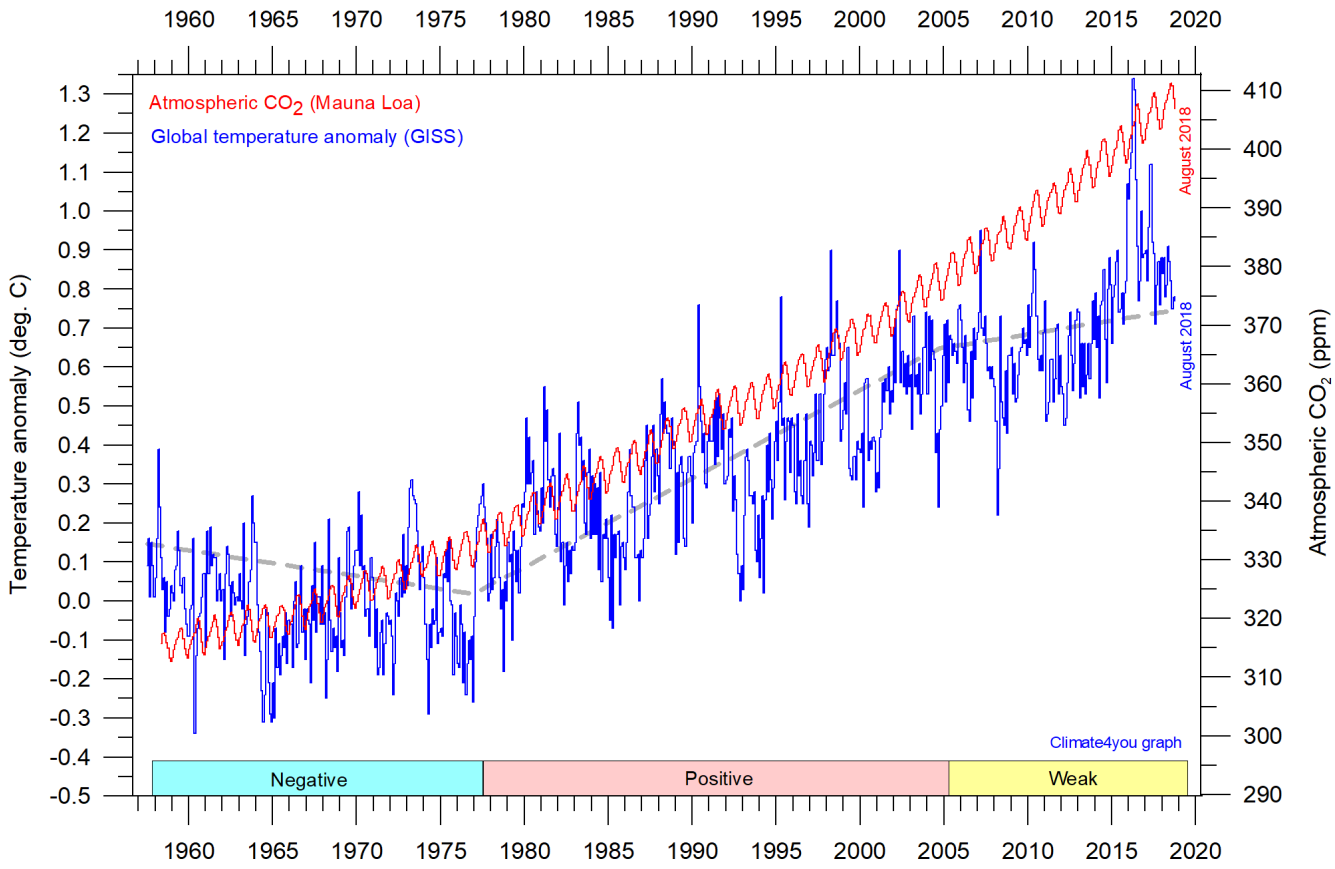
Atmospheric CO2 (Mauna Loa)
Global temperature anomaly (GISS)
August 2018
August 2018
Climate4you graph
Negative
Positive
Weak
Temperature anomaly (deg. C)
Atmospheric CO2 (ppm)
1960 1965 1970 1975 1980 1985 1990 1995 2000 2005 2010 2015 2020
1.3 1.2 1.1 1.0 0.9 0.8 0.7 0.6 0.5 0.4 0.3 0.2 0.1 0.0 -0.1 -0.2 -0.3 -0.4 -0.5
410 400 390 380 370 360 350 340 330 320 310 300 290

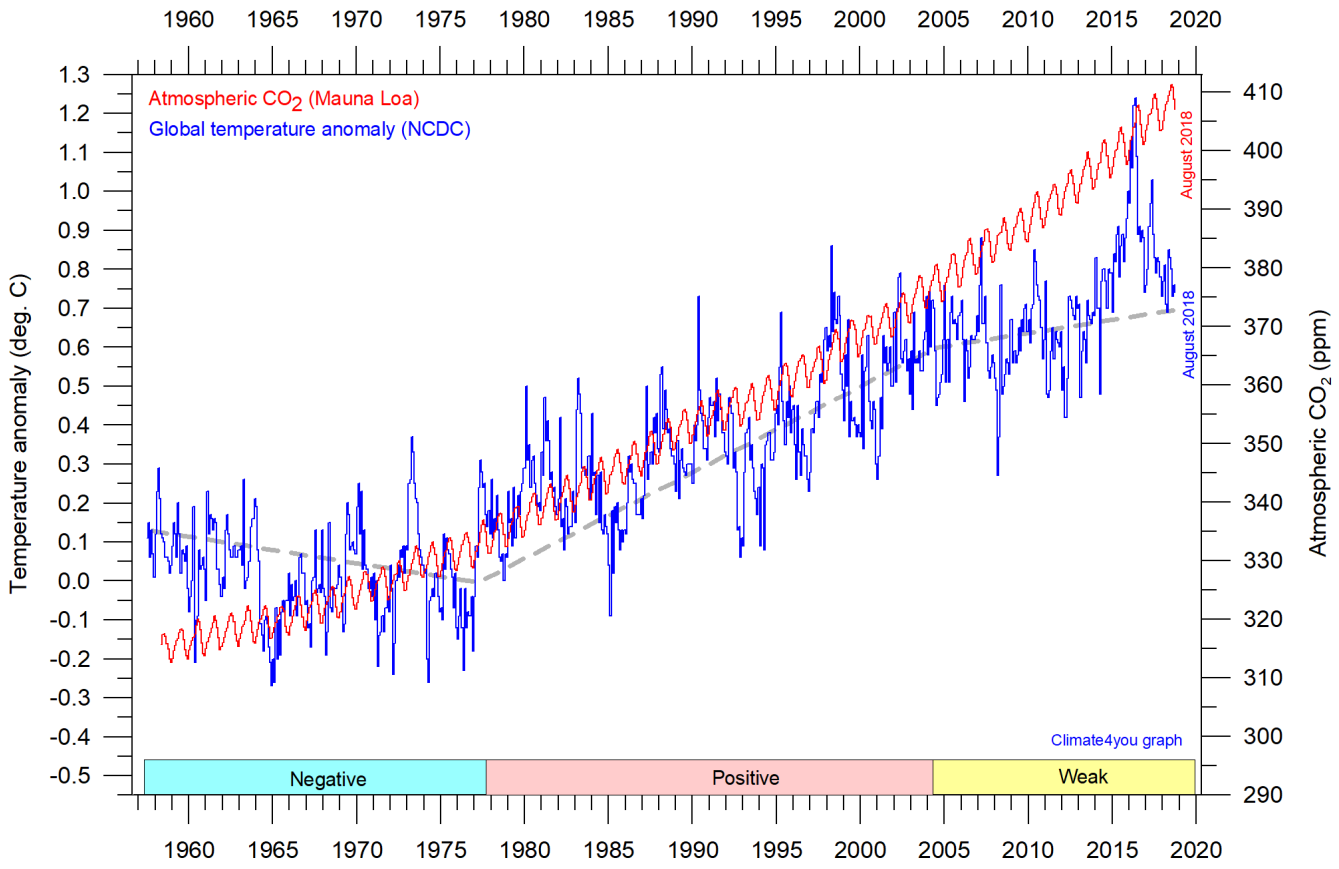

Diagrams showing UAH, RSS, HadCRUT4, GISS, and NCDC monthly global air temperature estimates (blue) and the monthly atmospheric CO_2 content (red) according to the Mauna Loa Observatory, Hawaii. The Mauna Loa data series begins in March 1958, and 1958 was therefore chosen as starting year for the diagrams. Reconstructions of past atmospheric CO_2 concentrations (before 1958) are not incorporated in this diagram, as such past CO_2 values are derived by other means (ice cores, stomata, or older measurements using different methodology), and therefore are not directly comparable with direct atmospheric measurements. The dotted grey line indicates the approximate linear temperature trend, and the boxes in the lower part of the diagram indicate the relation between atmospheric CO_2 and global surface air temperature, negative or positive. Please note that the HadCRUT diagram (p.43) is not yet updated beyond July 2018.

Most climate models are programmed to give the greenhouse gas carbon dioxide CO_2 important influence on global temperature. It is therefore relevant to compare different temperature records with measurements of atmospheric CO_2, as shown in the diagrams above.

Any comparison, however, should not be made on a monthly or annual basis, but for a longer time, as other effects (oceanographic, etc.) may well override the potential influence of CO_2 on short time scales such as just a few years. It is of cause equally inappropriate to present new meteorological record values, whether daily, monthly or annual, as support for the hypothesis ascribing high importance of atmospheric CO_2 for global temperatures. Any such meteorological record value may well be the result of other phenomena.

What exactly defines the critical length of a relevant period length to consider for evaluating the alleged importance of CO_2 remains elusive and represents a theme for discussion. However, the length of the critical period must be inversely proportional to the temperature sensitivity of CO_2, including feedback effects. If the net temperature effect of atmospheric CO_2 is strong, the critical period will be short, and vice versa.

However, past climate research history provides some clues as to what has traditionally been considered the relevant length of period over which

to compare temperature and atmospheric CO_2. After about 10 years of concurrent global temperature- and CO_2-increase, IPCC was established in 1988. For obtaining public and political support for the CO_2-hyphotesis the 10-year warming period leading up to 1988 most likely was important. Had the global temperature instead been decreasing, politic support for the hypothesis would have been difficult to obtain.

Based on the previous 10 years of concurrent temperature- and CO_2-increase, many climate scientists in 1988 presumably felt that their understanding of climate dynamics was sufficient to conclude about the importance of CO_2 for global temperature changes. From this it may safely be concluded that 10 years was considered a period long enough to demonstrate the effect of increasing atmospheric CO_2 on global temperatures.

Adopting this approach as to critical time length (at least 10 years), the varying relation (positive or negative) between global temperature and atmospheric CO_2 has been indicated in the lower panels of the diagrams above.

Latest 20-year QC1 global monthly air temperature changes, updated to August 2018

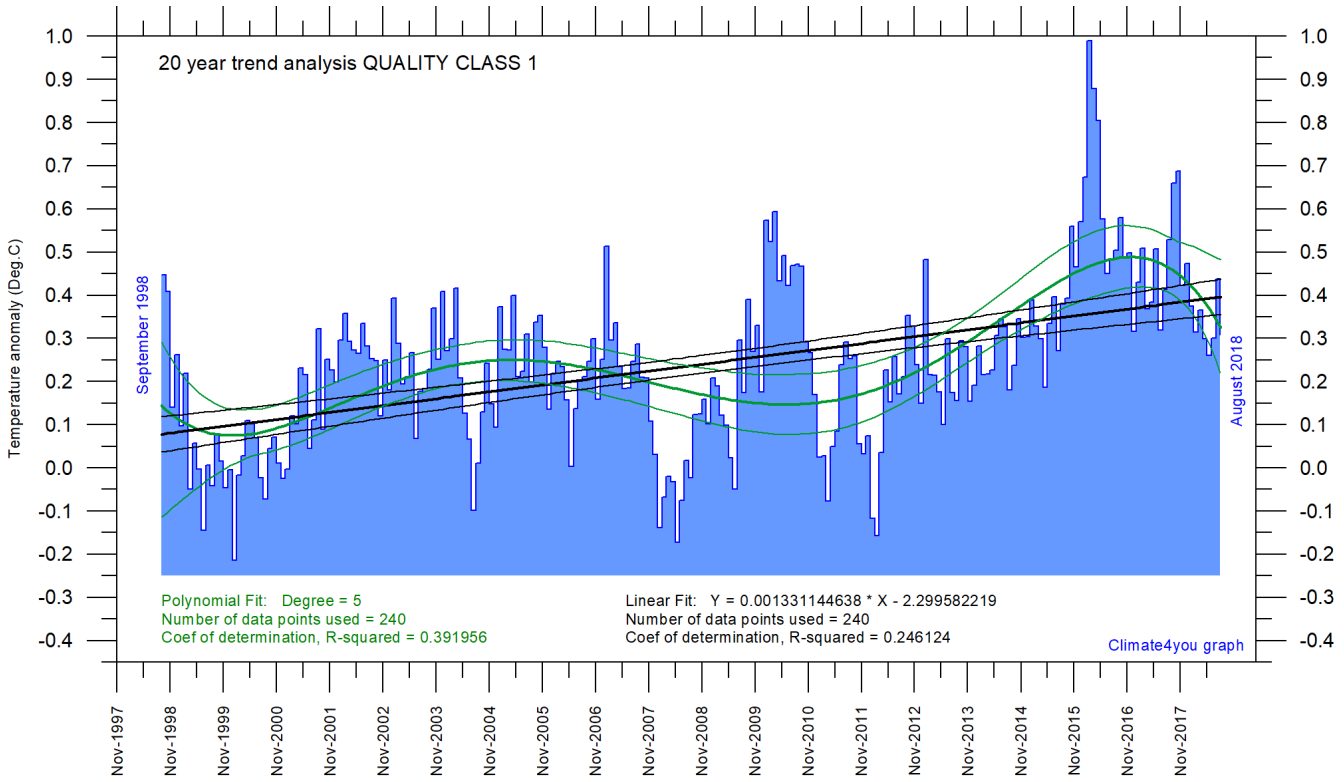

Last 20 years' global monthly average air temperature according to Quality Class 1 (UAH and RSS; see p.10) global monthly temperature estimates. The thin blue line represents the monthly values. The thick black line is the linear fit, with 95% confidence intervals indicated by the two thin black lines. The thick green line represents a 5-degree polynomial fit, with 95% confidence intervals indicated by the two thin green lines. A few key statistics are given in the lower part of the diagram (please note that the linear trend is the monthly trend).

In the ongoing climate debate the following about the global surface air temperature is often put forward: Is the surface air temperature still increasing or has it essentially been stable during the last 10-15 years?

The diagram above may be useful in this context and demonstrates the differences between two often used statistical approaches to determine recent temperature trends. Please also note that such fits only attempt to describe the past, and usually have limited predictive power. In addition, before using any linear trend (or other) analysis of time series a proper statistical model should be chosen, based on statistical justification.

For temperature time series, there is no *a priori* physical reason why the long-term trend should be linear in time. In fact, climatic time series often have trends for which a straight line is not a good approximation, as can clearly be seen from several of the diagrams in the present report.

For an excellent description of problems often encountered by analyses of temperature time series analyses, please see Keenan, D.J. 2014: Statistical Analyses of Surface Temperatures in the IPCC Fifth Assessment Report.

Sunspot activity and QC1 average satellite global air temperature, updated to August 2018

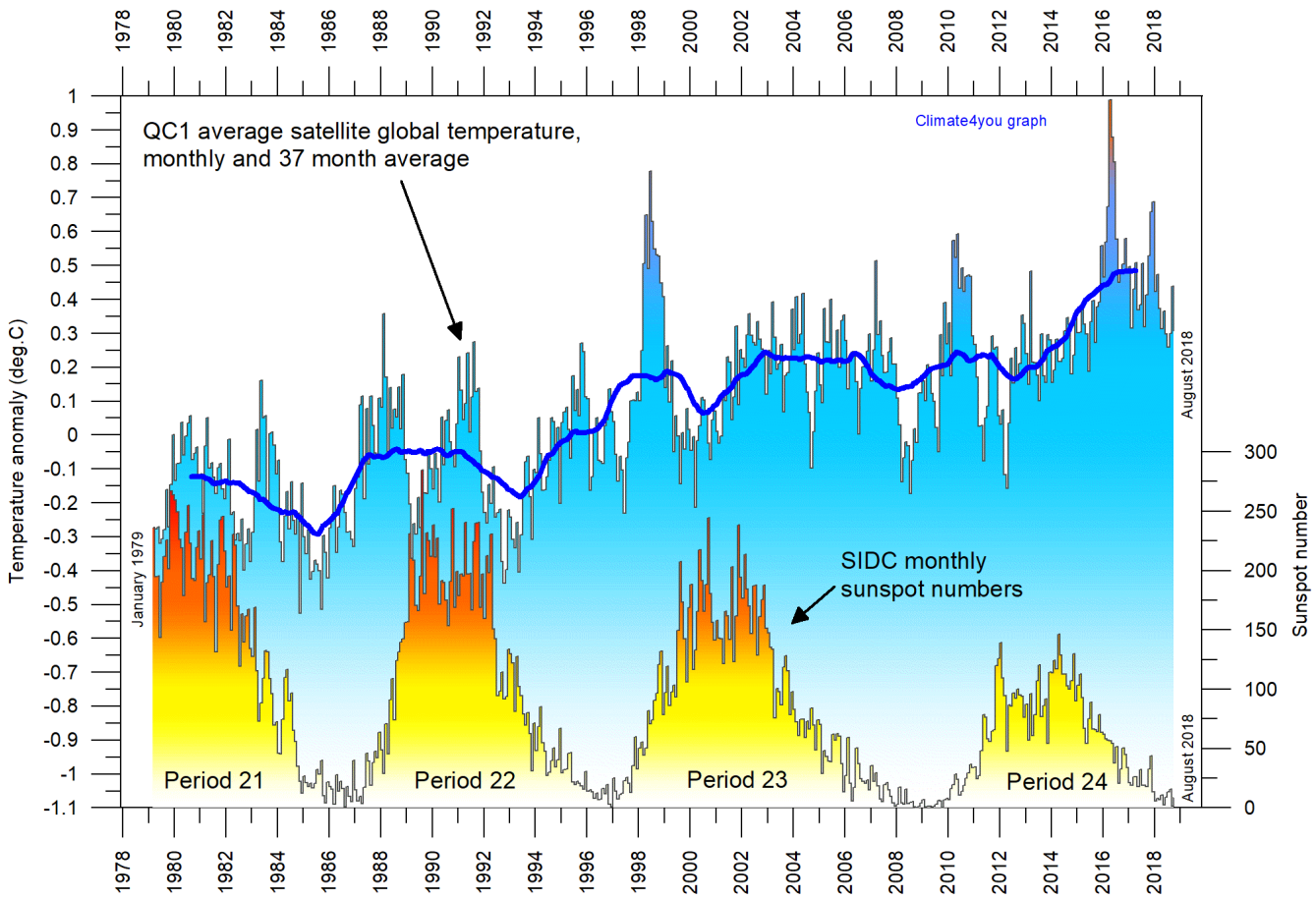

Variation of global monthly air temperature according to Quality Class 1 (UAH and RSS; see p.4) and observed sunspot number as provided by the Solar Influences Data Analysis Center (SIDC), since 1979. The thin lines represent the monthly values, while the thick line is the simple running 37-month average, nearly corresponding to a running 3-year average. The asymmetrical temperature 'bump' around 1998 is influenced by the oceanographic El Niño phenomenon in 1998, as is the case also for 2015-16.

2002: New knowledge obtained on Kilimanjaro glaciers

The stratovolcano Kilimanjaro (5895 m asl.) in northeastern Tanzania (left). The Furtwängler Glacier on the summit plateau of Kilimanjaro (right). The vertical ice cliffs are about 40 m high.

Kilimanjaro (5895 m asl.) is an inactive stratovolcano in northeastern Tanzania, near the border to Kenya. Kilimanjaro is also the tallest free-standing mountain in the world, rising 4,600 m from the surrounding plains. The first official climb of the highest summit was on 6 October 1889 by the German Hans Meyer, the Austrian Ludwig Purtscheller, guided by the Marangu army scout Yohanas Kinyala.

The glaciers on Kilimanjaro have attracted much recent interest, especially in relation to global temperature changes. The Furtwängler Glacier (see illustration above) is located near the summit and is a remnant of a bigger icecap which once crowned the summit of Mount Kilimanjaro. This glacier is named after Walter Furtwängler, who along with Ziegfried Koenig, were the fourth to ascend to the summit of Kilimanjaro in 1912. Furtwängler Glacier has lost much of its previous volume since first visited by Meyer and Purtscheller in 1889. Between 1912 and the 2000, about 80 percent of the glacier ice on the mountain disappeared.

A detailed analysis of six ice cores retrieved from the ice fields on the summit of Kilimanjaro shows that those glaciers began forming about 11,700 years ago (Thompson et al. 2002). The ice core records from the Furtwängler Glacier suggests conditions at the Summit of Kilimanjaro today are returning to that characteristic for the site 11,000 years ago.

For decades it has been known that solar radiation and sublimation, not air temperature, are the primary factors for loss of ice from tropical glaciers. In the tropics glaciers exist only at the highest elevations, and their size is controlled more by seasonal changes in precipitation than by air temperatures. Observations of the volume change of glaciers on Kilimanjaro suggest their total volume decreased by 66 percent from 1889 to 1953.

The balance between energy inputs and energy outputs are important to understand 20th century glacier reduction at Kilimanjaro. The primary input of energy is short-wave solar radiation, while ice loss is primarily by way of sublimation, the transition of ice directly to water vapour. Because neither solar radiation and sublimation depends primarily on surface air temperatures, air temperature change does not have a big role in the loss of ice from tropical glaciers. This also applies to glaciers on Kilimanjaro, as can be seen from the fact that the ice on Kilimanjaro forms high vertical walls (see illustration above) and finger-like features called penitents (see illustration below), the result of sublimation driven by direct radiation from the sun, rather than ablation caused by warm air.

Examples of ice and snow penitentes from tropical areas. The individual blades are between 1.5 and 2m in height but may be as high as several meters. Because penitentes are formed by sublimation driven by direct solar radiation, their axis indicates the approximate position of the sun at noon at this latitude and time of the year. Snow penitentes was first described by Darwin (1839). *The term penitente date back at least to the beginning of the Little Ice Age, referring to Los Penitentes, the flagellant orders in Spain and Italy.*

A prolonged dry period may be responsible for the shrinking glaciers on Kilimanjaro. Kaser et al (2004) found that a marked drop in atmospheric moisture at the end of the 19th century and the ensuing drier climatic conditions are likely to represent the main driver for 20th century glacier retreat on Kilimanjaro. Independent surface observations of water levels from nearby Lake Victoria suggest that water levels have been declining since the end of the 19th century (Thompson et al. 2002), lending support to the notion that the present glacier retreat is caused by more dry conditions, and that the large extent of the glaciers observed by Meyer and Purtscheller in 1889 was the result of a more humid period in eastern Africa at that time, rather than to lower air temperatures.

The ice core from from the Furtwängler Glacier (Thompson et al. 2002) yield evidence of three catastrophic droughts in the tropics 8,300, 5,200 and 4,000 years ago. The ice core also suggests a much wetter environment near Kilimanjaro 9,500 years ago, contemporary with the existence of Megalake Chad in the Sahara region. The ice core also showed a 500-year period beginning around 8,300 years ago when methane levels in the ice dropped rapidly, suggesting that several lakes of Africa were beginning to dry up. Usually,

atmospheric methane levels are assumed to reflect, among other things, the extent of the tropical wetlands.

In addition, the ice core showed an abrupt depletion in oxygen-18 isotopes that may signal a second drought event occurring around 5,200 years ago (Thompson et al. 2002). This coincides with the period when anthropologists believe people in the region began to come together to form cities and social structures. Prior to this, the population of mainly hunters and gatherers had been more scattered. A third marker type in the ice cores is a visible dust layer dating back to about 4,000 years ago (Thompson et al. 2002). This is interpreted as marking a severe 300-year drought which struck the region. Historical records show that a massive drought hit the Egyptian empire at the time and threatened the rule of the Pharaohs. Until this time, people in Africa had been able to exist and thrive in areas that are now just barren Sahara Desert.

REFERENCES:

Kaser, G., Hardy, D.R., Olg, T.M., Bradley, R.S. and Hyera, T.M. 2004. Modern Glacier Retreat on Kilimanjaro as Evidence of Climate Change: Observations and Facts. *International Journal of Climatology* 24, 329–339.

Thompson, L.G., Mosley-Thompson, E., Davis, M.E., Henderson, K.A., Brecher, H.H., Zagorodnov, V.S., Mashiotta, T.A., Lin, P-N., Mikhalenko, V.N., Hardy, D.R. and Beer, J. 2002. Kilimanjaro ice core records: Evidence of Holocene climate change in tropical Africa. *Science* 298, 589-593.

*****

All diagrams in this report, along with any supplementary information, including links to data sources and previous issues of this newsletter, are freely available for download on www.climate4you.com

Yours sincerely,

Ole Humlum (Ole.Humlum@gmail.com)

September 19, 2018.